



Grant Agreement No.: 226479

# SafeLand

Living with landslide risk in Europe: Assessment,  
effects of global change, and risk management strategies

7<sup>th</sup> Framework Programme  
Cooperation Theme 6 Environment (including climate change)  
Sub-Activity 6.1.3 Natural Hazards

## Deliverable 1.4

Guidelines for use of numerical codes for prediction of climate-induced  
landslides

Work Package 1.2 – Geomechanical analysis of weather-induced triggering  
processes

Deliverable/Work Package Leader: EPFL

Revision: 3

March, 2011

| Rev. | Deliverable Responsible | Controlled by | Date       |
|------|-------------------------|---------------|------------|
| 0    | EPFL                    | -             | 31.07.2010 |
| 1    | EPFL                    | -             | 15.12.2010 |
| 2    | EPFL                    | FUNAB         | 20.03.2011 |
| 3    | EPFL                    | FUNAB         | 23.03.2011 |

## SUMMARY

This deliverable addresses as a summary of deliverable D1.2 the different key physical mechanisms in landslides and the mathematical frameworks that have been developed in the soil mechanics community to model the time-dependent processes of water flow, pore pressure dissipation and deformation in soil slopes. Guidelines are presented for landslide modelling which provide the user in the first place with some information on the utility of numerical codes. In the second place, these guidelines allow the user to identify the necessary code components for a given landslide problem, select the necessary and most important field data for the model and perform the modelling steps, including data pre-processing, the actual numerical calculation, as well as the post-processing of the results. The geomechanical codes used in the SafeLand project are evaluated with respect to the availability of components which are necessary or which allow to obtain additional expertise on different, particular landslide problems. The last section is dedicated to a discussion on the use of geomechanical modelling for early-warning systems and the prediction of the behaviour of large landslides under different climatic scenarios.

## CONTRIBUTORS

- **Lead partner responsible for the deliverable:**

EPFL

*Deliverable prepared by:*

L. Laloui

J. Eichenberger

A. Ferrari

- **Partner responsible for quality control:**

FUNAB

*Deliverable reviewed by:*

M. Pastor

- **Contributors to the deliverable:**

AMRA: L. Picarelli, E. Damiano, L. Comegna

CNRS: J.-P. Malet, A. Spickermann

FUNAB: M. Pastor, J.A. Fernández Merodo, P.Mira, D.Manzanal

UNISA: L. Cascini, G. Sorbino, S. Cuomo

UPC: E. Alonso, N. Pinyol

## Table of contents

|          |   |           |
|----------|---|-----------|
| <b>1</b> | <b>Challenges in numerical modelling of landslides</b>                                      | <b>4</b>  |
| <b>2</b> | <b>Key issues in numerical modelling of climate induced landslides</b>                      | <b>6</b>  |
| 2.1      | Modelling procedures in the landslide community (EPFL)                                      | 6         |
| 2.1.1    | <i>Numerical modelling for landslide problems</i>   | 6         |
| 2.1.2    | <i>Interdisciplinary process of landslide modelling</i>                                     | 6         |
| 2.2      | Conceptual modelling of slope-relevant processes  | 8         |
| 2.2.1    | <i>Physical processes in landslides subjected to rainfall infiltration (EPFL)</i>           | 9         |
| 2.2.2    | <i>Hydraulic concepts for landslide modelling (UNISA)</i>                                   | 11        |
| 2.2.3    | <i>Mechanical concepts for landslide modelling (FUNAB)</i>                                  | 16        |
| 2.2.4    | <i>Hydro-mechanical couplings (UPC)</i>   | 21        |
| 2.2.5    | <i>Requirements for numerical codes (EPFL)</i>  | 25        |
| 2.3      | Input data for numerical models from site investigations, field and laboratory tests (AMRA) | 34        |
| 2.3.1    | <i>Monitoring for selection of appropriate initial conditions</i>                           | 34        |
| 2.3.2    | <i>Hydraulic properties</i>   | 34        |
| 2.3.3    | <i>Stiffness and strength properties</i>  | 36        |
| 2.4      | Guidelines for the use of numerical codes   | 38        |
| 2.4.1    | <i>Numerical modelling methods used in the landslide community (EPFL)</i>                   | 38        |
| 2.4.2    | <i>Preprocessing for numerical simulations (UPC)</i>  | 39        |
| 2.4.3    | <i>Numerical issues in transient slope analysis (FUNAB)</i>                                 | 41        |
| 2.4.4    | <i>Postprocessing: output data and analysis of results (CNRS)</i>                           | 46        |
| 2.5      | Use of numerical codes for landslide early-warning and long-term predictions (EPFL)         | 50        |
| <b>3</b> | <b>Performance of numerical codes</b>   | <b>52</b> |
| 3.1      | Performance check of codes for slope scale analysis (EPFL)                                  | 52        |
| 3.2      | Performance check of codes for regional scale analysis (UNISA)                              | 56        |
| <b>4</b> | <b>Conclusions</b>  | <b>65</b> |
| <b>5</b> | <b>References</b>   | <b>66</b> |

## 1 CHALLENGES IN NUMERICAL MODELLING OF LANDSLIDES

The numerical modelling of landslides is part of a multidisciplinary process, starting from in-situ investigations and continuous measurements to identify the landslide and its behaviour as a function of external, climatic factors and its geological and hydrogeological structure. Laboratory tests are conducted to determine in more detail the behaviour of the geomaterials composing the landslide. A geological model is built based on the available field data which allows characterising the landslide in more detail. Governing mechanisms are identified or at least hypotheses on possible mechanisms are formulated. In some cases, eventually the cause of the instability is determined. The geological and geotechnical characterisation of the landslide is important for the following modelling steps. The choice of adequate constitutive models for soils and rocks for the numerical modelling depends on the knowledge and lessons gained from the geological model and the field- and laboratory tests conducted on the different geomaterials. The actual process of numerical modelling itself is subject of technical issues related to the codes and calculation methods, the translation of geological and geotechnical input data into the model and the assumptions made based on geological and engineering expertise. Finally the results from the numerical models can help in understanding the role of different complex physical processes in each specific case study. They complete or revise the first output of the geological expertise. In some cases, they identify critical issues which result in further, more detailed and precise site investigations. The complete modelling process is subsequently reiterated. Of course, the results from numerical models need to go through a post-processing where engineering expertise is again an important factor for the correct output evaluation. Once the model is judged trustworthy based on a validation process, it can be used to simulate the landslide behaviour under variable environmental conditions in order to assess its susceptibility to accelerate and eventually fail. In the same way, a valuable assessment can be given on the efficiency of construction measures for risk mitigation.

This deliverable aims at addressing key issues in numerical modelling of climate-induced landslides and at providing general guidelines for the use of numerical codes for landslide modelling. Numerical models for landslide initiation and propagation have been strongly developed in the geotechnical community over the past 20 years and entered largely into the practicing engineering community hand in hand with the increasing capacities of personal computers. They serve engineers as useful tools for the qualitative and quantitative analysis of complex boundary value problems to which landslides belong.

Many model types exist and are used in the SafeLand community (c.f. deliverable D1.2) for different types of landslides and related phenomena. In the second chapter, the reader is given an overview of the classes of modelling tools and procedures for landslide analysis. The understanding of their physical and mathematical frameworks and basic assumptions are important pre-requisites in order to be able to choose an adequate model for a particular landslide problem. At this end, a synthesis on the conceptual modelling of slope-relevant processes is presented. First, physical mechanisms encountered in landslides subjected to external climate factors are recalled. Second, the general hydraulic and mechanical concepts for landslide modelling are presented, as well as the mathematical framework for the introduction of hydromechanical coupling processes in numerical codes.

Geotechnical site investigations, field- and laboratory tests are useful for characterising the involved geomaterials and are necessary for determining the parameters of the constitutive models. As evoked before, the landslide expertise is an iterative process where often the numerical model needs supplementary, more detailed information based on a first run of

analysis. At this end, a synthesis of field investigation methods, field- and laboratory tests and more precisely the inputs they can provide for numerical models is presented.

Guidelines for the different steps in geomechanical, finite element modelling of landslides are provided. Typically, finite element codes are composed of a pre-processor where the problem is defined, a finite element processor and a post-processor for reading the output results. Critical issues involved in each of the three steps are discussed. In order to capture various key physical mechanisms in landslide processes, the numerical codes need to fulfil a certain number of conceptual modelling requirements. The relation between the conceptual modelling requirements and the physical landslide mechanisms is presented in a clear table format and is intended to support the modeller in selecting the necessary ingredients so that he can subsequently choose an adequate numerical code.

Modelling tools for qualitative and quantitative analyses and forward predictions of potentially unstable slopes are frequently used in engineering expertise, but they are still not used as part of modern early-warning systems. Indeed, early-warning systems based on critical threshold values of rainfall and landslide displacement rates or other sensor measurements are well known and relatively simple to implement in practice and seem to be the only reasonable measure to alert in the case of superficial instability processes (i.e. soil slips and debris flows), but their accuracy and effectiveness for risk mitigation in cases of large, slow moving landslides with recurrent reactivation phases is questionable. In this sense, chapter four opens a discussion on the subject of early-warning systems and their enhancement with deterministic and statistical, computational methods. Perspectives for future developments in geotechnical monitoring are suggested, considering in particular developments in structural and system monitoring which have been made in other engineering disciplines.

The third chapter gives an overview of the different numerical codes for slope- and regional-scale analyses used in the SafeLand community and their modelling components. The performance check of the codes allows the user to identify useful tools for a particular analysis.

## **2 KEY ISSUES IN NUMERICAL MODELLING OF CLIMATE INDUCED LANDSLIDES**

### **2.1 MODELLING PROCEDURES IN THE LANDSLIDE COMMUNITY (EPFL)**

#### **2.1.1 Numerical modelling for landslide problems**

Landslides are manifold in types and behaviours (c.f. deliverable D1.1). Their kinematics vary from slow moving (cm/y) to fast moving landslides (m/s) and their volumes vary from a couple to several million cubic meters. They have a distinct time history and involve different kinds of geomaterials, from fine clays and granular soils to jointed rocks. Shallow slips and debris flows are most often triggered during heavy rainfall or snow melt and affect superficial soil layers in mostly steep slopes. Large landslides display most often continuous displacements with possible reactivation phases during which displacement rates may strongly increase. Whereas in the case of shallow slips and debris flows it is mostly dealt with first-time failures, deep-seated landslides commonly have a long history of movement. The kinematics of both, shallow and deep-seated landslides is most often governed by climatic conditions influencing the hydraulic regime and the mechanical response of the slope. In order to cope with the tremendous variety, the material and structural complexity of landslides, numerical models have been developed.

Too often, analytical solutions are oversimplifying the problem and missing key physical processes in natural slopes due to the numerous assumptions related to material behaviour and problem geometry that have to be made. The aim of the numerical modelling tools is to gain insights in the complex behaviour of instable or potentially instable slopes and to present that information in understandable form. Based on physical concepts of the mechanical or hydromechanical behaviour of geomaterials and more advanced geological representations of the landslide problem, the numerical codes basically aim at simulating the slope behaviour as a consequence of external hydraulic and/or mechanical perturbations or variations of time-dependent internal variables (damage, aging, etc.). The numerical codes presented in deliverable D1.2 and frequently used in the geomechanical community are based on deterministic, physical models. In recent years, more and more statistical concepts are combined with the deterministic codes in order to cope with imprecision and uncertainties related to material properties and their spatial distribution. The guidelines for the use of numerical codes in this deliverable focus however on the commonly used deterministic numerical models which are briefly recalled and classified in section 2.4.1.

Geomechanical models are useful tools for evaluating the stability of potentially instable slopes, but also for predicting future slope behaviour for different climate scenarios. In consulting expertise, they are often used to assess the effectiveness of planned constructive remedial measures or the likelihood for mass acceleration and subsequent damaging effects on infrastructures in the case of generally slow moving landslides sensitive to certain rainfall events. These geomechanical modelling tools occupy an essential part in the quantitative risk assessment of landslides and help understanding the underlying physical processes in natural slopes.

#### **2.1.2 Interdisciplinary process of landslide modelling**

Numerical modelling is not a standalone process, but rather joins an interdisciplinary process involving geologists, hydrologists and engineers (Figure 1). The general landslide problem definition is subject of preliminary geological models. These models allow identifying mechanisms of instability and defining the geometry and geological structure of natural slopes

which serve as basic source for the definition of problem geometry, spatial variations of material layers and for a rough, first choice of constitutive models in numerical codes. The accuracy of the numerical model depends mainly on the accuracy of the geological model which on its turn depends on the efforts invested for acquiring field information. It has to be kept in mind that the geological model itself is already a conceptualised, simplified representation of the reality (process A in figure 1). The understanding of the overall geological structure, the hypotheses on mechanisms and instability driving factors in the slope form the basic guidelines for the engineer performing the numerical modelling part. Due to the complexity of most landslides and the limitations of numerical models, only some aspects can be analysed at once. The choice of the numerical modelling strategy and the most important factors to consider is strongly based on the expertise gained from the geological model (process B in figure 1).

Many components of the geological model are more qualitative than quantitative. They may be classified in 4 categories:

1. Structure
  - Slope geometry,
  - Structural units of the region (i.e. fault orientation, joints or discontinuities, etc.),
  - Tectonics of the area (formation of the massif, initial stresses, etc.)
  
2. Geomaterial
  - Classification of involved geomaterials,
  - Basic material properties from field and simple laboratory tests (i.e. porosity,

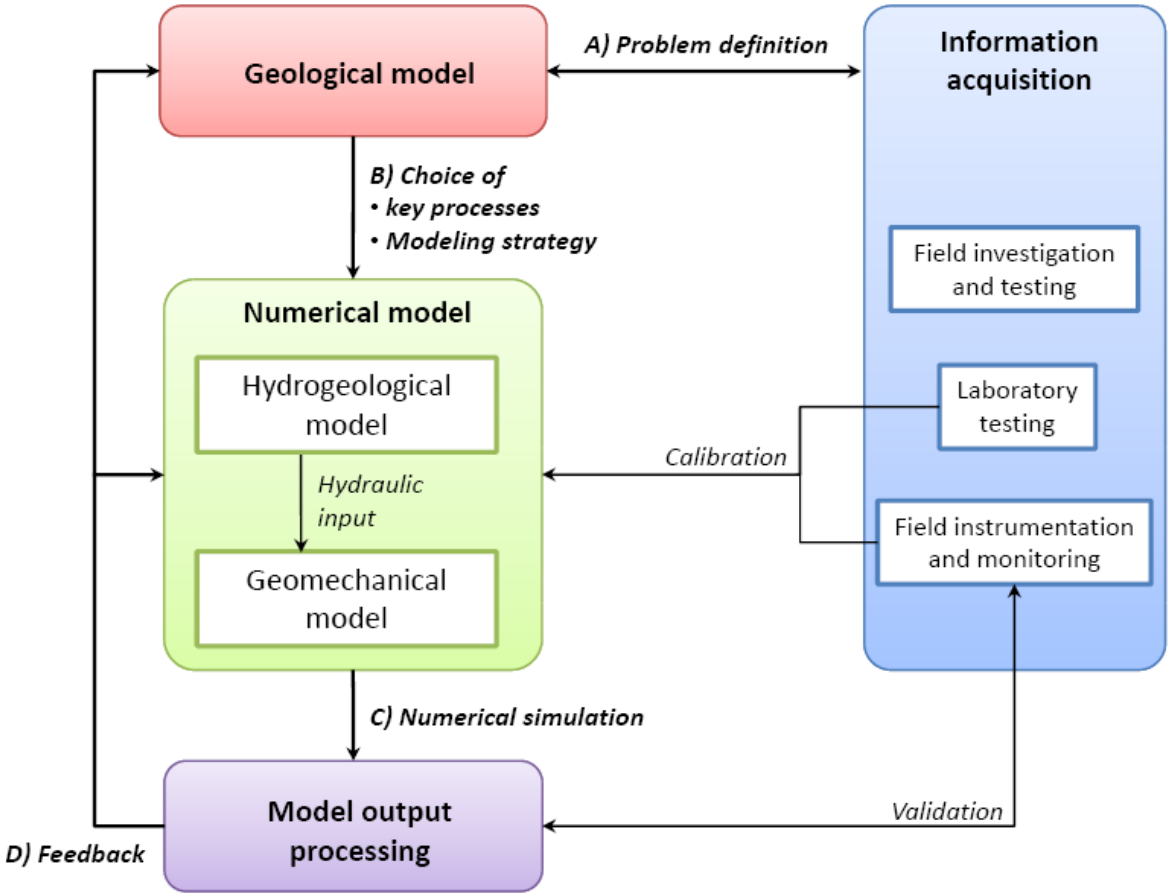


Figure 1: Interdisciplinary, iterative process of landslide modelling

- relative density, shear strength, stiffness),
  - Basic mechanical properties of rock joints
3. Movement
- Geomorphologic features (glacier erosion, river toe erosion, scarps, etc.),
  - Information from monitoring data on recent movements (i.e. surface and inclinometer measurements)
4. Hydrology/Hydrogeology
- Groundwater/Subsurface regime (pore pressures, flow rates, permeabilities, preferential flowpaths, moisture contents, etc.),
  - Surface regime (i.e. runoff, infiltration rates, etc.),
  - Climatic conditions (i.e. rainfall patterns, snow melt, temperature, humidity, etc.)

Geomechanical models of landslides, especially the more sophisticated ones, need to be fed with a large number of hydraulic and mechanical input parameters and their response depends strongly on imposed initial and boundary conditions. Consequently, they rely firstly on the geological and geotechnical reconnaissance of the landslide and secondly on a number of adequate material tests and field measurements in order to determine and quantify the key physical parameters. The mechanical response of natural slopes is most often governed by the subsurface hydraulic regimes which depend on time-dependent variations of subsurface flows and rainfall infiltration. Thus, special care must be taken to the hydrological aspects when modelling weather-induced landslides. Hydrogeological, numerical models are very often used separately to infer appropriate initial and boundary hydraulic conditions and to provide geomechanical models with calibrated hydraulic conductivity fields and time series of pore pressure fields (see also section 2.2.2). The numerical analysis is always subject of specific numerical problems related to the employed method and the problem type (process C in figure 1). Detailed procedures for the numerical analyses of the transient slope stability are presented in section 2.4.3.

Output results obtained from numerical models may confirm qualitatively assumed behaviour and key processes in a landslide and quantify them. Very often, numerical simulations reveal critical mechanisms and landslide critical rainfall scenarios which haven't been pointed out in precedent geological analyses. In this sense, numerical models can really be seen as a complementary tool for landslide expertise. The results of numerical simulations may also point out issues which deserve further detailed geological and geotechnical investigation (process D in figure 1). In this case, the whole process from data acquisition to numerical simulations is reiterated. By exploiting all possible scenarios of climate change, numerical simulations offer in the framework of risk management valuable information to define preventive measures and support advanced early warning systems.

## **2.2 CONCEPTUAL MODELLING OF SLOPE-RELEVANT PROCESSES**

Numerical models solve the landslide boundary value problem via integration of the discretized physical time and space problem for which a mathematical framework is formulated, and appropriately defined boundary and initial conditions. The construction of the mathematical framework including geomaterial constitutive models is a process of conceptualisation of the real physical problem. It consists of idealisations and simplifications and therefore contains always limitations. This section presents first the physical processes

that have been identified in different types of landslides. The following sub-sections present the different mathematical concepts on which the numerical codes are based, and finally these concepts are used to formulate requirements for adequate process modelling.

### **2.2.1 Physical processes in landslides subjected to rainfall infiltration (EPFL)**

There are various physical processes in soil slopes leading to failure. This section addresses the different features and physical processes separately for shallow slips and flow-type failures and deep-seated, generally slow-moving landslides. The mathematical, geomechanical code requirements which result from the different landslide features and physical processes are presented separately in section 2.2.5.

#### ***2.2.1.1 Shallow slips and flow-type failures***

Shallow slips and flow-type failures are without any doubt the most frequently triggered types of landslide. They are most often triggered during heavy rainfalls of short duration and are commonly encountered in steep slopes with angles higher than 25° (Iverson et al. 1997). Other than natural causes, anthropogenic factors play an important role in the triggering process as well (see deliverable D1.6). Failure takes most often place in 1 to 2 meters depth as a direct consequence of rainfall infiltration in initially partially saturated soils. Their volumes and kinematic features are however highly variable, depending on site conditions, material type and their morphological history.

The following list attempts to summarise particular features and processes related to these shallow landslides:

- *Majority of first-time failures*  
At some point during rainfall infiltration, slow, downward slope movements start to develop. Deformations localise in some cases to form narrow bands of high soil distortion and fracturation, in others they are observed to be distributed in a diffuse manner in the whole soil slope and become noticeable as surface settlements.
- *Steep slopes*  
Shallow slips and debris flows mostly occur in steep slopes where a water table is absent and the slope angle exceeds the internal friction angle. The stability prior to a catastrophic event is mainly sustained due to the positive capillary effects.
- *Partial saturation*  
The voids in the solid skeleton are filled at the same time with water and air in variable quantities. The degree of water or air saturation changes primarily as a function of external climate conditions. Depending on how much water fills the voids, the flow of water through the soil is more or less facilitated. At low degrees of water saturation, air fills the majority of the voids and minor water flow takes place along the grain surfaces. In contrary, if the degree of water saturation is high, the liquid phase occupies the majority of the voids and the flow is facilitated due to the continuity of the liquid phase throughout the porous medium.  
Liquid and gas phase have their own pressures and form curved interfaces, else known as contractile skins (Fredlund and Rahardjo 1993). These “menisci” between the grains depend on the water pressure relative to the air pressure and the size of the voids. They interact with the soil particles by exerting attracting forces for which a quantitative measure at macroscopic level called matric suction is defined. The higher the difference between air and water pressure, i.e. matric suction, the higher is the measured soil strength and stiffness.
- *Soil type and initial state*

Shallow slips and flow-type failures are observed in coarse and fine-grained deposits and residual soils. The soil composition is highly variable from well-graded to poorly-graded. Due to their genesis and shallow depths, stresses are rather low in the shallow soil covers and the soils are often in a loose or medium dense state. Especially loose and poorly-graded soils have a collapsible nature. They show high losses of volume due to slight perturbations of the stress state and are prone to flow-type failures. Denser soils dilate upon shearing and often develop into slip failures where blocks of soil move over a distinct sliding surface.

- *Strong local material heterogeneities*  
Shallow failures involve mostly small volumes of soil (couple of tens to hundreds of cubic meters). Site-related factors play an important role for the predisposition of a slope to fail. These factors include soil roots and the presence of multiple soil layers leading to preferential failure zones due to contrasts in mechanical properties and permeability which create preferential flow paths and govern the evolution of pore pressures (Johnson and Sitar 1990).
- *Strong relation between surface and subsurface processes*  
Shallow failures are directly related to external climate factors (rainfall, snow melt, temperature). Hydrological processes are the first link in the chain of processes leading to failure. These processes include water infiltration into soil, evaporation/evapotranspiration and run-off generation.
- *Post-failure kinematics*  
The mass transport after failure is of variable nature. Some slope failures end up in slow-moving slips with short run-out distances, others into extremely rapid fluid-like landslides moving over long distances.

### **2.2.1.2 Deep-seated landslides**

Large landslides present typically a volume of more than 1 million cubic meters. Slope angles for these types of slides in Switzerland are typically between 10° and 20°, with higher angles in alpine regions (Vulliet 1986). Due to their large extent (several km<sup>2</sup>) they show very often significant hydraulic and mechanical heterogeneities leading to different movement patterns within the sliding body. Large landslides are gravity-driven processes which are typically in a state of more or less constant movement with possible reactivation phases. They show however considerable differences among each other with respect to their velocities. Slow-moving landslides may reach velocities up to 1.6m/year and rapid-moving landslides reach velocities higher than 1.8m/h (Cruden and Varnes 1996; WP-WLI 1995).

The following list presents some relevant features and processes in deep-seated landslides:

- *Majority of post-glacial slides with reactivation phases*  
Slow-moving landslides are mostly encountered in regions which have been subjected to a relatively fast deglaciation period. Most large landslides have been moving for thousands of years. In most cases, movement takes place along pre-existing slip surfaces. The movement pattern is generally regular, but longer wet periods can lead to acceleration phases.
- *Groundwater fluctuations*  
Climatic conditions are the main factors for changing movement activity, even if the variations of the hydrogeological and climatic conditions are in most cases not very marked (Castelli et al. 2009). Large landslides present commonly a groundwater table primary subjected to seasonal fluctuations. Pore pressures along the failure plane are mostly positive. Fracture flow can play an important role in the hydrogeological

system of the landslide. In the case of first-time failures, exceptional climate conditions are often the cause of instability.

- *Kinematic features*

Slow-moving landslides are slides which have either experienced progressive displacements over long time periods and are still active or went through a fast episode of movement in the past and now are only affected by residual movements. Such creeping behaviour (2-5mm/year) is in some cases associated to displacements due to seasonal groundwater table fluctuations (Alonso et al. 2003; Picarelli et al. 2004) and in other cases is told to be little affected by external events (Macfarlane 2009).

For cases of first time failure, rapid movements may arise for example from a sudden decrease in shear strength, as encountered in brittle materials such as fractured rock slopes or overconsolidated clays. In stiff clays, the progressive development of the failure surface decreases the average strength of the soil mass at collapse (Skempton 1964; Bjerrum 1967; Potts et al. 1997).

- *Changes in geometry and boundary conditions*

Very often, large landslides are affected by changes in geometry caused for example by toe erosion from a river.

## 2.2.2 Hydraulic concepts for landslide modelling (UNISA)

In order to model the water flow through an aquifer the groundwater flow equation needs to be integrated in the numerical code. Therefore, a mass balance for the fluid phase, along with Darcy's law, must be performed. The resulting groundwater flow equation is a diffusion equation describing the general case of transient flow.

Hydrogeological triggering is commonly known as one of the main natural landslide initiation mechanisms. Hydrogeological triggering can be generally defined as a decrease in shear strength due to an increase in pore-water pressure on the potential failure surface which finally results in a slope failure. Pore-water pressure increases may be directly related to rainfall infiltration and percolation (saturation from above) or may be the result of the build-up of a perched water table or a groundwater table (saturation from below). Whatever is the particular process, an adequate analysis of pore water pressure variations induced by changes in hydraulic boundary conditions is the key factor for the assessment of landslides' hydrogeological triggering.

In order to achieve this goal, the scientific literature proposes a variety of mathematical models that differ with reference both to the scale of analysis (i.e. local or regional) and to the adopted conceptual framework. In general, whatever is the scale of analysis, these models can be broadly grouped in the following three categories: "hydrogeological models", "hydrological models" or "black-box models", and "mixed-type models" (Cascini and Versace 1986; Cancelli et al. 1987, Sorbino 1994).

The first group includes models simulating the physical processes regulating seepage in porous media; the second group, models allowing the determination of mathematical relationships between some of the physical factors involved, overlooking strictly hydrogeological and geotechnical aspects; the third, models which, while taking account of some physical aspects of a given problem, employ calculations that are typical of the "hydrologic models".

As extensively discussed in Cascini (1996), it is neither possible nor profitable to determine which is the best among several available models or approaches. It is, vice versa, important to choose the most appropriate model to deal with the particular problem under examination, taking into account the quality as well as quantity of available experimental data, and the objectives to be attained. Due to the objectives of the present deliverable, in the following attention will be focused on the hydrogeological models and, particularly, on the differential equations governing the flow of fluids through porous media.

### 2.2.2.1 Mathematical Framework

Soils and rocks are geomaterials with voids which can be filled with water, air, and other fluids. They are, therefore, multiphase materials, exhibiting a mechanical behaviour governed by the coupling between all the phases. Pore pressures of fluids filling the voids play a paramount role in the behaviour of a soil structure, and indeed, their variations can induce the attainment of failure conditions leading to the onset of landslides.

In order to properly reproduce the interactions among the different phases, it is necessary to use: 1) a mathematical model describing the coupling between pore fluids and soil skeleton; 2) a suitable constitutive relationship able to describe the soil behaviour; and 3) a numerical model where 1) and 2) are implemented.

To the authors' knowledge, these have not been done yet in a full satisfactory manner, and until such tools are available, simplified models have to be carefully used. Hereafter, a mathematical framework is described mainly derived from the fundamental contributions of Zienkiewicz et al. (1980, 1999).

It is assumed that the soil (mixture) consists of a solid skeleton and two fluid phases, water and air, which fill the voids. The skeleton is made of particles of density  $\rho_s$  with porosity  $n$  (volume percent of voids in the mixture) and void ratio  $e$  (volume of voids per unit volume of solid fraction). If water ( $w$ ) and air ( $a$ ) have a density  $\rho_w$  and  $\rho_a$  respectively and they are assumed not miscible, it is possible to define the density  $\rho^{(\alpha)}$  of the phase  $\alpha$  ( $\alpha = w, a$ ) as:

$$\rho^{(\alpha)} = nS_{r\alpha}\rho_\alpha \quad (2.2.2.1)$$

where  $S_{r\alpha}$  represents the degree of saturation of the phase  $\alpha$  (i.e. the volume of voids occupied by it).

The density of the solid skeleton is thus defined by:

$$\rho^{(s)} = (1-n)\rho_s \quad (2.2.2.2)$$

and the density of the mixture  $\rho$  is given by:

$$\rho = \rho^{(s)} + \rho^{(w)} + \rho^{(a)} \quad (2.2.2.3)$$

If  $v^{(\alpha)}$  and  $v^{(s)}$  are the velocities of the phase  $\alpha$  and of the solid, it is possible to define for each phase the velocity relative to the soil skeleton. This so-called Darcy's velocity  $w^{(\alpha)}$  of phase  $\alpha$  is given by:

$$w^{(\alpha)} = nS_{r\alpha}(v^{(\alpha)} - v^{(s)}) \quad (2.2.2.4)$$

As for the stresses, by defining the tensile stresses as positive and assuming the solid grains as incompressible, it is possible to define the effective stress tensor  $\sigma'$  as:

$$\sigma' = \sigma + I\bar{p} \quad (2.2.2.5)$$

where  $\sigma$  is the total stress tensor acting on the mixture,  $I$  is the second order identity tensor and  $\bar{p}$  is the averaged pore pressure defined by:

$$\bar{p} = S_{rw}P_w + S_{ra}P_a \quad (2.2.2.6)$$

Once the above quantities are defined, the mathematical framework for analysing the coupling between pore fluids and soil skeleton can be derived by imposing the conservation of the mass and momentum for the phases and the mixture.

The mass balance of the solid skeleton and fluid phases are given by:

$$\begin{aligned} \frac{D^{(s)}}{Dt} [(1-n)\rho_s] + (1-n)\rho_s \operatorname{div} v^{(s)} &= 0 \\ \frac{D^{(\alpha)}}{Dt} (nS_{r\alpha}\rho_\alpha) + nS_{r\alpha}\rho_\alpha \operatorname{div} v^{(\alpha)} &= 0 \end{aligned} \quad (2.2.2.7)$$

The balance of mass equation of the mixture can be obtained by adding the mass balance equations of all the phases, leading to the following equation:

$$\frac{D^{(s)}}{Dt} \rho + \rho \operatorname{div} v_s + \sum_{\alpha=1}^{N_\alpha} \operatorname{div} (\rho_\alpha w_\alpha) = 0 \quad (2.2.2.8)$$

The balance of momentum for the solid phase is represented by the equation:

$$\rho_s \frac{D^{(s)} v^{(s)}}{Dt} = \rho_s b + \operatorname{div} \sigma_s + R_s \quad (2.2.2.9)$$

where  $R_s$  is the term representing the drag forces due to all fluid phases and  $b$  is the body forces vector.

As for the fluid phases, the balance of momentum is furnished by:

$$\rho_\alpha \frac{D^{(\alpha)} v^{(\alpha)}}{Dt} = \rho_\alpha b + \operatorname{div} \sigma_\alpha + R_{s\alpha} \quad (2.2.2.10)$$

where  $R_{s\alpha}$  is the drag force representing the interaction between the solid skeleton and the pore fluid  $\alpha$ .

The term  $R_{s\alpha}$  can be assumed to follow Darcy's law, so obeying to the equation:

$$R_{s\alpha} = -\frac{1}{\bar{k}_\alpha} w^{(\alpha)} \quad (2.2.2.11)$$

In above,  $\bar{k}_\alpha$  is the permeability matrix for the phase  $\alpha$ , and it is defined by:

$$\bar{k}_\alpha = \frac{k_{r\alpha} K^{\text{int}}}{\mu_\alpha} \quad (2.2.2.12)$$

where  $k_{r\alpha}$  is the relative permeability of the phase  $\alpha$  which depends on  $S_{r\alpha}$ ,  $\mu_\alpha$  is the dynamic viscosity of the phase  $\alpha$  and  $K^{\text{int}}$  is the intrinsic permeability matrix. It should be noted that the permeability defined by eq. (2.2.2.12) has dimensions  $L^3 T/M$ . In geotechnical engineering, the permeability is more frequently defined in a slight different way that is linked to the equation (2.2.2.12) by the relation:

$$k_\alpha = \rho_\alpha b \bar{k}_\alpha \quad (2.2.2.13)$$

with dimensions of L/T.

By introducing the property of the material derivative of a magnitude  $\xi$ , i.e.:

$$\frac{D^{(\alpha)}\xi}{Dt} = \frac{D^{(s)}\xi}{Dt} + (v^{(\alpha)} - v^{(s)})grad\xi = \frac{D^{(s)}\xi}{Dt} + \frac{w^{(\alpha)}}{nS_{r\alpha}}grad\xi \quad (2.2.2.14)$$

and taking into account of the relations (2.2.2.11) and (2.2.2.12) equation (2.2.2.10) can be written as:

$$\rho_{\alpha} \left( \frac{D^{(s)}v^{(s)}}{Dt} + c.t. \right) = \rho_{\alpha}b + div\sigma_{\alpha} - \frac{1}{\bar{k}_{\alpha}}w^{(\alpha)} \quad (2.2.2.15)$$

where the correcting term  $c.t.$  is given by:

$$c.t. = \frac{D^{(s)}}{Dt} \left( \frac{w^{(\alpha)}}{nS_{r\alpha}} \right) + \frac{w^{(\alpha)}}{nS_{r\alpha}}gradv^{(s)} + \frac{w^{(\alpha)}}{nS_{r\alpha}}grad \left( \frac{w^{(\alpha)}}{nS_{r\alpha}} \right) \quad (2.2.2.16)$$

The balance momentum of the mixture can be derived by adding equation (2.2.2.9) and equation (2.2.2.15) for each of the fluid phases, so obtaining:

$$\rho \frac{D^{(s)}v_s}{Dt} + c.t.1 = \rho b + div\sigma + c.t.2 \quad (2.2.2.17)$$

where the correcting terms are given by:

$$c.t.1 = \sum_{\alpha=1}^{N_{\alpha}} nS_{\alpha}\rho_{\alpha} \left\{ \frac{D^{(s)}}{Dt} \left( \frac{w_{\alpha}}{nS_{\alpha}} \right) + \frac{w_{\alpha}}{nS_{\alpha}}gradv_s + \frac{w_{\alpha}}{nS_{\alpha}}grad \left( \frac{w_{\alpha}}{nS_{\alpha}} \right) \right\} \quad (2.2.2.18)$$

and

$$c.t.2 = \sigma_s \cdot grad n - \sum_{\alpha=1}^{N_{\alpha}} \sigma_{\alpha} \cdot grad(nS_{\alpha}) \quad (2.2.2.19)$$

Once defined suitable constitutive or rheological laws aimed to determine the state of stress for all constituents, the above mass and momentum balance equations allow modelling the mechanical coupling among the soil particles and the pore fluids when the movement of both solid and fluid phases is relevant (Pastor et al. 2004). This is, for instance, the case of the propagation phase of catastrophic fast slope movements like debris-flows, rock avalanche, mudslide, and so on.

### 2.2.2.2 Modelling alternatives

The above general equations can be rewritten in a simpler manner if some hypotheses are introduced. Particularly, if it is assumed that pore air pressure is constant and equal to the atmospheric pressure, and that relative velocities and accelerations of fluids relative to solid skeleton are small, the general equations of the previous paragraphs can be cast in terms of velocity of the solid skeleton and Darcy's velocities of pore water. By adopting these hypotheses, the averaged pore pressure defined by the equation (2.2.2.6) reduces to:

$$\bar{p} = S_{rw}p_w \quad (2.2.2.20)$$

and the effective stress tensor to the equation:

$$\sigma' = \sigma + S_{rw}p_w I \quad (2.2.2.21)$$

By neglecting the acceleration of water relative to soil grains the balance of momentum equation for the mixture (2.2.2.15) can be written as:

$$\operatorname{div}(\boldsymbol{\sigma}' - \bar{p}\mathbf{I}) + \rho \mathbf{b} = \rho \frac{d\mathbf{v}}{dt} \quad (2.2.2.22)$$

while, the balance momentum of the pore water (2.2.2.15) becomes:

$$\operatorname{grad} p_w + \rho_w \mathbf{b} - \frac{1}{k_w} \mathbf{w} = \rho_w \frac{d\mathbf{v}}{dt} \quad (2.2.2.23)$$

As for the balance of mass for the water, the following volume deformations  $d\vartheta_i$  in the mixture are considered:

a) Deformation of soil skeleton:

$$d\vartheta_1 = S_{rw} \operatorname{tr}(d\boldsymbol{\varepsilon}) = S_{rw} d\varepsilon_v \quad (2.2.2.24)$$

where  $d\boldsymbol{\varepsilon}$  is the increment of the strain tensor,  $\operatorname{tr}$  denotes the trace operator and  $d\varepsilon_v$  is the increment of volumetric strain.

b) Increase in water storage:

$$d\vartheta_2 = n dS_{rw} = \frac{\partial S_{rw}}{\partial p_w} dp_w = C_s dp_w \quad (2.2.2.25)$$

c) Deformation of pore water induced by pore pressure:

$$d\vartheta_3 = \frac{n S_{rw}}{K_w} dp_w \quad (2.2.2.26)$$

where  $K_w$  is the volumetric stiffness of pore water.

d) Deformation of soil grains caused by pore pressure:

$$d\vartheta_4 = \frac{1-n}{K_s} d\bar{p} = \frac{1-n}{K_s} \left( S_{rw} + p_w \frac{C_s}{n} \right) dp_w \quad (2.2.2.27)$$

where  $K_s$  is the volumetric stiffness of soil particles.

Taking account of the above volume deformations in the mixture, the mass balance of the pore water given by eq. (2.2.2.7) can be rewritten as:

$$\operatorname{div} \mathbf{w} + \frac{1}{Q^*} \frac{dp_w}{dt} + S_{rw} \operatorname{tr} \left( \frac{d\boldsymbol{\varepsilon}}{dt} \right) + C_s \frac{\partial p_w}{\partial t} = 0 \quad (2.2.2.28)$$

where

$$\frac{1}{Q^*} = \left[ \frac{n S_{rw}}{K_w} + \frac{1-n}{K_s} \left( S_{rw} + p_w \frac{C_s}{n} \right) \right] \quad (2.2.2.29)$$

Balance of mass and momentum of the pore water can be combined leading to the following equation:

$$\left( C_s + \frac{1}{Q^*} \right) \frac{dp_w}{dt} + S_{rw} \operatorname{div} \mathbf{v} - \operatorname{div}(k_w \operatorname{grad} p_w) = 0 \quad (2.2.2.30)$$

where the term  $\text{div}(-\rho_w b + \rho_w dv/dt)$  has been neglected assuming that body forces are independent by space coordinates and the space derivative of accelerations are assumed to be small. Equations (2.2.2.22) and (2.2.2.30) have to be complemented by a kinematic relation linking velocities to rate of deformation tensor, and a suitable constitutive or rheological law.

This simplified coupled stress-strain model have been recently used for simulating the failure stage of earthquake-induced landslides of the flow-type (Fernandez-Merodo et al. 2004; Pastor et al. 2004) and for the propagation stage of rainfall-induced landslides of the flow-type (Pastor et al. 2008). Indeed, it could be profitably used for the simulation of the failure and postfailure stages of landslides of the flow type. However, advanced constitutive models have to be used to reproduce postfailure phenomena such as liquefaction (Sladen et al. 1985; Chu et al. 2003) and instability phenomena (Darve and Laouafa 2000). Since the failure and postfailure stages of the landslides can be generally separately addressed, a more simplified versions of this model can be usefully derived, aimed to their application in case only the failure stage is of concern.

Indeed, within the same mathematical framework, an uncoupled stress-strain model can be obtained based on further simplifying assumptions. Particularly, if the deformation rate can be neglected without appreciable errors and if water and grain compressibility are assumed as negligible, equation (2.2.2.30) finally reduces to:

$$C_s \frac{dp_w}{dt} - \text{div}(k_w \text{grad} p_w) = 0 \quad (2.2.2.31)$$

Equation (2.2.2.31) is the well-known Richards' equation governing transient water flow through a rigid fully saturated or saturated-unsaturated porous media. For the numerical integration of Richards' equation it is necessary to provide the soil-water characteristic curve (i.e. the functional relationship between soil suction ( $p_a - p_w$ ) and the saturation degree ( $S_{rw}$ )), as well as the permeability function  $k_w = k_w(S_{rw})$  of the medium.

Once the appropriate initial and boundary conditions of the integration domain have been defined, the spatial and temporal variation of pore-water pressures  $p_w$  can be computed through the numerical resolution of (2.2.2.31).

From equation (2.2.2.22), by neglecting the deformation rate, we obtain:

$$\text{div}(\sigma' - \bar{p}I) + \rho b = 0 \quad (2.2.2.32)$$

from which the state of stress can be computed based on known pore-water pressures  $p_w$ . Finally, deformations and displacements are computed through a suitable constitutive equation of the soil skeleton.

It should be noted that by adopting the above equations, the averaged pore pressure  $\bar{p}$  influences the mechanical behaviour but, in turn, the latter does not influence the former. Consequently, the uncoupled model can be usefully applied for the simulation of the failure stages of both slides and slides turning into flows only if drained conditions are assumed.

## 2.2.3 Mechanical concepts for landslide modelling (FUNAB)

### 2.2.3.1 Introduction

A landslide can be considered as the failure of a geostucture. Indeed, modelling of landslides presents the same difficulties found when analyzing failure of geomaterials and geostuctures.

The study of failure conditions has attracted the attention of researchers since the early works of Coulomb (1773). Historically, three main lines of dealing with the problem and obtaining solutions were followed: (i) The slip line method, (ii) Limit theorems for plastic collapse, and (iii) limit equilibrium methods. All of them provide information on failure loads and mechanisms, but not on post failure phenomena. Since both, material behaviour and kinematics of failure are strongly variable from one landslide type to another, these simple methods of slope stability analysis cannot be applied in all cases as explained below.

Both, the limit theorems of plastic collapse and the limit equilibrium methods are based on two assumptions: (i) failure conditions takes place at the strength envelope, and (ii) there exists a surface where failure takes place. This corresponds to a type of failure which is referred to as “*localized*”. These conditions are not always satisfied, as observed in the case of loose, collapsible materials, where instability and failure take place at effective stresses below the Mohr Coulomb strength envelope, and where failure is observed to occur in a much larger volume of soil. This type of failure has been described as “*diffuse*”.

Localized failure is found in overconsolidated materials presenting softening, while the diffuse mode is typical of soils having a low relative density and a tendency to compact when sheared. Failure takes place not in a narrow limited zone, but in a much larger mass of soil. Rising pore pressures during rainfall events may cause a loss in shear strength leading to liquefaction of the soil or conditions close to it. This mechanism is believed to play an important role in landslides of the flow type.

Localized failure is characterized by a concentration of strain in very narrow and limited zones, where the phenomenon is idealized assuming there exists a discontinuity in the strain or its rate (weak discontinuity). In the case of soils, the most frequent case is that of discontinuities in the shear strain, which are referred to as shear bands. They can evolve into discontinuities in the displacement and velocity fields (strong discontinuity). Failure mechanism is interpreted as a relative sliding of two regions where deformations are small.

Diffuse failure is related to instabilities of material behaviour in loose soils. The study of these instabilities is still a young area of research. It is worth mentioning the work of Darve (1995) and Nova (1994) on constitutive instabilities and di Prisco et al. (1995) on the stability of shallow submerged slopes where liquefaction induced by sea waves can be triggered, and Darve and Laouafa (2000, 2001) and Fernández Merodo et al (2004) on diffuse mechanisms of failure in catastrophic landslides. An updated account of work done in this area can be found in Nicot and Wan (2008).

### **2.2.3.2 Basic mechanical concepts**

In all models used to describe and characterize failure we find the following ingredients: (i) a mathematical model describing the balance of mass and linear momentum for the soil skeleton and the pore fluids, (ii) a constitutive equation describing the behaviour of soil skeleton –and of its pore fluids-, and (iii) a numerical model where the mathematical and constitutive models are discretized.

The first ingredient describes the coupling between the different phases of the porous media which is dealt with in detail in section 2.2.4. The third ingredient will be analyzed in section 2.4.3 devoted to numerical issues in transient slope analysis. Here we will concentrate on constitutive modelling from the point of view of the modelling of landslide triggering.

We must point out that there exists many types of landslides, and some of them cannot be studied from a continuum mechanics point of view. In such cases, the slope is formed by blocks which may move relative to each other and discrete element method should be

favoured for modelling purposes. This section focuses on “localized” and “diffuse” mechanisms in the framework of continuum mechanics in order to relate them to the constitutive properties of the material.

Catastrophic landslides are characterized by an acceleration of the soil mass which is believed to be caused by a decrease of strength, which in turn is quite often related to “softening” of the material. However, it is important to precise what is really softening. Let us consider the following three triaxial tests: (i) Consolidated Drained behaviour of a dense sand, (ii) Consolidated Undrained behaviour of a very loose sand, and (iii) Consolidated Undrained behaviour of an overconsolidated clay. Figure 1 illustrates these cases.

In the figure, we have depicted: (a) deviatoric stresses versus axial strain, (b) stress paths on  $p'$ - $q$  space, and (c) the mobilized stress ratio ( $q/p'$ ) versus axial strain. If we assume that soil strength is of frictional nature, the stress ratio ( $q/p'$ ) is the determinant indicator for the analysis of the soil response. In all three cases shown in Figure 2, we can see that only the CD response of dense sand and the CU response of the slightly overconsolidated clay present a decrease of strength. On the contrary, the CU response of the very loose sand is characterized by a monotonically increasing stress ratio. However, the peak in deviatoric stress is much more important in the latter. The conclusion is that softening is not responsible for all fast landslides. The phenomenon of liquefaction needs to be considered as well. Therefore, liquefaction is in many occasions responsible for diffuse failure mechanisms and fast catastrophic landslides while softening can be associated with localized mechanisms such as planar or circular slides.

It is crucial to model the increase of pore pressures leading to liquefaction presented in loose or meta-stable deposits. Liquefaction of loose sands has been studied in detail during the last decades, but the collapse of meta-stable soils such as those of volcanic origin has received

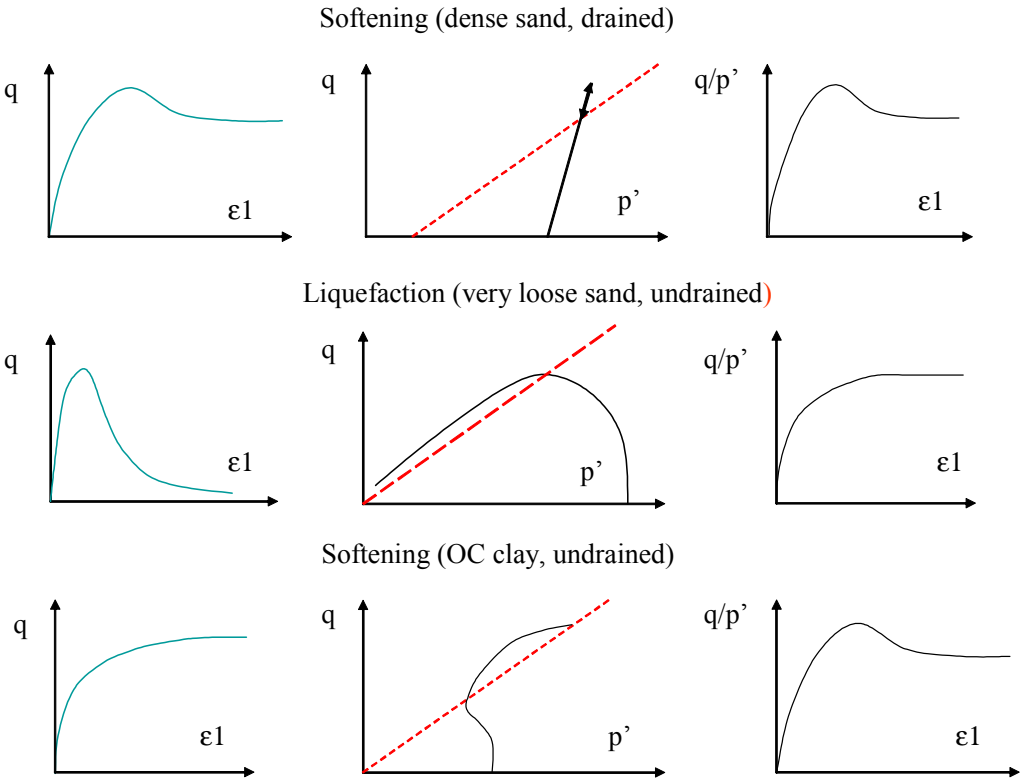


Figure 2: Softening of geomaterials

less attention from researchers. To illustrate the destructive power of landslides triggered in such soils, the case of El Salvador earthquakes of 2001 can be mentioned, where a large number of fast landslides were triggered. In that case, the soils were unsaturated even during the failure process. Long distances and velocities of propagation can be related to a collapse of soil structure causing a rise of the air pressure in the pores due to the soil's tendency to compact. Of course, time of pressure dissipation is small, but the landslide propagation times were smaller than 10 s.

### ***2.2.3.3 Classes of constitutive models for landslide modelling***

#### Failure loci

In many occasions, the behaviour of the material can be considered elastic up to failure. In that case, failure coincides with the plastic yield limit and there is no post-yield behaviour, that is to say no hardening or softening of the material. In addition to the elastic component, a simple yield criterion completes in that case the idealised description of a geomaterial as elastic-perfectly plastic. In addition to Coulomb, who in 1773 proposed the simple yet effective criterion which is still used today, we have the failure loci proposed by Tresca (1864) and Von Mises and Huber (1913), which are pressure independent.

In the family of pressure dependent yield surfaces, the Drucker-Prager (1952) surface is also very common. It can be viewed as an extension of the Mohr-Coulomb pyramid. The surface in the space of principal stresses is a cone.

Pressure independent loci can be applied only to purely cohesive soils in conditions of fast undrained loading. In general, it is much more reliable to perform a coupled analysis with a Mohr Coulomb or Drucker-Prager criterion.

One word of caution is worth addressing to the modeller dealing with the Mohr-Coulomb and Drucker-Prager failure criterion. As shown in Figure 3 in an isotropic plane, the Mohr Coulomb failure criterion represents a hexagon while that of Drucker-Prager is a circle. If the analyst is given the friction angle, he will have to choose a particular value of the Drucker Prager parameter controlling the cone angle in such a way that it coincides with the Mohr Coulomb criterion under specific conditions. It is possible to choose a cone coinciding with the outer vertexes of the hexagon, (outer cone), or with the inner (inner cone) or an intermediate position for plane strain problems. However, the choice of the outer cone results in higher friction angle in extension which in some cases may even be physically unreasonable.

#### Classical plasticity models

We will define by Classical Plasticity models those using yield surfaces which coincide with the failure loci. The size of the yield surface is controlled by the cohesion and the angle of friction in the case of Mohr Coulomb and Drucker-Prager criteria. The important point here is that softening can be introduced just by using suitable laws describing how these strength parameters decrease with the plastic deviatoric strain, for instance. In this way, localized failure can be reproduced.

Another important aspect influencing failure is the dilatancy angle, or in other words, the non associative nature of the plastic flow rule. An associated flow rule –yield surface coincides with the plastic potential- can be used for soils showing a highly dilatant behaviour. However, the use of an associated flow rule for a soil in undrained conditions at failure (i.e. constant volume during deformation) leads to decreasing pore pressures at yielding instead of developing large plastic strains.

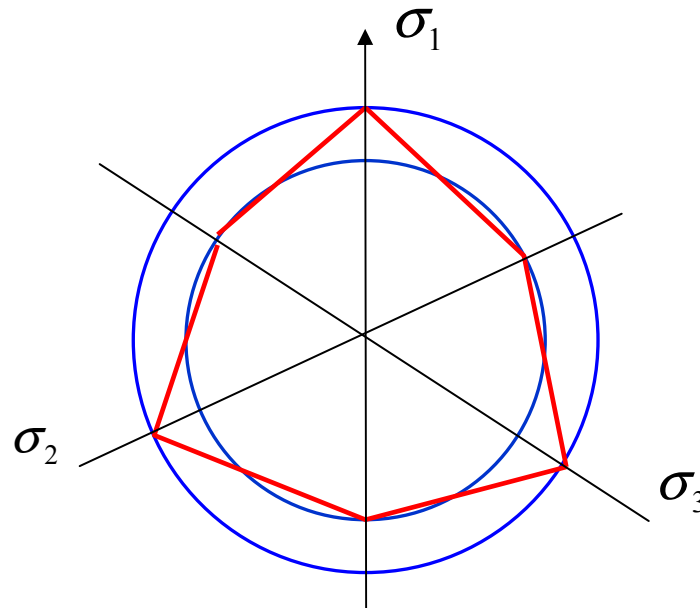


**Figure 3: Mohr-Coulomb pyramid and possible Drucker Prager cones in an isotropic plane. The choice of the outer cone for numerical modelling results in a higher friction angle in extension. In some cases the angle may reach physically unreasonable values.**

It is important to notice that classical plasticity models can provide an approximation to localized failure problems, but they will never be able to reproduce liquefaction or failure of loose meta-stable soils leading to diffuse, catastrophic mechanisms of failure.

### 3.3 Cam Clay based models

Most of the models used today in geotechnical engineering practice are based on the Critical State theory developed at Cambridge University in the period 1955 to 1968 (see for instance Roscoe et al. 1963).

The main ingredients of these models are: (i) there exists a state at which the soil flows once residual conditions have been reached (ii) the observed soil behaviour can be modelled within the plasticity framework using associative flow rules which are closed surfaces, and (iii) the size of the yield surface depends on the void ratio. A hardening rule obtained in isotropic compression tests relates the size of the yield surface and the plastic volumetric deformation.

The initial Cam Clay model is useful for normally consolidated clays, and can also reproduce –with some limitations- the behaviour of overconsolidated clays.

The model has been further extended to describe the behaviour of sands by Nova (1977) and Wilde (1977). This extension provides a simple way to model the behaviour of both dense and loose sands, including especially the liquefaction phenomena. The main ingredients of the model are (i) use of a non associative flow rule, and (ii) use of both volumetric and deviatoric hardening.

In some cases, we find landslides occurring in collapsible materials, for which we need to introduce a new extension. It is worth mentioning here the work of Nova and Lagioia (1995).

One of the most important extensions of Cam Clay theory is that of Alonso et al. (1990) who formulated the first consistent model for unsaturated soils. It is worth mentioning the contributions of Bolzon, Schrefler and Zienkiewicz (1996) and its extension by Santagiuliana and Schrefler (2006), Loret and Khalili (2000), Gallipoli, Gens, Sharma and Vaunat (2003),

Tamagnini (2004), Tamagnini and Pastor (2004), Fernandez Merodo, Tamagnini, Pastor and Mira (2005), Laloui and Nuth (2005), and Manzanal et al. (2008, 2009).

The described models are able to provide an accurate approximation of the constitutive behaviour of soils in slopes where landslides are triggered. They are more advanced than the two first categories described in the text, but they are able to describe both localized and diffuse failure caused by monotonic loads.

### 3.4 Models for cyclic and dynamic loading

Even if landslides related to external climate factors (e.g. rainfall, snow melt) can be studied in a quasi static, transient, monotonic framework, we have to remember that climate is essentially of cyclic nature, with daily, seasonal and yearly variations. Therefore, the constitutive models have to be able to reproduce accurately this cyclic behaviour. This can be especially relevant in unsaturated soils with drying-wetting cycles.

We refer the interested reader to Chapter 4 of the textbook of the late Prof.O.C.Zienkiewicz on geomaterials modelling (Zienkiewicz et al. 1999) where models for cyclic and dynamic loading are described in detail.

### 3.5 Time dependent models. Viscoplasticity

Landslides present quite frequently a viscous type of behaviour with deformation and movements accumulating over time. In addition to the relation with seasonal changes of moisture, water table levels, rain, etc, it is important to consider the possibility of viscoplastic behaviour of the material.

Viscoplastic models have been used in the literature to describe this behaviour, see for instance Corominas et al. (2005) and Herrera et al. (2009).

There exist different types of viscoplastic models, such as the Perzyna, Duvaut-Lions or consistent type. Among them, the most used type is that of Perzyna.

Perzyna models can be developed in a straightforward manner from classical plasticity models, using their yield surface, potential surface and hardening rule. The main difference resides in the fact that (i) stress states outside the yield surface are admissible, and (ii) the rate of viscoplastic strain depends on how far the stress state is located from the yield surface.

In some cases, such as those described above, simple infinite slope models have been developed which exhibit viscous bottom friction and provide a simple yet accurate description of the landslide evolution.

## **2.2.4 Hydro-mechanical couplings (UPC)**

Pore water pressure distribution, whether positive for the case of saturated soils or negative for partial saturation, is one of the most important factors in slope stability. Pore water pressure increment results in a reduction of the frictional component of the strength while in unsaturated conditions, suction leads to increments of the strength. A good understanding of slope movements often requires approximating appropriately the pore water pressure distribution inside the slope.

Changes in hydraulic and mechanical boundary conditions will affect the pore water pressure distribution. Changes in the boundary total stress will induce, in general, a change in pore pressure. The sign and intensity of pore pressures depend on the constitutive (incremental strain-effective stress) behaviour of the soil skeleton. For the simple case of an elastic soil

skeleton, changes in pore water pressure will be equal to the change in mean, octahedral, stress. If dilatancy (positive or negative sign) is present due to shear effects, additional pore pressures, positive or negative will be generated.

Changes in hydraulic boundary conditions resulting in an unbalanced state will induce flow that also affects the resulting pore water distribution in time. The flow mainly depends on the soil permeability and soil stiffness, which controls the storage or source term associated with changes in effective stress. In addition, permeability is not a constant hydraulic parameter, but also depends on the void ratio which varies with the effective stress.

Therefore, an appropriate hydro-mechanical coupled formulation will be necessary to capture the pore water pressure distribution and, therefore, to understand the slope stability. In order to do so, a comprehensive formulation for a fully hydro-mechanical formulation, valid for saturated and unsaturated conditions, is presented below.

In what follows, it will be considered that the state variables (unknowns) are: solid displacements,  $\mathbf{u}$  (three spatial directions) and liquid pressure,  $P_l$ . Balance of momentum for the medium as a whole is reduced to the equation of stress equilibrium together with a mechanical constitutive model which relates stresses with strains. Strains are defined in terms of displacements. Small strains and small strain rates for solid deformation are assumed. Advective terms due to solid displacement are neglected once the formulation is written in terms of material derivatives (in fact, material derivatives are approximated as eulerian time derivatives). In this way, volumetric strain is properly considered.

The governing equations for non-isothermal multiphase flow of water and gas through porous deformable saline media have been presented by Olivella *et al.* (1994). A derivation is given in this reference, and only a description of the reduced formulation for hydro-mechanical problems is presented in this deliverable.

Mass balance of solid present in the medium is written as:

$$\frac{\partial}{\partial t}(\rho_s(1-\phi)) + \nabla \cdot (\mathbf{j}_s) = 0 \quad (2.2.4.1)$$

where  $\rho_s$  is the mass of solid per unit volume of solid and  $\mathbf{j}_s$  is the flux of solid. From this equation, an expression for porosity variation can be obtained if the flux of solid is written as the velocity of the solid multiplied by volumetric fraction occupied by the solid phase and the density, i.e.  $\mathbf{j}_s = \rho_s (1-\phi) \frac{d\mathbf{u}}{dt}$  :

$$\frac{D_s \phi}{Dt} = \frac{(1-\phi)}{\rho_s} \frac{D_s \rho_s}{Dt} + (1-\phi) \nabla \cdot \frac{d\mathbf{u}}{dt} \quad (2.2.4.2)$$

The material derivative with respect to the solid is defined as:

$$\frac{D_s(\bullet)}{Dt} = \frac{\partial}{\partial t} + \frac{d\mathbf{u}}{dt} \cdot \nabla(\bullet) \quad (2.2.4.3)$$

Equation (2.2.4.2) expresses the variation of porosity caused by volumetric deformation and solid density variation.

In the following it is assumed that the water component and the liquid phase are the same. The total mass balance of water is expressed as:

$$\frac{\partial}{\partial t}(\rho_w S_w \phi) + \nabla \cdot (\mathbf{j}_w) = f^w \quad (2.2.4.4)$$

where  $S_w$  is the degree of saturation of water,  $\rho_w$  is the water density,  $\mathbf{j}_w$  is the flux of water, and  $f^w$  is an external supply of water. Water flux is a combination of a Darcy flux and an advection caused by the solid motion:

$$\frac{\partial}{\partial t}(\rho_w S_w \phi) + \nabla \cdot \left( \rho_w \mathbf{q}_w + \rho_w \phi S_w \frac{d\mathbf{u}}{dt} \right) = f^w \quad (2.2.4.5)$$

The use of the material derivative leads to:

$$\phi \frac{D_s(\rho_w S_w)}{Dt} + \rho_w S_w \frac{D_s \phi}{Dt} + \rho_w S_w \phi \nabla \cdot \left( \frac{d\mathbf{u}}{dt} \right) + \nabla \cdot (\rho_w \mathbf{q}_w) = f^w \quad (2.2.4.6)$$

The mass balance of solid is introduced in the mass balance of water to obtain, after some algebra:

$$\frac{\phi S_w}{\rho_w} \frac{D_s \rho_w}{Dt} + \phi \frac{D_s S_w}{Dt} + S_w \frac{(1-\phi)}{\rho_s} \frac{D_s \rho_s}{Dt} + S_w \nabla \cdot \left( \frac{d\mathbf{u}}{dt} \right) + \frac{1}{\rho_w} \nabla \cdot (\rho_w \mathbf{q}_w) = \frac{1}{\rho_w} f^w \quad (2.2.4.7)$$

This equation has four storage terms, related to:

Water compressibility since  $\frac{1}{\rho_w} \frac{d\rho_w}{dp_w} = \frac{1}{K_w}$  is the volumetric compressibility of water,

Retention curve storativity since  $\frac{dS_w}{dp_w}$  is obtained from the retention curve.

Solid compressibility since  $\frac{1}{\rho_s} \frac{d\rho_s}{dp} = \frac{1}{K_s}$  is the compressibility of the soil particles.

Soil skeleton compressibility since the divergence of solid velocity can be transformed into  $\nabla \cdot \left( \frac{d\mathbf{u}}{dt} \right) = \frac{d}{dt}(\nabla \cdot \mathbf{u}) = \frac{d\varepsilon_v}{dt}$ , and  $\frac{d\varepsilon_v}{dt} = \frac{d\varepsilon_v(\boldsymbol{\sigma}', p_w)}{dt} = \frac{d\varepsilon_v}{d\boldsymbol{\sigma}} \frac{d\boldsymbol{\sigma}}{dt} + \frac{d\varepsilon_v}{dp_w} \frac{dp_w}{dt}$  is the volumetric strain

rate that should be calculated with an appropriate constitutive model for the soil. The mechanical model may include effective or net stress terms (volumetric or deviatoric) or suction terms. Effective or net stress has to be considered here as the total stress minus the water pressure or the air pressure, respectively, for saturated or unsaturated conditions. The final terms are left as a function of total stress.

The relative importance of the different terms depends on the conditions of the soil. For instance, for saturated conditions the second term disappears. When the compressibility of the skeleton is large, the compressibility of the particles is negligible. The compressibility of the water may be negligible in some cases but it is not possible to neglect it in general for hard soils.

The final objective is to find the unknowns from the governing equations. Therefore, the dependent variables will have to be related to the unknowns in some way. Doing this in the last equation leads to:

$$\begin{aligned} \frac{\phi S_w}{K_w} \frac{dp_w}{dt} + \phi \frac{dS_w}{dp_w} \frac{dp_w}{dt} + S_w \left( \frac{\partial \varepsilon_v}{\partial \boldsymbol{\sigma}} \frac{d\boldsymbol{\sigma}}{dt} + \frac{\partial \varepsilon_v}{\partial p_w} \frac{dp_w}{dt} \right) + \frac{1}{\rho_w} \nabla \cdot (\rho_w \mathbf{q}_w) &= 0 \\ \frac{\phi S_w}{K_w} \frac{dp_w}{dt} + \phi \frac{dS_w}{dp_w} \frac{dp_w}{dt} + S_w \frac{\partial \varepsilon_v}{\partial \boldsymbol{\sigma}} \frac{d\boldsymbol{\sigma}}{dt} + S_w \frac{\partial \varepsilon_v}{\partial p_w} \frac{dp_w}{dt} &= -\frac{1}{\rho_w} \nabla \cdot (\rho_w \mathbf{q}_w) \end{aligned} \quad (2.2.4.8)$$

where the compressibility of the solid particles has been neglected and the source/sink term is assumed to be zero. The material derivatives have been approximated as eulerian.

This equation allows the calculation of the pressure development for a soil subjected to changes in total stress in the following way:

$$dp_w = \frac{-S_w \frac{\partial \epsilon_v}{\partial \sigma} d\sigma - \frac{dt}{\rho_w} \nabla \cdot (\rho_w \mathbf{q}_w)}{\frac{\phi S_w}{K_w} + \phi \frac{dS_w}{dp_w} + S_w \frac{\partial \epsilon_v}{\partial p_w}} \quad (2.2.4.9)$$

Deformation is assumed negative in compression from these equations, and stress is also negative in compression. This implies that  $d\sigma$  is negative in compression (loading) and produces positive pressure increments. Note that the general stress tensor is maintained because volumetric deformations can be induced by any stress variation (not only isotropic). For instance, dilatancy is a volumetric expansion induced by shear.

In equation (2.2.4.9), the volumetric deformation derivatives  $\frac{\partial \epsilon_v}{\partial \sigma}$  and  $\frac{\partial \epsilon_v}{\partial p_w}$  should be calculated with an appropriate constitutive model. These are volumetric deformation terms and can be obtained from a model for unsaturated soils such as the elastoplastic model BBM (Alonso *et al*, 1990). A general equation, including the effect of effective or net stresses and the effect of suction, is written as:

$$\begin{aligned} d\sigma' &= \mathbf{D}d\epsilon + \mathbf{h}ds \\ d\epsilon &= \mathbf{D}^{-1}d\sigma' - \mathbf{D}^{-1}\mathbf{h}ds \\ d\epsilon_v &= \mathbf{m}'d\epsilon = \mathbf{m}'\mathbf{D}^{-1}d\sigma' - \mathbf{m}'\mathbf{D}^{-1}\mathbf{h}ds \\ \mathbf{m}' &= [1 \quad 1 \quad 1 \quad 0 \quad 0 \quad 0] \end{aligned} \quad (2.2.4.10)$$

Where suction can be defined as  $s = \max(p_a - p_w, 0)$  and effective or net stress as  $\sigma' = \sigma + \max(p_a, p_w)$ . This is valid for saturated and unsaturated conditions, and considers stresses in compression as negative quantities. The model parameters are included in  $\mathbf{D}$  which is the stiffness tensor (6x6) or constitutive matrix for changes in net or effective stress and  $\mathbf{h}$  which is the constitutive vector for changes in suction. Both are nonlinear functions.

Note that the derivatives of volumetric deformation needed in Equation (2.2.4.9) can be obtained in the following way:

$$\frac{\partial \epsilon_v}{\partial \sigma} = \frac{\partial \epsilon_v}{\partial \sigma'} \frac{\partial \sigma'}{\partial \sigma} \quad \text{and} \quad \frac{\partial \epsilon_v}{\partial p_w} = \frac{\partial \epsilon_v}{\partial \sigma'} \frac{\partial \sigma'}{\partial p_w} + \frac{\partial \epsilon_v}{\partial s} \frac{\partial s}{\partial p_w} \quad (2.2.4.11)$$

By comparison with Equation (2.2.4.10), the following terms are obtained:

$$\frac{\partial \epsilon_v}{\partial \sigma'} = \mathbf{m}'\mathbf{D}^{-1} \quad \text{and} \quad \frac{\partial \epsilon_v}{\partial s} = -\mathbf{m}'\mathbf{D}^{-1}\mathbf{h} \quad (2.2.4.12)$$

The nonlinear elastic part of the BBM model, gives the following volumetric deformation:

$$d\epsilon_v = \frac{\kappa}{1+e} \frac{dp'}{p'} + \frac{\kappa_s}{1+e} \frac{ds}{s+0.1} \quad (2.2.4.13)$$

Where,  $e$  is void ratio,  $\kappa$  and  $\kappa_s$  are material parameters,  $p'$  is the mean net or effective stress which is defined as  $p' = (\sigma_x + \sigma_y + \sigma_z) / 3 + \max(p_a, p_w)$ , and  $s$  is suction.

The preceding formulation provides a reasonably complete formulation of hydro-mechanical interactions. It incorporates coupling in two directions:

Hydraulic  $\rightarrow$  Mechanical effects

Mechanical  $\rightarrow$  Hydraulic effects

The first coupling is obvious if one considers the effective stress definition. The second coupling is in general less significant, but some relevant cases (rapid drawdown) are also examples of important coupling.

The outlined formulation may also handle saturated and unsaturated soil states and their evolution:

Saturated  $\rightarrow$  Non saturated

Non saturated  $\rightarrow$  Saturated

The first case leads typically to an increase in safety. The second one is one of the main reasons for sliding, especially shallow landsliding.

## 2.2.5 Requirements for numerical codes (EPFL)

Landslides present a large variety of types and movement patterns due to the different soil types, geological and topographical contexts, as well as the hydrogeological predisposition factors involved. Most of them have rainfall input as trigger in common. This section presents first a catalogue of information requested from geomechanical models for various types of landslides. Second, model outputs are highlighted which are necessary to give quantitative answers to the various requested information. Also, model requirements are formulated for the different types of outputs. The last section presents a synthesis of the requirements that have to be met by physically-based models in order to reproduce the different features of the reviewed shallow and deep-seated landslide phenomena. The objective is to guide the user in choosing the necessary model ingredients and analysis procedures for different problem types and scales.

### 2.2.5.1 Requested information from geomechanical models

Geomechanical models are useful tools for the quantitative analysis of hillslope processes. Depending on the model type, the geomechanical analysis can help answer a certain number of fundamental questions on landslide hazard:

1. Location, released landslide volume and frequency of landslide events?
2. Proneness of a slope to fail under certain environmental conditions?
3. Quantitative measure of slope stability?
4. Prediction of the time of failure?
5. Landslide type?
6. Probable movement pattern?

Empirical methods based on statistical landslide analysis (e.g. ID models, see also SafeLand D1.5) are widely used for the identification of hazard regions and landslide frequency, but they can only give partial answers to some of the addressed questions above. Since they don't

consider explicitly the physical hillslope processes, but only external climatic agents and the statistics of past landslide events, empirical methods are only applicable at representative, regional scales for which important predisposition factors for slope failure are the same. Within their limits, deterministic models are able to give more or less accurate answers to the addressed questions above. One specific model alone is however incapable of answering all questions. Due to their need of detailed data input, the application of deterministic models is mostly limited to slope-scale which is one of the reasons why statistical methods are most often used at regional scale. Nevertheless, deterministic analyses using simple representations of the problem can be used in some cases at regional scale (e.g. Godt et al. 2008; Sorbino et al. 2007).

### ***2.2.5.2 Outputs and basic requirements of geomechanical models***

The different outputs of numerical models are supposed to support landslide hazard assessment and decisional processes for risk mitigation. They can also be used to define thresholds for slope stability in an early warning system or to predict the possible future behaviour of a slope for various environmental scenarios. The engineer needs to decide which type of model output is most significant for a specific problem, considering also scale and precision issues. Outputs from physical models give information on the expected quantitative evolution of physical field variables (e.g. pore pressure distribution, soil displacements and stresses) and slope stability. In the following, necessary outputs for answering the catalogue of questions addressed in the precedent section are highlighted. Also, basic conceptual requirements to get the desired outputs are summarised.

#### *1. Location, released landslide volume and frequency of landslide events?*

In local 2D or 3D slope-scale models, the location of a landslide is given exactly with respect to local slope geometry as a result of a limit equilibrium analysis (e.g. slice methods) or a stress-strain analysis (e.g. FEM, FDM). In the limit equilibrium method, the shape of the failure surface is predefined while it results naturally through strain localisation in a stress-strain analysis. One-dimensional models considering stationary or transient vertical rainfall infiltration coupled with infinite slope stability calculations are commonly used at local scale for shallow translational slides and at regional scale for early-warning systems and hazard mapping (e.g. Godt et al. 2008). They primary aim at giving an answer concerning the frequency or likelihood of shallow landslide events to occur, but they oversimplify the material failure process.

In order to locate a landslide in a numerical model, the mobilised, failed mass needs to be differentiated from the stable soil mass. Indicators are plastic shear strains and horizontal displacements in continuum models or slip surfaces with associated minimum safety factors in limit equilibrium methods (see also section 2.4.1). The volume of the failed soil mass can be estimated from the slope geometry and the calculated failure mechanism. An exact prediction of the landslide mass for rainfall-induced, first-time failures is however not an easy task: the correct failure mechanism needs to be captured in the numerical model (e.g. failure due to loss of suction stress or mounding of the groundwater table) which depends strongly on soil heterogeneities, initial hydraulic conditions, soil properties and rainfall pattern (see also SafeLand D1.2, chapter 4.1.2.4 for more details).

#### *2. Proneness of a slope to fail under certain environmental conditions?*

Landslide early warning consists in practice in defining threshold values of measured entities (e.g. displacement rates of a landslide, groundwater level, rainfall intensity, duration, cumulative rainfall, etc.) based on which a warning signal is triggered. Risk prevention consists however also in assessing the proneness of a given slope to fail for certain scenarios.

This means that the current hydraulic and mechanical state of a slope, as well as the environmental conditions which can lead to slope failure need to be determined. It requires a detailed analysis of the hydromechanical slope behaviour in order to determine the various factors controlling failure. Shallow rainfall-induced landslides involve mostly granular soils in steep terrain and represent first-time failures. Failure is most often a direct consequence of rainfall infiltration and its effects on pore water pressure distributions in the soil (suction stress and/or groundwater table variations). Hence, hydraulic soil characteristics, transient water storage and pore pressure dissipation are the most critical elements to include in the analysis. Therefore, the hydraulic model needs to be able to calculate saturated and unsaturated, time-dependent flow and pore pressure dissipation (e.g. solve Richard's equation: mass conservation for liquid phase combined with generalised Darcy's law). The hydraulic component of the code needs to include a retention model, a soil water relative permeability function and the possibility to define variable initial and boundary conditions to account for soil moisture content, pore pressures and their variations prior to and during a triggering rainfall event. The transient pore pressure field can be introduced in a mechanical calculation for slope stability (e.g. stress-strain or limit equilibrium). In most cases of shallow landslides, the model is not required to present a coupling from the mechanical to the hydraulic part, i.e. a semi-coupled hydromechanical approach is sufficient to deal with the problem. Pore pressures calculated in an adequate hydraulic model can be exported and introduced either as boundary conditions at each calculation timestep in a multiphase, time-dependent mechanical stress-strain model (e.g. Tacher et al. 2005; François et al. 2007; Ferrari et al. 2009) or they can be used to calculate effective stresses and variations in shear strength in single-phase approaches (solid stress-strain analysis or limit state methods, e.g. Blatz et al. 2004; Gasmo et al. 2000; Cho and Lee 2001; Collins and Znidarcic 2004; Rahardjo et al. 2007). The full hydromechanical coupling becomes necessary when undrained conditions occur, as for example in collapsible soils (e.g. loose sands, pyroclastic soils) and soft clays possessing high deformability, as well as for modelling post-failure phenomena (e.g. Alonso et al. 2003; Fernandez Merodo et al. 2004). In that case, the code needs to solve simultaneously mass conservation for all phases (solid, liquid, gas) and balance of linear momentum.

In semi- and fully coupled hydromechanical approaches, the mechanical model needs an appropriate effective stress framework to deal with variably saturated and unsaturated conditions in the soil.

In deep-seated landslides the two-way hydromechanical coupling (hydraulic → mechanical and also mechanical → hydraulic coupling) plays more often an important role: rock fracture width variations are seen to influence flow characteristics noticeably and undrained conditions due to rapid mass movements may lead to sudden high increases of pore water pressures along the slip surface.

### 3. *Quantitative measure of slope stability?*

Part of landslide hazard assessment consists in identifying controlling factors for failure and determination of their threshold values for slope stability. Slope stability needs to be defined in some mechanical terms. Commonly, the safety of a slope is defined by the use of a factor of safety (FoS). In simplest terms, the factor of safety is defined by Duncan (1996) as *"the factor by which the shear strength of the soil would have to be divided to bring the slope into a state of barely stability equilibrium"*. Expressing the shear strength by the Mohr-Coulomb criterion, the mobilised shear strength  $\tau_f$  can be expressed as a function of the factor of safety as (Duncan and Wright 2005):

$$\tau_f = \frac{c'}{F_s} + \sigma_n' \frac{\tan \phi'}{F_s} \quad (2.2.5.1)$$

Values for the safety factor  $F_s$  above 1 represent a stable configuration, a safety factor equal to 1 corresponds to the limit equilibrium and all values below 1 correspond to an unstable configuration.

The shear strength reduction method (SSRM) is a technique to obtain the factor of safety by means of a finite element simulation (Zienkiewicz et al. 1975; Griffiths and Lane 1999). Compared to the limit equilibrium method, no assumption needs to be made on the shape of the failure surface and soil anisotropy can be considered without taking any particular measures. The most probable failure mechanism results naturally from the stress-strain analysis. The principle of this technique is to reduce the shear strength parameters in elasto-plastic models until a plastic mechanism occurs and the numerical code diverges. The shear strength parameters  $c'$  and  $\phi'$  are reduced by incrementally increasing the coefficient  $F_s$  for which the maximum corresponds to the actual safety factor of the slope.

Another technique for determining the factor of safety is the so-called gravity increase method (GIM). It consists in gradually increasing the gravity until a failure mechanism develops and the numerical code diverges (Swan and Seo 1999; Li et al. 2009). The material parameters are kept constant. The safety factor is defined as the ratio between the maximum trial gravity and the initial earth gravity.

#### *4. Prediction of the time of failure?*

Analogue to the first question, the timing of failure can only be estimated if the correct failure mechanism is captured in the numerical model and if the related transient processes are exactly simulated. Compared to the questions of landslide location and proneness of slopes for failure, the prediction of the time of failure is probably the most difficult answer to obtain. In practical terms, a real-time warning system which includes the predictions of numerical simulations relies above all on in-situ real-time measurements of relevant field variables at relevant locations.

#### *5. Landslide type?*

Some shallow landslides move as a rigid block over short distances, while others mobilize into debris flows with long run-out distances. In order to give some information on the proneness of a slope to fail and develop into one of the two landslide types, the slope model needs a fully coupled hydromechanical framework and advanced constitutive features, especially for collapsible soils. Most debris flows are observed to mobilise from shallow slips as a consequence of static liquefaction due to the soil undergoing rapid volumetric compaction and reaching quasi full saturation. In the unsaturated range and under certain stress conditions, soil compaction can be a consequence of the phenomenon of wetting pore collapse. Commonly, the concept of a loading collapse curve is used in constitutive models to reproduce compressive deformations on a wetting path in the stress space (Alonso et al. 1990). Other constitutive models describe the compaction tendencies of saturated, bonded granular soils due to mechanical perturbations which lead to undrained loading and the onset of liquefaction (e.g. Fernandez Merodo et al. 2004). Diffuse failure modes in soil slopes subjected to rain infiltration have also been studied under the light of the second-order work criterion as opposed to conventional elasto-plasticity (Darve and Laouafa 2000; Lignon et al. 2009). Modelling the initiation of debris flows requires that the constitutive model is capable of reproducing the volumetric compaction of certain soils. In elasto-plastic models, this is achieved by means of the dilatancy rule.

### 6. *Probable movement pattern?*

Most of the geomechanical codes have been developed to model the landslide behaviour in the pre-failure and failure stage. More recently, the soil mechanics community is focusing on the modelling of the post-failure stage, i.e. the run out of rapid, fluidised masses (see deliverable D1.6 of WP 1.2). For those cases, geomechanical models aim at giving quantitative answers concerning the probable movement pattern of the travelling soil mass, its velocity, impact on obstacles and location of deposition. These models require a sound calibration of rheological parameters and a precise surface topography.

Large, slow moving landslides displaying from time to time large displacements (couple of meters) can have a considerable impact on infrastructures (e.g. La Frasse landslide, D1.3 WP 1.2). These large landslides are in a state of continuous movement. They are in most cases whether stable nor really instable. Rather than the question of slope stability, the questions of the probable displacement rates and movement patterns are of interest. In order to model large, localised displacements along a preexisting slip surface, interface elements need to be incorporated in the numerical code which have a large strain formulation. A simple frictional law for the interface is insufficient for the correct prediction of displacement rates since the instable mass will simply move infinitely as soon as the shear strength along the interface exceeds the shear strength. An elastic-viscoplastic constitutive model can be used for the interface in that case.

Apart from elasto-viscoplastic constitutive models for finite elements, non-linear viscous models are often used to reproduce the displacement rates of large landslides. In that approach, the soil is modelled as a non-Newtonian viscous body with rate-dependent stress. Many viscous-type sliding law functions are defined in the literature and commonly used by many authors, because they are above all relatively simple to fit to inclinometer readings and can be integrated in conceptual and simplified analytical models (e.g. van Asch et al. 2007; Puzrin and Sterba 2006). However, the viscous behaviour of the landslide reproduced by the numerical model doesn't reflect the actual soil viscosity measured in the laboratory.

#### ***2.2.5.3 Key elements in continuum models for the analysis of rainfall-induced landslides***

Model requirements can also be formulated from the point of view of landslide types. Modelling first-time failures or reactivated landslides requires different code components. In shallow landslides the unsaturated zone is most often of particular importance while the groundwater table often reaches the ground surface for many deep-seated landslides. Hydromechanical couplings may be less important in granular soils than in fine-grained soils, depending on their tendency to contract upon wetting. Table 1 summarizes the various model components and their relative importance with respect to the modelling of shallow or deep-seated landslides. Shallow landslides are divided into those which take place in dense or medium dense granular soils and those which take place in fine-grained or collapsible soils. Slow moving, creeping landslides are distinguished from landslides with display common rapid reactivation phases. A legend for Table 1 is given beforehand which enables to understand its lecture.

Legend of Table 1:

0: not required or not always necessary

1: necessary component

a: basic requirement

b: key requirement

2: sufficient in some cases

3: insufficient

4.x : to consider in particular case x

Case 4.1: Anisotropic permeability is mainly due to the stratification of sediments, but in surface close zones, it may also originate from root systems. As the void ratio of soils decreases during consolidation, anisotropic permeability increases (Chapuis and Gill, 1989). Anisotropic permeability can be important in overconsolidated clays and dense sands.

Case 4.2: Anisotropic permeability can be an important feature in stratified and poorly cemented rock slopes for the correct calculation of pore water pressure distributions after rainfall events (Dong et al. 2006). Deep-seated landslides in overconsolidated clays and soft rocks (e.g. shales) often have preferential flow paths for groundwater due to dominant fractures and faults. Flow characteristics of fracture families can be approximated in a continuum mechanics approach with anisotropy in the permeability tensor.

Case 4.3: Anisotropic deformability and shear strength may arise in some cases due to the presence of fractures with inferior mechanical properties, predominantly oriented in a single direction. In others, mechanical anisotropy is inherent to the soil or rock type (e.g. shales).

Case 4.4: Plastic swelling becomes a necessary component to consider in the case of active clays. During rainfall events, such soils undergo strong swelling which leads to an increase in total and shear stresses within the soil slope. Shallow failures in active clay slopes are numerous reported (e.g. Ng et al. 2003; Stimpson et al. 1987).

Case 4.5: Wetting pore collapse might lead to important variations in soil porosity. In natural conditions, this phenomenon is particularly pronounced in regions where the climatic conditions are not conducive to development of long-term saturated conditions within the soil (Bell, 2000).

Case 4.6: Olivares and Tommasi (2008) present the hypothesis of temperature changes in soil slopes originating from volcanic activities and which lead to vapour condensation. Subsequent to an increase in water content, suction decreases or positive pore pressures can develop and trigger shallow landslides.

Case 4.7: Vardoulakis (2000) presented a possible coupled hydromechanical mechanism of frictional heating of the failure plane leading to catastrophic landslides. The heat generated by friction along a failure plane gives rise to pore pressures which are unable to dissipate in time.

Case 4.8: Permafrost has a positive effect on soil strength in many slopes in Alpine regions. Frozen soil strength and its variation with temperature changes can be considered to investigate the effects of climate change on slope stability (Andersland and Ladanyi, 2004).

**Table 1: Components of geomechanical models and their relative importance for the reproduction of different landslide phenomena.**

| Topic                     | Specification             | Component   | Shallow landslides – First-time failures |                                    | Deep-seated landslides       |                           |
|---------------------------|---------------------------|---|--|------------------------------------|------------------------------|---------------------------|
|                           |                           |   | Dense granular soils                     | Fine-grained and collapsible soils | Slow moving/ creeping slopes | Rapid reactivation phases |
| <b>Problem definition</b> | Slope geometry            | Slope angle, shape of slope and meshing of domain | 1a                                       | 1a                                 | 1a                           | 1a                        |
|                           | Soil stratigraphy         | Material layers                                   | 1a                                       | 1a                                 | 1a                           | 1a                        |
|                           | Pre-existing slip surface | Interface elements for large strains              | 0  | 0                                  | 2                            | 1b                        |
|                           |                           | Material layer for shear zone with small strains  | 0  | 0                                  | 1a                           | 3                         |
|                           | Boundary conditions       | Hydraulic   | 1b                                       | 1b                                 | 1b                           | 1b                        |
|                           |                           | Mechanical  | 1a                                       | 1a                                 | 1a                           | 1b                        |
|                           | Initial conditions        | Hydraulic   | 1b                                       | 1b                                 | 1a                           | 1a                        |
|                           |                           | Mechanical  | 1b                                       | 1b                                 | 1a                           | 1a                        |
| <b>Material</b>           | Phases                    | Single phase approach                             | 2  | 3                                  | 2                            | 3                         |
|                           |                           | Two- or three phase approach                      | 0  | 1a                                 | 0                            | 1a                        |
| <b>Analysis type</b>      | Steady state analysis     | No time dependency                                | 2  | 3                                  | 3                            | 3                         |
|                           | Transient analysis        | Time dependency of hydromechanical processes      | 0  | 1b                                 | 1a                           | 1b                        |
|                           |                           | Hydromechanical coupling                          | Semi-coupled approach                    | 2                                  | 3                            | 2                         |
|                           | Fully coupled approach    |   | 0  | 1b                                 | 0                            | 1b                        |

Table 1: continuation (1/2)

| Topic   | Specification   | Component  | Shallow landslides – First-time failures |                                    | Deep-seated landslides       |                           |
|---|---|--|--|------------------------------------|------------------------------|---------------------------|
|   |   |  | Dense granular soils                     | Fine-grained and collapsible soils | Slow moving/ creeping slopes | Rapid reactivation phases |
| <b>Governing equations</b>                                | Equilibrium   | Balance of linear momentum                                   | 1a                                       | 1a                                 | 1a                           | 1a                        |
|   | Time-dependent flow of fluids through soils, uncoupled approach | Mass conservation for fluids                                 | 2  | 3                                  | 2                            | 3                         |
|   | Time-dependent flow of fluids through soils, coupled approach   | Coupled mass conservation for solid and fluids               | 0  | 1b                                 | 0                            | 1b                        |
| <b>Material behaviour: Hydraulics</b>                     | Fluid flow  | Darcy's law  | 1a                                       | 1a                                 | 1a                           | 1a                        |
|   | Anisotropic permeability  | Second-order permeability tensor                             | 4.1                                      | 4.1                                | 4.2                          | 4.2                       |
|   | Permeability in unsaturated soils                               | Hydraulic conductivity curve                                 | 1b                                       | 1b                                 | 0                            | 0                         |
|   | Water retention for unsaturated soils                           | Soil water characteristic curve                              | 1b                                       | 1b                                 | 0                            | 0                         |
| <b>Material behaviour: Mechanics</b><br><i>Plasticity</i> | Soil stiffness depending on confining pressure                  | Non-linear elasticity  | 0  | 0                                  | 1a                           | 1a                        |
|   | Anisotropic deformability or shear strength                     | Transversal, elastic isotropy, anisotropic elasto-plasticity | 0  | 0                                  | 4.3                          | 4.3                       |
|   | Stress redistribution due to material yielding                  | Yield criterion  | 1b                                       | 1b                                 | 0                            | 1b                        |
|   | Onset of failure  | Hardening plasticity   | 1b                                       | 1b                                 | 0                            | 1b                        |

Table 1: continuation (2/2)

| Topic                                | Specification                               | Component  | Shallow landslides – First-time failures        |                                    | Deep-seated landslides       |                           |    |
|--------------------------------------|---|--|---|------------------------------------|------------------------------|---------------------------|----|
|                                      |   |  | Dense granular soils                            | Fine-grained and collapsible soils | Slow moving/ creeping slopes | Rapid reactivation phases |    |
| <b>Material behaviour: Mechanics</b> | Dilatancy                                   | Non-associative plasticity   | 1b  | 1b                                 | 0                            | 1b                        |    |
|                                      | Instability phenomena                       | Dilatancy, constitutive features for volume compaction, second-order work criterion, ... | 0   | 1b                                 | 0                            | 0                         |    |
|                                      | <i>Viscosity</i>                            | Soil creep   | Non-linear viscous or elasto-viscoplastic model | 0                                  | 0                            | 1b                        | 1b |
|                                      |   | Stress relaxation  | Non-linear viscous or elasto-viscoplastic model | 0                                  | 0                            | 1b                        | 1b |
| <i>Capillary effects</i>             | Effects of capillary on stress state        | Effective stress framework for unsaturated soils   | 1b  | 1b                                 | 0                            | 0                         |    |
|                                      | Shear strength increase                     | Extension of yield surface as a function of capillary stress                             | 1b  | 1b                                 | 0                            | 0                         |    |
|                                      | Volumetric changes during wetting           | Elastic swelling   |   | 1a                                 | 1a                           | 0                         | 0  |
|                                      |   | Plastic swelling   |   | 0                                  | 4.4                          | 0                         | 0  |
| Wetting pore collapse                |   |  | 0   | 4.5                                | 0                            | 0                         |    |
| <b>Temperature effects</b>           | Phase changes: Water vapour ↔ liquid water  | Heat conservation equation, water and vapour mass balance, heat transfer equation        | 0   | 4.6                                | 0                            | 4.7                       |    |
|                                      | Effects of temperature on material strength | Yield function depending on temperature  | 4.8   | 4.8                                | 0                            | 0                         |    |

## **2.3 INPUT DATA FOR NUMERICAL MODELS FROM SITE INVESTIGATIONS, FIELD AND LABORATORY TESTS (AMRA)**

Geomechanical models are becoming more and more sophisticated as they evolve to reproduce more realistically physical subsoil processes which change as a function of continuous variation of boundary conditions related to weather and climate. As a consequence, numerical modelling of slope behaviour requires in a first step the determination and understanding of a great number of necessary weather and climate parameters, as well as of the hydraulic and mechanical soil parameters. In a second step, the model parameters are calibrated based on laboratory testing and field monitoring and finally the numerical model is validated.

The objective of this section is to present some laboratory and field tests, as well as site investigation methods, and to suggest the best procedures and parameters to reach the goal of a correct analysis. At the same time, the constraints and limits of the adopted procedures are stressed out. Since rainfall or snow melting leads to water infiltration and subsequent change in the internal state of stress, special attention is given to the hydrological aspects.

### **2.3.1 Monitoring for selection of appropriate initial conditions**

The correct definition of *initial conditions* is crucial in order to obtain accurate results from numerical simulations. To this end, in-situ monitoring is a fundamental tool. Boreholes allow to obtain the stratigraphic profile and to recover soil samples for the determination of their physical properties.

The groundwater regime can be investigated through the installation of:

- piezometers or standpipes (readings should cover long time lengths);
- tensiometers in unsaturated shallow deposits.

Since natural slopes often present a complex structure with possible preferential flow path and other singularities, instruments should be installed at different locations and depths. Attention has to be paid to the quality of readings that can be affected by errors. For example, when using hydraulic piezometers, it is important to check impermeability of the junctions or that no occlusions occur in the tubes. Similarly, tensiometers must be regularly checked in order to avoid the accumulation of air bubbles. Remote monitoring may lead to this inconvenience if periodical inspections and servicing of the instruments are not performed: in this case, a high amount of data can be acquired, but the quality might be inferior.

In recent years, the use of TDR probes to monitor the volumetric water content in response to precipitations or to changes in air temperature and humidity is becoming widespread. Such a technique relies on the relationship between the bulk soil dielectric permittivity,  $\epsilon_r$ , and the volumetric water content,  $\theta$ , which is generally based on the so-called “universal calibration relationship” (Topp et al., 1980). However, in some cases (Greco et al., 2010; Regalado et al., 2003; Tomer et al., 1999), such a relationship is quite rough and leads to errors in the assessment of the water content.

### **2.3.2 Hydraulic properties**

In order to assess the hydraulic characteristics of soils, laboratory or site tests must be performed on high quality natural samples.

a) The *soil-water retention curve* may be investigated through:

- tests in pressure plates or volume extractors: by the axis translation technique, such tests allow to assess the link between matric suction and water content following drying and wetting procedures. Only under the assumption of rigid skeleton it is possible to evaluate the parameters which describe the curve, i.e. the air-entry value  $(u_a - u_w)_b$ , or AEV, the residual degree of saturation,  $S_{rr}$ , and the pore size index,  $\lambda$ . For granular soils, these tests do not allow to investigate the saturation zone of the retention curve and thus to determine the air-entry value;
- tests in a suction controlled oedometer and in a suction controlled triaxial apparatus: the suction controlled apparatus allows to determine the soil-water retention curve (hence, the parameters  $(u_a - u_w)_b$ ,  $S_{rr}$ ,  $\lambda$ ) taking into the account the soil compressibility during the test itself. In this way the degree of saturation (or volumetric water content) - suction relationship is directly obtained; the coefficient of compressibility at given stress levels can also be determined;
- tests in hanging water column by progressive desaturation of initially saturated soil samples to an established energy state: the test is very useful for granular soils since it allows to exploit the very narrow air-entry region and part of the capillary zone of the water characteristic function and, hence, to determine the parameter  $(u_a - u_w)_b$ ;
- drying and wetting tests using a minitensiometer installed in the specimen: even though this technique causes some disturbance, it seems useful in the investigation of the characteristic curve of granular soils both in drying and wetting paths when approaching the saturation zone. Even though this is an unconventional test (and for this reason it is not recommendable), it is quite common, cheap and quick.

The experimental results obtained by described tests can be fitted by one of the formulations proposed in literature in order to obtain the parameters required by numerical codes (i.e. the parameters  $\alpha$ ,  $m$ ,  $n$ ,  $\theta_r$ ,  $\theta_s$  in the equation of Van Genuchten (1980) adopted in the I-MOD3D code, or Gardner's parameter  $\bar{\alpha}$  adopted in the TRIGRS code). Since only some numerical codes offer the possibility to account for hysteretic behaviour of soil, the procedure adopted in the laboratory (drying or wetting) has to be carefully considered when extracting the parameters.

b) The *coefficient of permeability* can be obtained through:

- standard permeameter tests on saturated soil specimens under constant or variable head. These provide a direct measurement of the saturated coefficient of permeability  $k_s$  (m/s);
- the steady-state methods under constant hydraulic head gradient across an unsaturated soil specimen for given suction and water content. The test can be repeated for different suction values providing the coefficient of permeability,  $k_w$  (m/s), with respect to the water phase;
- instantaneous profile methods (unsteady-state method) which provide the coefficient of permeability with respect to the water phase of unsaturated soils during water-flow processes.

The non homogeneity of soils and the presence of open discontinuities and cracks make often in situ tests more suitable for geotechnical purposes.

Field tests include:

- permeability tests: the coefficient of permeability under the groundwater level,  $k_s$ , can be measured by falling or constant head tests in wells, standpipes or in wells with monitoring piezometers. All tests can be performed by pumping or injecting water. In general, tests based on pumping water out of the well may be performed only under the ground-water level and lead to an overestimation of the hydraulic conductivity; the opposite occurs with tests based on injecting water. Good quality data can be obtained by performing both types of tests in order to compensate the potential errors;
- instantaneous profile method (unsteady-state method) suitable for low plasticity soils: it provides a direct value of the coefficient of permeability,  $k_w$  (m/s), in unsaturated soils with respect to the water phase.

It is worth noting that the measurement of the coefficient of permeability in unsaturated conditions is very difficult in both laboratory and site since the procedure requires keeping a constant degree of saturation during water-flow in steady-state tests or the measurement of a number of variables in unsteady-state tests. More usual are the indirect methods starting from the evaluation of soil water characteristic curve or analyzing the transient phase of suction equalization in tests performed in suction controlled apparatuses or in a volume extractor. The experimental values of  $k_w$  under given values of suction can be fitted by different permeability functions proposed in literature and implemented in numerical codes (Brooks & Corey, 1964; Gardner, 1958; et al.).

Difficulties arise when evapotranspiration plays a non negligible role in the hydraulic balance. In this case only monitoring of weather and site conditions can help. Actually, the installation of a weather station for monitoring of rainfall, wind speed, relative humidity of air and air temperature is necessary but not sufficient, since the evapotranspiration is governed by other parameters as well which are difficult to determine, such as the net radiation, the ground surface albedo, etc.. Only through the back-analysis of data obtained in well instrumented sites, a set of parameters can be selected for the numerical model. Otherwise, lysimeter tests can be adopted for the evaluation of actual surface ET released by plants, vegetation, crops, but they are difficult and expensive.

Numerical codes typically include theoretical or empirical formulations for the evaluation of actual evapotranspiration: in any case they need a set of weather parameters (maximum and minimum values of air temperature; maximum and minimum values of relative humidity of air; rainfall; average wind speed) that can be obtained only through in situ monitoring.

### 2.3.3 Stiffness and strength properties

Numerical codes offer a set of advanced models for the analysis of the mechanical behaviour of soils. Naturally, advanced approaches require in parallel an advanced soil characterization.

Laboratory testing has the advantage of directly measuring the mechanical soil parameters, but generally cannot be performed on *granular soils* unless using sophisticated sampling procedures, because of the difficulty to recover high quality samples. To this end, *penetration tests* are currently adopted. These have the advantage to investigate the soil response with continuity along one or more verticals. Both standard (SPT) and cone penetration tests (CPT) allow to evaluate the relative density  $D_r$  and the friction angle  $\phi'$  through empirical correlations. This is also the limit of the approach. Similarly, empirical correlations can be found linking the Young modulus  $E$  to the cone resistance  $q_c$  (Schmertmann et al., 1978; et al.).

The characterization of *fine-grained soils* can be obtained by laboratory tests. For most applications on saturated soils, a conventional triaxial apparatus is sufficient.

The Young's modulus,  $E$ , and shear modulus,  $G$ , which govern the *elastic* behaviour of soils can be obtained from the initial stage of a drained triaxial compression test by plotting the deviator stress,  $q$ , against the axial,  $\epsilon_a$ , or deviator strain,  $\epsilon_q$ . Note that other devices, such as the oedometer apparatus, or field geophysical tests, can be used to infer the elastic properties of soils, but the obtained parameters are not individual properties ( $E$ ,  $\nu$  or  $G$ ,  $K$ ), but some composite quantity which can provide one of these parameters, if assumptions are made about the others (Wood, 2004).

The Mohr-Coulomb failure criterion is most commonly adopted in *elastic-perfectly plastic models*. An elastic-perfectly plastic model with a Mohr-Coulomb failure criterion requires the definition of the elastic properties and of some strength properties: for example, the maximum angle of shearing resistance used to analyze drained problems, or a limiting shear stress used to analyze undrained conditions in cohesive soils, in conjunction with some information about the induced volume change through, for example, an angle of dilation. In this case too, compression triaxial tests can be used. The value of the parameter  $M$ , which defines the yield function, can be related to the angle of shearing resistance  $\phi$  of the soil, while the definition of the plastic potential function which describes the plastic deformation mechanism at the current stress state, requires the evaluation of another property,  $M^*$ , that must be linked to the angle of dilation  $\alpha$ .

The Cam-clay model requires the definition of other properties:

- two elastic properties: the bulk modulus,  $K$ , which is non linear and depends on the current stress level, and the shear modulus,  $G$ . The elastic volumetric response ( $K$ ) can be linked to the slope  $\kappa$  of the unload-reload line in the semi-logarithmic compression plane;  $G$  is assumed constant and can be directly determined from the initial soil behaviour in any compression test;
- two plastic properties:  $M$  ( $q/p'$ ), which controls the shape of the yield locus assumed as an elliptical surface passing through the origin of the stress plane, and the size of the ellipse,  $p'_0$ ;
- a hardening rule which describes the dependence of the size of the yield locus  $p'_0$  on the plastic strains; the hardening rule involves an additional soil parameter,  $\lambda$ , corresponding to the slope of the normal compression line in the compression plane.

Therefore, for the definition of Cam-clay parameters, as well as for those characterizing other elastoplastic models, both triaxial and oedometer tests are needed.

The modelling of unsaturated soils is more difficult. The shear strength of unsaturated specimens can be measured by suction-controlled triaxial tests which require the adoption of independent mean net stress and suction (by means of axis-translation technique). These tests enable to evaluate the effect of matric suction on the shear strength (Fredlund and Rahardjo, 1993).

For the Barcelona Basic Model (Alonso et al., 1990) there are not well established methods for selecting parameter values. This model requires three groups of parameters:

- the elastic parameters ( $\kappa$ ,  $\kappa_s$ ,  $G$ );
- the plastic parameters ( $\lambda(0)$ ,  $\beta$ ,  $r$ ,  $N(0)$ ,  $p^0$ );
- the strength parameters ( $M$ ,  $k$ )

while the isotropic preconsolidation stress at null suction ( $p_o^*$ ) defines the initial soil condition.

The three parameters describing the elastic behaviour and the two parameters describing the shear strength can be selected by analogous procedures as those adopted for saturated soils models, while the determination of the five parameters controlling the virgin loading under isotropic stress state is more difficult. In fact, each of these parameters governs more than one aspect of the soil behaviour and an iterative process is needed until a satisfactory match of the experimental data is reached (Mattsson et al., 2001; Wheeler et al., 2002).

It is worth noting that a series of laboratory tests aimed at investigating the soil behaviour under loading and unloading cycles (both in terms of suction and net stress) are needed to extrapolate such parameters. There is not a unique combination of tests but, in general the following ones are needed:

- a saturated and a suction controlled isotropic compression test including multiple loading/unloading cycles under different values of suction and multiple wetting/drying paths under different mean net stresses;
- triaxial tests including a combination of loading/unloading cycles for different values of suction and multiple wetting/drying paths under different mean net stresses before shearing.

## **2.4 GUIDELINES FOR THE USE OF NUMERICAL CODES**

### **2.4.1 Numerical modelling methods used in the landslide community (EPFL)**

#### ***2.4.1.1 Slope stability analysis methods: a brief historical review***

As it is the case for every problem in geotechnical engineering, a complete theoretical solution for a landslide problem must satisfy the following four conditions (Potts and Zdravkovic 1999):

- Equilibrium,
- Compatibility,
- Material constitutive behaviour,
- Boundary and initial conditions.

Ever since, closed form solutions and in particular analytical and numerical approximations of exact solutions have been developed for landslide problems in geotechnical engineering. Alexander Collin (1846) made already an early attempt to mathematically calculate slope stability. Fellenius (1927) proposed an analytical method for the undrained analysis of slopes in 1918, developed the first slice method in 1927 and ended up with the well known Swedish method, else known as ordinary method of slices in 1936. Taylor (1937) refined the Swedish method, proposing the Taylor's stability chart in 1937. Petterson (1955) back-calculated, by means of the limit equilibrium method, the stability of a circular failure of a slope in Goetheburg from 1916. In the same year, Bishop (1955) published the limit equilibrium method for circular failures well known as Bishop's simplified method of slices. Morgenstern and Price (1965) proposed a slice method which satisfies not only the moment equilibrium, but also force equilibrium in both directions for two-dimensional problems. In order to perform stability analyses including possible random, non-circular failure surfaces, Janbu (1973) proposed the method for generalised slip surfaces. Many other researchers further developed their own limit equilibrium methods mainly based on distinct assumptions on the distribution of inter-slice and basal forces (e.g. Spencer, 1967). Latest developments on the

limit equilibrium method were focused amongst others on 3D-effects, improved searching routines for critical failure surfaces and the incorporation of unsaturated soil mechanics (Cheng and Lau 2008).

These simple, basically analytical methods of slices which are nowadays solved numerically are used widely in engineering practice and in the scientific community. These analytical solutions fail however to satisfy all four requirements formulated above. In particular, they are inaccurate for modelling the material behaviour throughout the entire loading history. The finite element method which dates back to the late 1950's (Turner et al. 1956; Clough 1960; Argyris 1960) was the first numerical method with enough flexibility for the treatment of material heterogeneity, non-linear deformability (especially plasticity), complex boundary and initial conditions and gravity (Jing and Hudson 2002). A complete hydromechanical analysis by means of the finite element method can actually satisfy all four theoretical requirements cited above. The price to pay is primary a noticeably higher model complexity and user input requirements compared to simple methods.

#### **2.4.1.2 Numerical codes used in the SafeLand project**

Table 2 gives an overview of the numerical codes used in the SafeLand project. A more detailed description of these codes can be found in deliverable D1.2 of WP 1.2. The finite element method is visibly the most used slope analysis technique. Meshless methods are recently employed in the soil mechanics community for post-failure simulations (e.g. Pastor et al. 2008; Zabala and Alonso, 2010). An application of the material point method (MPM) to landslides is shown in section 4.1.3.2 of deliverable D1.2 and the smoothed particle hydrodynamics method (SPH) and its application to run out modelling are presented in deliverable D1.6.

**Table 2: Numerical analysis methods used in the SafeLand landslide community**

| Method                          | Code acronym  | Reference            |
|---------------------------------|---|----------------------|
| Limit equilibrium method        | Geo-Slope: Slope/W  | WP1.2, D1.2          |
| Finite element method           | LAGAMINE, GeHoMadrid, Code BRIGHT, I-MOD 3D, ELLIPSIS, Z_Soil, PLAXIS, Geo-Slope: Seep/W, Vadose/W, Sigma/W | WP1.2, D1.2          |
| Finite difference/volume method | FLAC  | WP1.2, D1.2          |
| Meshless methods                | MPM, SPH  | WP1.2, D1.2 and D1.6 |

#### **2.4.2 Preprocessing for numerical simulations (UPC)**

The construction of a numerical geotechnical model and in particular, a model for a landslide, mainly requires two aspects:

- A mathematical model to establish equilibrium of forces, compatibility of strain and displacements and the definition of a constitutive model to describe the main aspects of the soil behaviour.
- A numerical model in which a simplified or idealized geometry and initial and boundary conditions are established and allow solving the equations of the model in space and time.

The ability to reproduce field conditions essentially depends on the following aspects:

- a. Ability of the chosen constitutive model to represent soil behaviour and relevant aspects for the case analysed. Several books and papers describe different constitutive models suitable for different cases (Zienkiewicz *et al.* 1999; Potts and Zdravkovic 1999). Some examples of particular features of constitutive models suitable for landslide modelling are given below:
  - The simulation of the progressive failure, often present in first-time landslides, requires advanced constitutive models. This phenomenon is associated with materials that exhibit a brittle behaviour, defined by a maximum peak value of strength and a low residual value. In order to capture this failure mechanism, a strength softening behaviour, dependent on the relative displacement, should be included. Early classical studies on this topic were published by Skempton (1967), Bjerrum (1967) and Bishop (1967, 1971). More recent contributions have been published by Cooper (1998), Potts *et al.* (1990) and Mesri and Shahien (2003).
  - Soil degradation by chemical, mechanical and environmental actions, often associated with clayey soil rocks and cemented soils. They are also responsible of slope stability problems. The constitutive model introduced in the simulation should be able to include such degradation. In the last decades, several authors have been working on this topic, proposing conceptual frameworks and advanced constitutive models (Leroueil and Vaughan, 1990; Burland, 1990; Gens and Nova, 1993; Kavvadas, 2000; Vaunat and Gens, 2004; Pinyol *et al.*, 2006).
  - The effect of suction in unsaturated soils induces increments of strength. The saturation of slopes by rainfall, underground flow or man-made actions, namely construction of dams and reservoirs, may induce the instability of slopes. In order to simulate them, the model should be able to capture the unsaturated behaviour of soils and the transition between unsaturated and saturated states. The model should include coupled hydro-mechanical effects. Several models for unsaturated soils have been published (Alonso *et al.*, 1990, 1992, 1999; Romero and Vaunat, 2000; Gallipolli *et al.* 2003; Tamagnini, 2004, among others).
  - Liquefaction under monotonic and cyclic loading processes is also involved in triggering landslides or their run-out. This phenomenon should be captured by the constitutive model. For more information on this topic, the reader is referred to the books of Zienkiewicz *et al.* (1999) and Jefferies and Benc (2006).
- b. Appropriateness of the numerical technique. Several options are available: limit equilibrium, finite elements, finite differences, SPH meshless models (Augarde and Heaney, 2009; Pastor *et al.*, 2009), Material Point Method (Sulsky and Schreyer, 1996; Zabala and Alonso, 2010), and Distinct Element Method.
- c. Correctness of the geometry and initial and boundary conditions. The user should define the appropriate geometry, initial and boundary conditions. In general, a construction procedure should be defined in different stages that simulate the problem. They are defined by means of different boundary conditions. Some relevant aspects of this stage are given below:

- The geometry of the model and its discretization should be conceived taking into account all the modelling stages. If there are curved boundaries or curved material interfaces, higher order elements, with mid-side nodes should be used. The size and number of elements depend largely on the material behaviour, since soil behaviour influences the final solution. In order to obtain accurate solutions and reduce as much as possible the computational cost, zones where unknowns vary rapidly need special attention and require refined mesh of smaller elements. In general, meshes of regular shaped elements will give the best results.
- Initial pore water pressure distribution should be in equilibrium with boundary conditions. If this is not the case, a stage to establish such equilibrium should be allowed.
- Initial conditions of stress and pore water pressures are often difficult to estimate in the case of landslides and they have relevant importance on results. As far as initial stresses are concerned, if no accurate data is available, they can be estimated by the so called  $K_0$  procedure. In this procedure, the stress distribution is characterized by an initial vertical effective stress distribution in equilibrium with the soil weight. The effective horizontal stresses are calculated as a function of effective vertical stress according to:  $K_0 \sigma'_{v,0}$ . Note that pore water pressure distribution should be known for this methodology to be applied.
- Flux boundary conditions are classified typically in two types (Newman or Cauchy type conditions). The water inflow or outflow can be imposed at points, lines or surfaces when a flow rate is prescribed. The mass inflow or outflow can be calculated by imposing a pressure in prescribed boundaries. Sometimes it is interesting to impose a seepage boundary condition (when only outflow for liquid phase is permitted).

Building an appropriate model requires experience and solid knowledge of the topics outlined above. Only a few general remarks can be given here. The reader may find useful to read some specialized texts, for instance Potts and Zdravkovic (1999).

### **2.4.3 Numerical issues in transient slope analysis (FUNAB)**

#### ***2.4.3.1 Introduction***

As mentioned in section 2.2.3 devoted to mechanical concepts, a landslide can be considered as the failure of a geostucture, and when modelled, care has to be taken on certain issues. The numerical modelling is just one more link in the modelling chain and its quality should be consistent with that of the other links (see chapter 2).

Advanced numerical modelling is based on:

- (i) Using a suitable mathematical model –transient or dynamic- able to take into account the coupling between solid skeleton and pore fluids,
- (ii) Choosing suitable constitutive models for the materials involved in the landslide,
- (iii) Selecting a suitable numerical model and the proper options required.

#### ***2.4.3.2 Main sources of inaccuracies***

The main sources of inaccuracy which can appear in numerical modelling of landslides can be grouped as follows:

(a1) *Proper modelling of the relevant hydrologic processes.* The model has to account for seasonal variations of the hydrological regime, including the position of the water table and the correspondent boundary conditions. Variation of reservoirs and lakes levels at the toe of slopes can be crucial.

(a2) *Initial conditions.* The response of a slope to external actions causing a landslide is greatly dependent on the assumed initial stresses. While in some cases the analyst can reproduce reasonably well the slope formation process –railroad and road cuts, mining heaps– in most cases it is a difficult if not an impossible task. If there exist different alternatives or assumptions, the analyst has to test all possible combinations studying the sensitivity of the triggering conditions to the initial stress field.

(b1) *Constitutive model.* We have already addressed in section 2.2.3 the importance of choosing a suitable constitutive model. If failure is of localized type, no classical plasticity of associative type will be able to predict a catastrophic failure. Moreover, the analysis will fall on the unsafe side, because peak friction is smaller than the residual friction angle used in the analysis.

(c1) *Model extension.* The temptation of saving computer time by using a reduced domain should be avoided, because deep seated failure surfaces will not be properly modelled. Indeed, the domain has to have an extension of at least twice the expected failure mechanism.

(c2) *Mesh size (1/2).* When dealing with softening materials and localized failure mechanisms the analyst should be aware of the following facts:

- The shear band is smeared over several element widths; therefore finer meshes will provide a much better resolution minimizing band diffusion.
- When using coarse meshes, the resulting failure mechanism will be more ductile, i.e., less “catastrophic” than the real one.
- The mathematical nature of the problem changes from elliptic to hyperbolic in transient problems, and from hyperbolic to elliptic in dynamics when using plasticity models. Regularization of the problem can be done by using (i) non local models, (ii) gradient models, (iii) Cosserat models and (iv) viscoplastic models (Vardoulakis and Sulem).

The results depend, therefore, in a spurious manner on the mesh size. Figure 4 illustrates the failure simulation of a soil beneath a rigid footing considering different mesh sizes. Shear band widths and failure loads vary as a function of the mesh size.

(c3) *Mesh structuring.* When preparing the finite element mesh, care should be taken in avoiding unnatural mesh structuring and alignment which can be produced by some pre-processors when choosing some meshing options. Most of displacement-based finite elements are dependent on mesh alignment. In order to illustrate this effect, we provide in figure 5 the example of a vertical cut on a purely cohesive soil which has been discretized with two different aligned meshed of linear triangles. It can be seen that failure mechanism captured by the wrong alignment provides a wrong failure mechanism.

(c4) *Mesh size (2/2).* In the case of dynamic problems, there exist numerical damping causing an spurious attenuation of the wave amplitude. This effect depends on the algorithm being used, on the Courant number (ratio of physical and numerical velocities) and the relation between the mesh size and the wave length. For a given Courant number, we have to choose element sizes smaller than 1/10 to 1/20 of the shorter propagation wavelength.

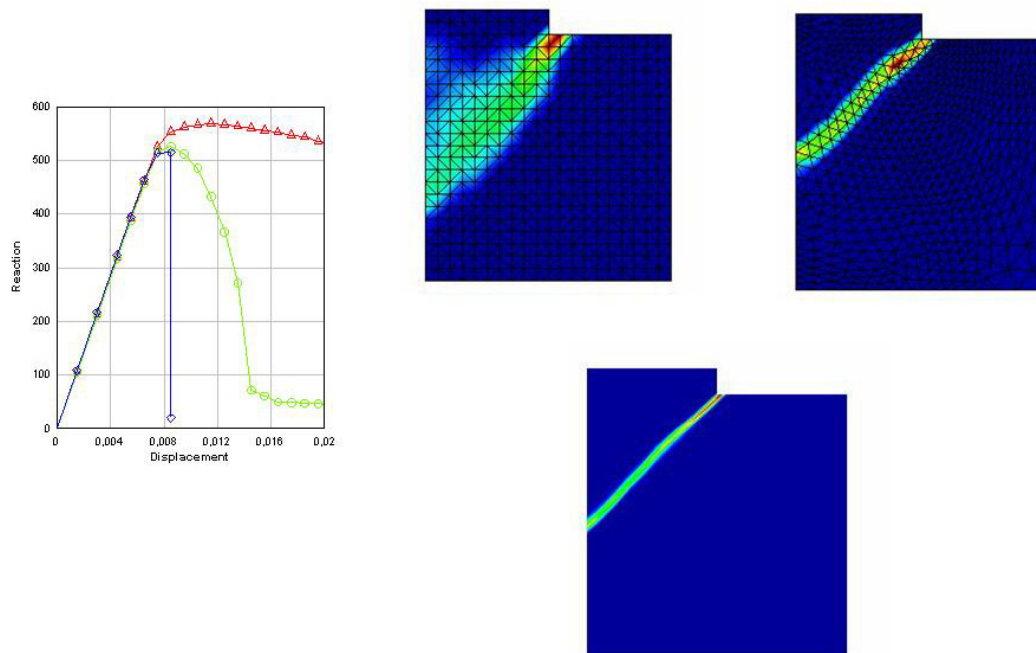


**Figure 4: Influence of mesh size on the fragility and the shear band width**

(d1) *Type of finite element.* In order to properly model failure problems and triggering of landslides, the following types of finite elements have to be used:

- Selective and reduced integration, using for instance quadratic quadrilaterals with a reduced integration rule for the volumetric component of the stiffness matrix. In the case of coupled problems, the interpolation of pore pressures is bilinear in 2D.
- Enhanced strain methods, introduced by Simo and Rifai (1990). The problem here is that this element –bilinear quadrilateral in 2D- cannot be used with a bilinear interpolation of the pore pressure unless stabilization techniques such as proposed by Mira et al (2003) are used.
- Mixed stress-velocity approximations, such as that introduced by Mabssout and Pastor (2003) allow the use of simple linear elements which are not affected by mesh alignment.

(d2) *Boundary conditions.* The numerical models used for the analysis of landslides have to have a limited extent. These boundaries are artificial, and require suitable boundary conditions. In the case of slow varying, transient problems, the boundary conditions can be of the prescribed displacement type, sometimes combined with zero shear stress. Concerning the pore pressures, the analysts frequently use no flux boundaries. In the case of dynamical problems, suitable radiation or transparent boundary conditions have to be chosen. Otherwise, waves originating within the domain will return to it, resulting sometimes in an unnatural amplification.

### 2.4.3.3 Strategies of analysis

#### (a) Quasi static versus dynamics

Even in the case of quasi static problems, where loads can be applied very slowly, accelerations can be produced once the load has exceeded its failure value. If the structure presents global softening, its strength will be decreasing, which will result in higher accelerations. In these cases the analyst must consider the possibility of performing a dynamic

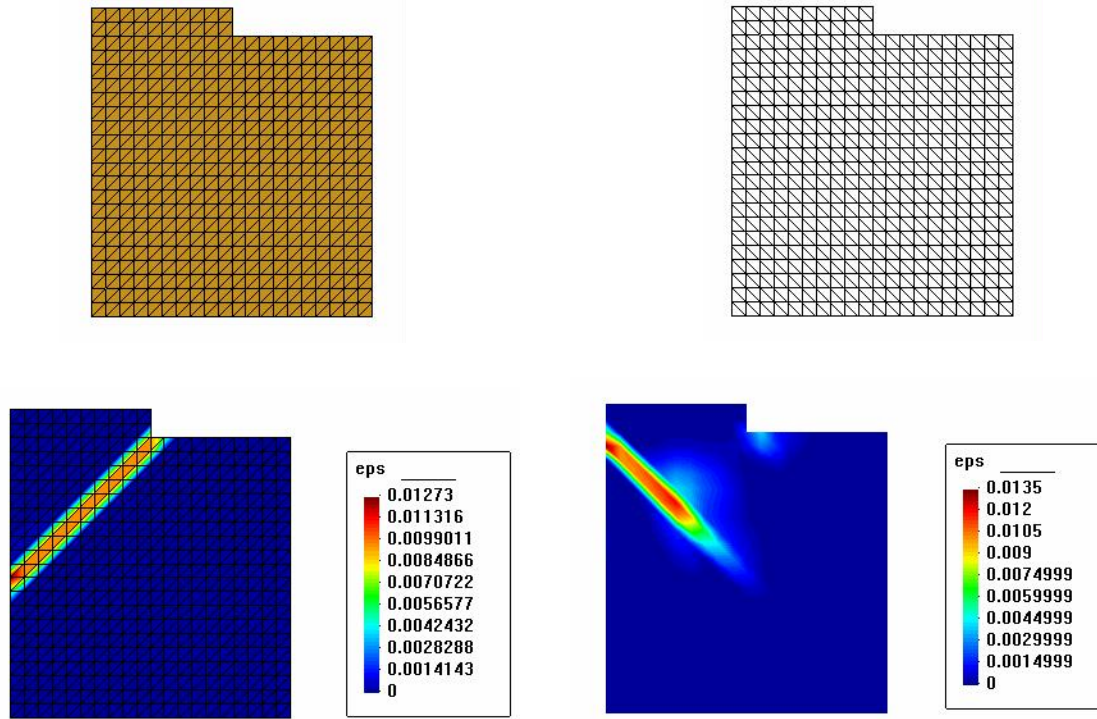


**Figure 5: Influence of mesh alignment in the computation of the failure mechanism of a vertical cut on a purely cohesive soil. A point load is applied at the center of a rigid footing on top of the cut.**

analysis including inertia terms in the mathematical model. This extends the validity of the simulation during the softening phase.

#### (b) Load or displacement control

In classical analysis of failure the analyst can choose between load and displacement control. Let us consider a slope at which top a distributed load –buildings, for instance- is being applied. A first strategy which can be chosen is to divide the load in a series of increments, and apply them until failure is reached. However, the last increment can create a load higher than the limit, and the solution algorithm will not converge. The analysis will end at the step 3, with a limit load between the values of increments 3 and 4.

Alternatively, the analysis can be performed controlling (imposing) the displacement at a certain control point. In this way it is possible to pass the limit load and enter the softening regime. It must be noticed that in highly nonlinear problems the size of the increment will influence the convergence. The ideal situation is to converge in some 5-8 iterations. Adaptive step size techniques can be used to increase or decrease the increment size in a linear manner having as a target the convergence in the required number of iterations.

#### (c) Time dependent problems

In some time dependent problems, where pore pressures vary, failure can arrive after some time has elapsed. This case occurs for example when analyzing the failure of a slope under rain using a transient analysis without inertia terms. Failure is characterized by an acceleration of the rate at which displacements are growing, and the program stops running as convergence is not attained. Figure 7 and 8 illustrate the development of a failure mechanism and horizontal displacements at middle height in a slope subjected to rainfall infiltration (Fernandez Merodo et al. 2004). Time to failure and the mobilised volume can be determined.

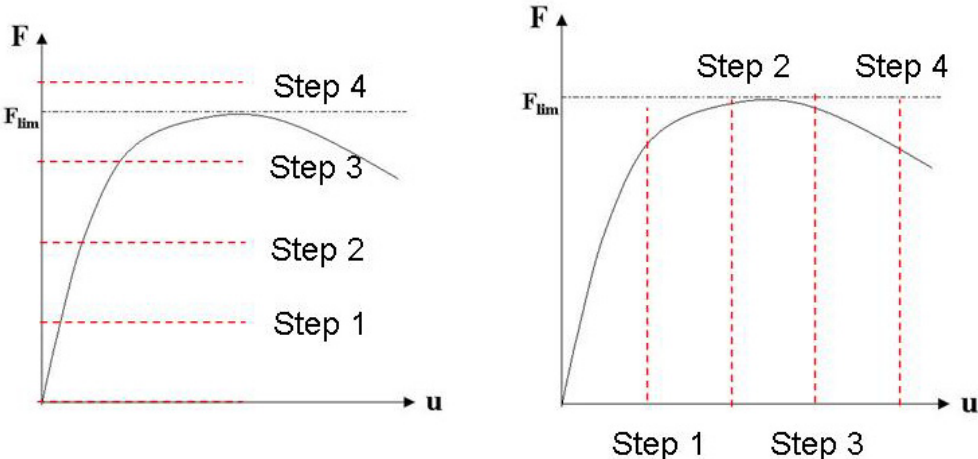


Figure 7: Load and displacement control strategies

(d) Stress reduction methods

One popular method used to assess the safety of slopes is the strength reduction method. It consists of reproducing the working conditions of a natural slope –initial stresses and pore pressures- and then to decrease its strength in a series of steps where steady state conditions or failure are attained. It is easy to apply in the case of purely cohesive or frictional soils, but much more difficult in cases where the constitutive models describing the materials of the slope are more complex. Even in the case of frictional cohesive materials, it is convenient to follow from an initial state several paths with a given combination of the reduction factors in both friction angle and cohesion.

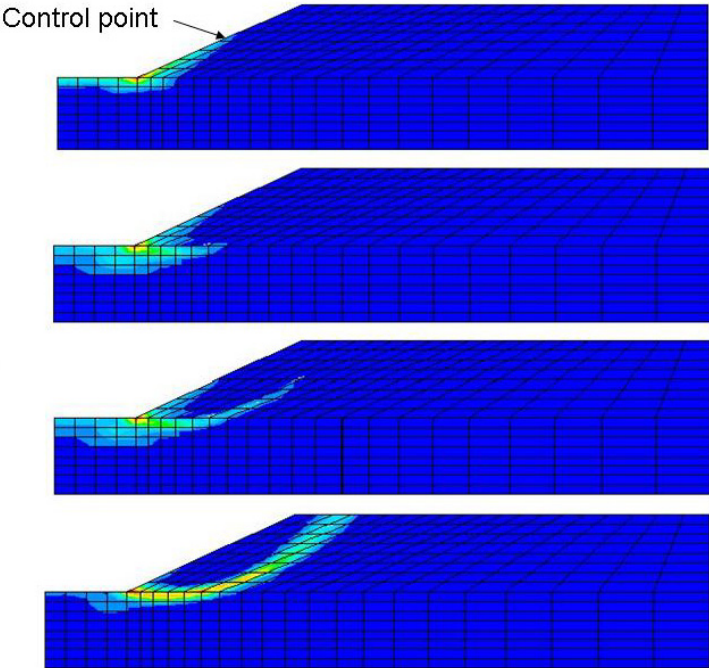
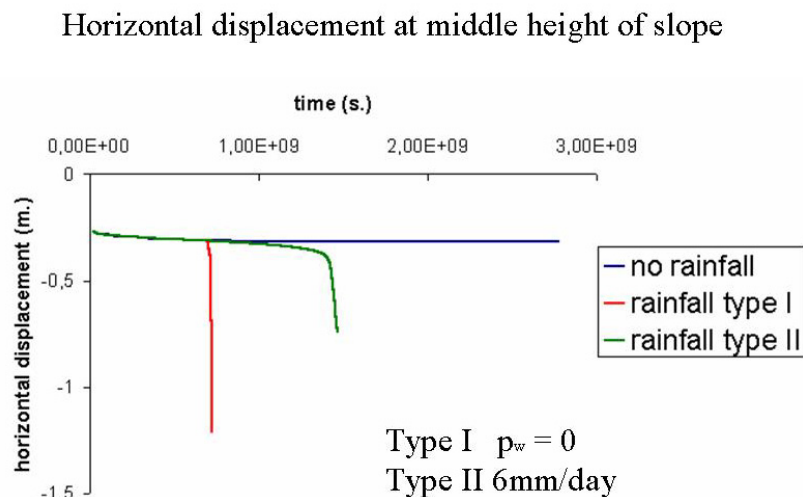


Figure 6: Cut slope failure induced by rain. Isolines of deviatoric plastic deformation.



**Figure 8: Cut slope failure induced by rain. Time evolution of horizontal displacements at mid height of slope for several alternative assumptions.**

#### 2.4.4 Postprocessing: output data and analysis of results (CNRS)

The last step of the modelling process is the post-processing. Due to the complex subsurface conditions, the complex hydraulic and mechanical conditions, and the coupled hydro-mechanical conditions within most landslides, numerical modelling of landslides is very difficult. To evaluate the modelling approach the analysis has to be interpreted using the results of the numerical simulation (output data). Typical output data in landslide modelling are stresses (total stresses, effective stresses, pore water pressures, excess pore water pressures), strains (shear strains, volumetric strains), displacements (total displacements, horizontal displacements, vertical displacements) and the development of these quantities in time using stress rates, strain rates and displacement rates (velocities). The analysis of such quantities allows a sound engineering judgment on the problem but the reliability of the model and the computed results has to be checked by comparing the output data with field measurements (c.f. figure 1 in section 2.1).

That means before predicting the future slope behaviour, numerical modelling of the past or present slope behaviour has to be performed. Then the model has to be validated by comparing the computed results with the past and present field data and given a positive comparison the validated model can be used to predict the behaviour of the investigated landslide problem.

Because of the large dimensions and heterogeneities of landslides it is not possible to monitor all the information necessary to characterize the real slope behaviour. The comparison of computed results and measurements is limited to certain features. Such features are the development and location of shear surfaces, the groundwater regime and the kinematics of landslides. In the following it is presented how these features can be monitored in the field and which output data is used, related to these features, to evaluate the numerical model.

##### 2.4.4.1 Development and location of shear zones

In the field the location of slip surfaces can be estimated by inclinometer measurements. Inclinometers can measure lateral movements or movement rates below the ground surface and provide information on the depth of landslide movements (landslide thickness) and the thickness of the shear zone (Cornforth 2005). An example of inclinometer measurements

installed at the Super-Sauze landslide in the South French Alps and the interpretation of the inclinometer readings of one location is given in Figure 9. The interpretation of the data measured with inclinometer F1 results in the existence of one shear zone in a depth of about 9.5 m with a thickness of 5 m.

In numerical modelling the initiation of failure, i.e. the development and the location of a shear zone for the localised failure type is indicated by following output quantities (dependent on the numerical code):

- irreversible strain rate, such as e.g. shear strain rate
- irreversible strain, such as plastic strain, equivalent plastic strain, equivalent viscoplastic strain (c.f. Figure 10)
- zero tension zones (zero tensile strength within zones/elements denotes the region in which tensile failure occurs)
- plasticity indicators (c.f. Figure 10)

In the modelling of the La Maina landslide in the Carnian Alps, Italy, Marcato et al. (2006) determine the position of slip surfaces using the maximum shear strength increment indicating the finite difference zones in which most intensive shear slip occurs. Slip surface development can be studied during the calculation of the first calculation phase without water, the second phase using the actual water table and the third phase where the water table is increased by 6 m. Whereas the shear zone is fragmented in the second phase, it is continuous in the third phase. The reliability of the results was checked by their comparison of failure surface location in the inclinometer holes with the depths calculated, i.e. calculated horizontal

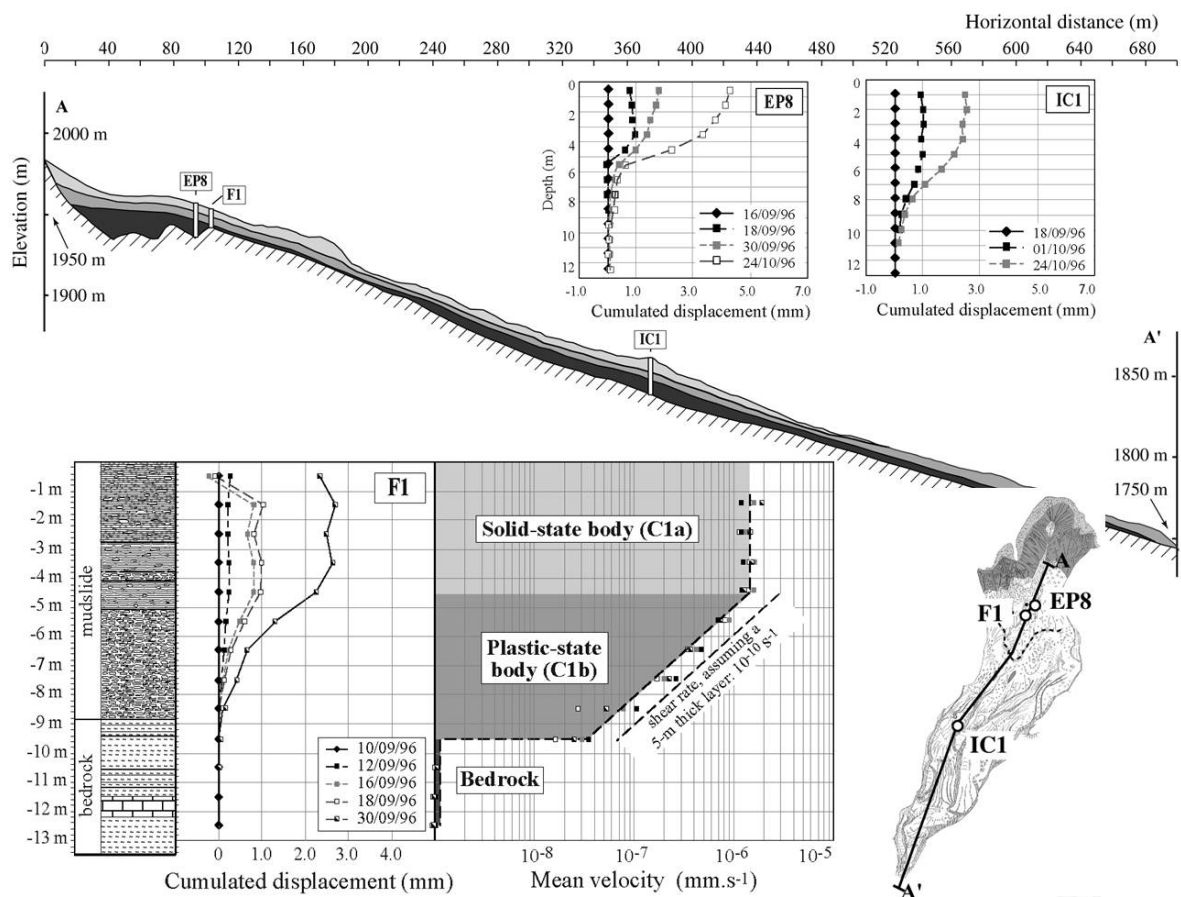


Figure 9: Inclinometer measurements of three different locations within the longitudinal profile of the Super-Sauze landslide (South French Alps) and interpretation of inclinometer data F1 (Malet, 2003).

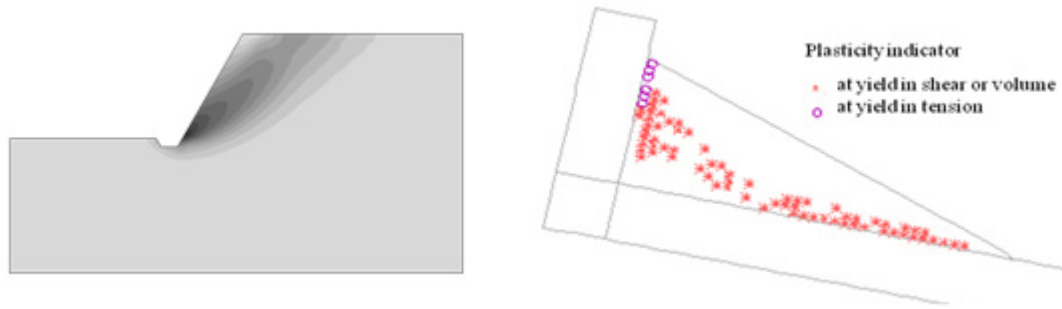


Figure 10: (a) Equivalent visco-plastic strains as output quantity to analyse the development and location of a shear zone/failure surface (Spickermann, 2008); (b) Plasticity indicators as output quantity to analyse the development and location of a shear zone/failure surface.

displacement curves and the location of measured slip zones is drawn for four inclinometers.

#### 2.4.4.2 Groundwater regime

The modelling of the groundwater regime can be validated by piezometric measurements. Piezometers measure pore water pressures and groundwater heads. With the advent of automatic data acquisition systems it is possible to monitor piezometric levels continuously, which is used e.g. to check the modelling of the groundwater response on rainfall.

In Malet et al. (2005) a coupled unsaturated/saturated model, incorporating Darcian saturated flow, fissure flow and meltwater flow is developed to forecast the future hydrological behaviour of the Super-Sauze landslide. The model is calibrated and validated on a database acquired on the site since 1997.

Figure 11 shows the location, the monitored groundwater levels and the simulation results of two piezometers, EV2 and BV16, after calibration.

#### 2.4.4.3 Landslide kinematics

Selected information on lateral displacements in depth is provided by inclinometer measurements. With this the movement of only certain points of a slope model can be

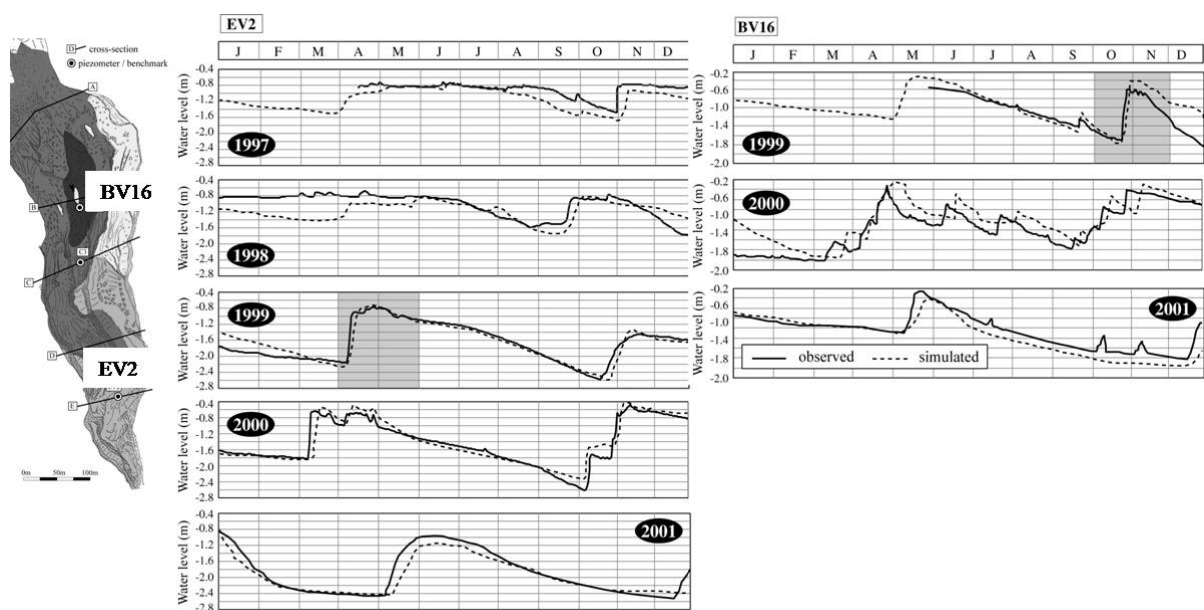


Figure 11: Hydrological model evaluation using monitored groundwater levels of the Super-Sauze landslide during the time period of 1997-2001.

compared with field data. Downhill monitoring by inclinometers is restricted to the recording of displacements in the range of cm. Wire extensometer devices may last working for several metres but measured displacements are global. The device can neither detect the vertical and the horizontal components of displacements nor identify the presence of several slip surfaces (Corominas et al. 2000).

Superficial ground movements can be surveyed continuously by theodolites, Electronic Distance Measurement (EDM) instruments and global positioning system (GPS) that require a system of local benchmarks that has to remain stable and visible during the course of investigation. Due to spatial and temporal heterogeneities such ground-based measurements are not accurate enough to fully describe the velocity field of a landslide. In the last few years, remote-sensing methods such as interferometry for radar data and image correlation for optical data have been developed allowing continuous superficial measurements of displacement fields. In Delacourt et al. (2007) these remote sensing techniques are reviewed and examples of applications are given. The methods are applied on sensors, i.e. radar, cameras or terrestrial 3D laser scanning. These sensors are attached to space or aerial platforms such as satellites, planes, and unmanned radio-controlled platforms (drones and

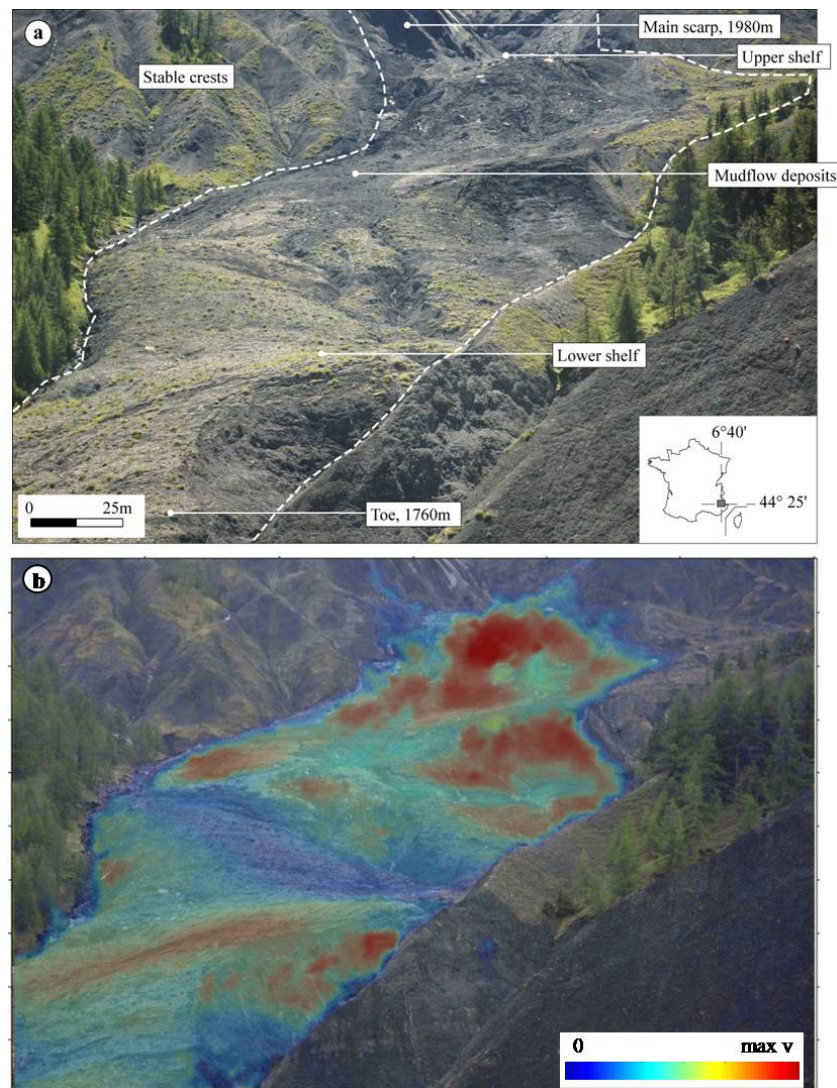


Figure 12: Velocity field at a certain time monitored by EOVS (School and Observatory of Earth Sciences, Strasbourg, France) using a high resolution optical camera located on a stable crest and digital image correlation (DIC).

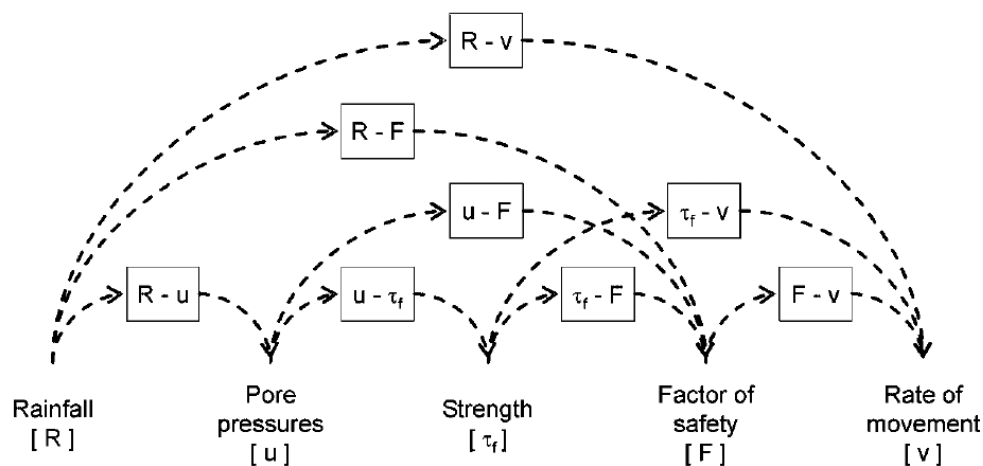


Figure 13: Conceptual schematization of the approaches used to model the kinematic response of landslides to rainfall (Calvello et al. 2008; modified from Leroueil 2001).

helicopters) or settled at fixed positions emplaced in the front of landslides. Figure 12 shows an example of the continuous monitoring of the displacement field at the Super-Sauze landslide using a high resolution optical camera located on a stable crest and digital image correlation (DIC).

In the past the comparison of measured and computed displacements were carried out at selective points on the landslide. Nowadays with the described monitoring techniques advanced three-dimensional model approaches can be evaluated in terms of superficial displacement fields.

Prediction of climate-induced landslide behaviour by means of e.g. hydro-mechanical modelling requires a first postprocessing phase, i.e. the foregoing validation of the model by comparing computed and measured quantities obtained in the past and a second postprocessing phase in which a future trend is predicted by interpreting the output data.

## 2.5 USE OF NUMERICAL CODES FOR LANDSLIDE EARLY-WARNING AND LONG-TERM PREDICTIONS (EPFL)

Many phenomenological or semi-physical based models have been developed at regional and slope scales associating slope failure to local threshold values with respect to rainfall intensity and duration (see R-F models in Fig. 13). Some methods interpret directly monitoring data to predict time of failure or velocity increase (see R-v models in Fig. 13) (Saito 1965; Kawamura 1985; Voight 1988). A major drawback of these phenomenological models is to rely on surface measurements of velocities, as well as on time-constant boundary conditions to predict failure (Eberhardt et al. 2008; Bonnard 2006). In the case of large, creeping landslides, Petley et al. (2008) reported that the Saito type of models only predict failure in the tertiary creep phase, but are not applicable for the slow-moving phase. According to Eberhardt et al. (2008), only a few cases have been reported where these techniques have been successfully applied as part of a reliable forward prediction. Other methods are more useful in that case as for example back-propagation algorithms or neural network tools (ANN). Artificial neural network tools have proven to be efficient for forward calculations of slow-moving landslides. More recently, neural network based constitutive models (NNCM) have been incorporated in finite element codes (Shin et al. 2000). The idea is to introduce the constitutive model as a neural network operator in the code. However, these networks which

are trained with test data sets from past measurements are incapable of predicting sudden acceleration phases originating from changing physical processes in the soil (Mayoraz and Vulliet 2002). Other recently developed systems, such as the evolutionary polynomial regression-based constitutive models (EPRCM) coupled with FEM (Javadi and Rezania 2009) may be more efficient and cheaper in a computational sense, but their response depends on the training data set as well.

Physically based models try to simulate the complex hydromechanical processes in landslides (i.e.  $R-u-\tau_r-F$ ,  $R-u-\tau_r-v$  in figure 13). They allow in many cases a better understanding of the slope behaviour and can simulate failure mechanisms accurately. However, these models need realistic, variable initial and boundary conditions and optimized input parameters for reliable predictions, especially related to climate change effects. The physical models can be enhanced with empirical relationships and input parameters can be inferred by means of backcalculation (Calvello et al. 2008).

Especially the availability of continuous records of both velocities and groundwater table in monitored landslides offers new possibilities for studying the dynamics of slow moving landslides (Gonzales et al. 2008; Eberhardt et al. 2008). The quality of prediction issued from statistical tools, such as ANN, can be increased due to the availability of larger datasets. As a consequence, mixed models with soft and hard computing components will certainly be a focus of attention in coming years.

### 3 PERFORMANCE OF NUMERICAL CODES

#### 3.1 PERFORMANCE CHECK OF CODES FOR SLOPE SCALE ANALYSIS (EPFL)

The numerical, physically-based codes which are used in the SafeLand project for the modelling of slope failure initiation have been described in deliverables D1.2. In this section, the various home-made and commercial codes are evaluated with respect to the code components summarised in section 2.2.5. This allows the user to identify the numerical code suitable for a solving a specific landslide problem. Table 3 presents the performance check for the home-made codes Lagamine, GeHoMadrid, Code\_BRIGHT, Ellipsis and I-Mod 3D. The evaluation of the commercial codes Z\_Soil, Flac, Plaxis and the GeoSlope package is shown in Table 4.

Table 3: Evaluation of home-made codes for the numerical analysis of landslides

| Topic              | Specification             | Component  | Home-made codes (reference: D1.2) |             |             |          |          |
|--------------------|---------------------------|--|-----------------------------------|-------------|-------------|----------|----------|
|                    |                           |  | Lagamine                          | GeHo Madrid | Code_BRIGHT | I-MOD 3D | ELLIPSIS |
| Problem definition | Slope geometry            | Slope angle, shape and domain meshing            | ✓                                 | ✓           | ✓           | ✓        | ✓        |
|                    | Soil stratigraphy         | Material layers                                  | ✓                                 | ✓           | ✓           | ✓        | ✓        |
|                    | Pre-existing slip surface | Interface elements for large displacements       | ✓                                 | ✓           | ✗           | ✗        | ✗        |
|                    |                           | Material layer for shear zone with small strains | ✓                                 | ✓           | ✓           | ✗        | ✓        |
|                    | Boundary conditions       | Hydraulic  | ✓                                 | ✓           | ✓           | ✓        | ✗        |
|                    |                           | Mechanical                                       | ✓                                 | ✓           | ✓           | ✗        | ✓        |
|                    | Initial conditions        | Hydraulic  | ✓                                 | ✓           | ✓           | ✓        | ✗        |
|                    |                           | Mechanical                                       | ✓                                 | ✓           | ✓           | ✗        | ✓        |
| Material           | Phases                    | Single phase approach                            | ✓                                 | ✓           | ✓           | ✗        | ✓        |
|                    |                           | Two- or three phase approach                     | ✓                                 | ✓           | ✓           | ✓        | ✗        |
| Analysis type      | Steady state analysis     | No time dependency                               | ✓                                 | ✓           | ✗           | ✓        | ✓        |
|                    | Transient analysis        | Time dependency of hydromechanical processes     | ✓                                 | ✓           | ✓           | ✓        | ✓        |
|                    | Hydromechanical coupling  | Semi-coupled approach                            | ✓                                 | ✓           | ✓           | ✗        | ✗        |

|                                       |  |  |   |   |   |   |   |
|---------------------------------------|--|--|---|---|---|---|---|
|                                       |  | Fully coupled approach                                       | ✓   | ✓ | ✓ | ✗ | ✗ |
| <b>Governing equations</b>            | Equilibrium                                    | Balance of linear momentum                                   | ✓   | ✓ | ✓ | ✗ | ✓ |
|                                       | Transient H, uncoupled HM approach             | Mass conservation for fluids                                 | ✓   | ✓ | ✓ | ✓ | ✗ |
|                                       | Transient, HM coupled approach                 | Coupled mass conservation for solid and fluids               | ✓   | ✓ | ✓ | ✗ | ✗ |
| <b>Material behaviour: Hydraulics</b> | Fluid flow                                     | Darcy's law  | ✓   | ✓ | ✓ | ✓ | ✗ |
|                                       | Anisotropic permeability                       | Second-order permeability tensor                             | ✓   | ✓ | ✓ | ✗ | ✗ |
|                                       | Permeability in unsaturated soils              | Hydraulic conductivity fct                                   | ✓   | ✓ | ✓ | ✓ | ✗ |
|                                       | Water retention for unsaturated soils          | Soil water characteristic curve                              | ✓   | ✓ | ✓ | ✓ | ✗ |
| <b>Material behaviour: Mechanics</b>  | Soil stiffness depending on confining pressure | Non-linear elasticity  | ✓   | ✓ | ✓ | ✗ | ✓ |
|                                       | Anisotropic deformability or shear strength    | Transversal, elastic isotropy, anisotropic elasto-plasticity | ✗   | ✗ | ✗ | ✗ | ✗ |
|                                       | Stress redistribution due to material yielding | Yield criterion  | ✓   | ✓ | ✓ | ✗ | ✓ |
| <i>Plasticity</i>                     | Onset of failure                               | Hardening plasticity   | ✓   | ✓ | ✓ | ✗ | ✓ |
|                                       | Dilatancy                                      | Non-associative plasticity                                   | ✓   | ✓ | ✓ | ✗ | ✓ |
|                                       | Instability phenomena                          | Dilatancy, constitutive features for volume compaction       | ✓   | ✓ | ✓ | ✗ | ✓ |
|                                       | <i>Viscosity</i>                               | Soil creep   | Non-linear viscous or elasto-viscoplastic model | ✗ | ✓ | ✓ | ✗ |
| Stress relaxation                     |  | Non-linear viscous or elasto-viscoplastic model              | ✗   | ✓ | ✓ | ✗ | ✓ |
| <i>Capillary effects</i>              | Capillary effects on stress state              | Effective stress framework for unsaturated soils             | ✓   | ✓ | ✓ | ✗ | ✗ |
|                                       | Shear strength increase                        | Extension of yield surface as a function of capillary stress | ✓   | ✓ | ✓ | ✗ | ✗ |

|                      |   |   |   |   |   |   |   |
|----------------------|---|---|---|---|---|---|---|
|                      | Volumetric changes during wetting           | Elastic swelling  | ✓ | ✓ | ✓ | ✗ | ✗ |
|                      |   | Plastic swelling  | ✗ | ✓ | ✓ | ✗ | ✗ |
|                      |   | Wetting pore collapse   | ✓ | ✓ | ✓ | ✗ | ✗ |
| <b>Temp. effects</b> | Heat and vapour diffusion                   | Fourier and Fick's law  | ✓ | ✗ | ✓ | ✗ | ✗ |
|                      | Phase changes: Water vapour ↔ liquid water  | Coupling between heat, water and vapour conservation equation | ✓ | ✗ | ✓ | ✗ | ✗ |
|                      | Thermal-induced elastic strains             | Thermo-elasticity   | ✓ | ✓ | ✓ | ✗ | ✓ |
|                      | Effects of temperature on material strength | Yield function and plastic potential depending on temperature | ✓ | ✗ | ✗ | ✗ | ✓ |

Table 4: Evaluation of commercial codes for the numerical analysis of landslides

| Topic                     | Specification             | Component  | Commercial codes (reference: D1.2) |   |             |  |
|---------------------------|---------------------------|--|------------------------------------|---|-------------|--|
|                           |                           |  | Z_Soil                             | PLAXIS<br><sup>1</sup> With<br>PLAXFLO<br>W | FLAC        | <sup>1</sup> Seep/W or<br><sup>2</sup> Vadose/W<br>+ <sup>3</sup> Sigma/W<br>or <sup>4</sup> Slope/W |
| <b>Problem definition</b> | Slope geometry            | Slope angle, shape and domain meshing            | ✓                                  | ✓   | ✓           | ✓  |
|                           | Soil stratigraphy         | Material layers                                  | ✓                                  | ✓   | ✓           | ✓  |
|                           | Pre-existing slip surface | Interface elements for large displacements       | ✓                                  | ✓   | ✓           | ✓ <sup>3)</sup>  |
|                           |                           | Material layer for shear zone with small strains | ✓                                  | ✓   | ✓           | ✓  |
|                           | Boundary conditions       | Hydraulic  | ✓                                  | ✓   | ✓           | ✓  |
|                           |                           | Mechanical                                       | ✓                                  | ✓   | ✓           | ✓  |
|                           | Initial conditions        | Hydraulic  | ✓                                  | ✓   | ✓           | ✓  |
|                           |                           | Mechanical                                       | ✓                                  | ✓   | ✓           | ✓  |
| <b>Material</b>           | Phases                    | Single phase approach                            | ✓                                  | ✓   | ✓           | ✓  |
|                           |                           | Two- or three phase approach                     | ✓<br>2phase                        | ✓<br>2phase                                 | ✓<br>3phase | ✓ <sup>3)</sup><br>2phase  |
| <b>Analysis type</b>      | Steady state analysis     | No time dependency                               | ✓                                  | ✓   | ✓           | ✓  |
|                           | Transient analysis        | Time dependency of hydromechanical processes     | ✓                                  | ✓   | ✓           | ✓  |

|                                       |  |  |  |                          |          |           |      |
|---------------------------------------|--|--|--|--------------------------|----------|-----------|------|
|                                       | Hydromechanical coupling                       | Semi-coupled approach  | ✓  | ✓                        | ✓        | ✓         |      |
|                                       |  | Fully coupled approach                                       | ✓  | ✓                        | ✓        | ✓ 3)      |      |
|                                       | Safety factor analysis                         | Shear strength reduction method                              | ✓  | ✓                        | ✓        | ✓ 3)      |      |
|                                       |  | Limit equilibrium  | ✗  | ✗                        | ✗        | ✓ 4)      |      |
| <b>Governing equations</b>            | Equilibrium                                    | Balance of linear momentum                                   | ✓  | ✓                        | ✓        | ✓         |      |
|                                       | Transient H, uncoupled HM approach             | Mass conservation for fluids                                 | ✓  | ✓                        | ✓        | ✓ 1) + 3) |      |
|                                       | Transient, HM coupled approach                 | Coupled mass conservation for solid and fluids               | ✓  | ✓ 1)                     | ✓        | ✓ 3)      |      |
| <b>Material behaviour: Hydraulics</b> | Fluid flow                                     | Darcy's law  | ✓  | ✓                        | ✓        | ✓         |      |
|                                       | Anisotropic permeability                       | Second-order permeability tensor                             | ✓  | ✓                        | ✓        | ✓         |      |
|                                       | Permeability in unsaturated soils              | Hydraulic conductivity fct                                   | ✓  | ✓ 1)                     | ✓        | ✓ 1)      |      |
|                                       | Water retention for unsaturated soils          | Soil water characteristic curve                              | ✓  | ✓ 1)                     | ✓        | ✓ 1)      |      |
| <b>Material behaviour: Mechanics</b>  | Soil stiffness depending on confining pressure | Non-linear elasticity  | ✓  | ✓                        | ✓        | ✓ 3)      |      |
|                                       | Anisotropic deformability or shear strength    | Transversal, elastic isotropy, anisotropic elasto-plasticity | ✓  | ✓<br>Elastic & elastopl. | ✓        | ✓ 3)      |      |
|                                       | <i>Plasticity</i>                              | Stress redistribution due to material yielding               | Yield criterion  | ✓                        | ✓        | ✓         | ✓    |
|                                       |  | Onset of failure   | Hardening plasticity                                   | ✓                        | ✓        | ✓         | ✓ 3) |
|                                       |  | Dilatancy  | Non-associative plasticity                             | ✓                        | ✓        | ✓         | ✓    |
|                                       | <i>Viscosity</i>                               | Instability phenomena  | Dilatancy, constitutive features for volume compaction | ✓                        | ✓        | ✓         | ✓ 3) |
|                                       |  | Soil creep   | Non-linear viscous or elasto-viscoplastic model        | ✓                        | ✓        | ✓         | ✗    |
| Stress relaxation                     |  | Non-linear viscous or elasto-viscoplastic model              | ✗  | ✓                        | ✓        | ✗         |      |
| <i>Capillary effects</i>              |  | Capillary effects on stress state                            | Effective stress framework for unsaturated soils       | ✓ Bishop                 | ✓ Bishop | ✓         | ✗    |

|                      |  |   |                               |                               |   |                            |
|----------------------|--|---|-------------------------------|-------------------------------|---|----------------------------|
|                      | Shear strength increase  | Extension of yield surface as a function of capillary stress  | ✓ due to $\sigma'$ definition | ✓ due to $\sigma'$ definition | ✓ | ✓ 3)<br>Mod. App. cohesion |
|                      | Volumetric changes during wetting  | Elastic swelling  | ✓                             | ✓                             | ✓ | ✓                          |
|                      |  | Plastic swelling  | ✗                             | ✗                             | ✗ | ✗                          |
|                      |  | Wetting pore collapse   | ✗                             | ✗                             | ✗ | ✗                          |
| <b>Temp. effects</b> | Heat and vapour diffusion  | Fourier and Fick's law  | ✓                             | ✗                             | ✓ | ✗                          |
|                      | Phase changes: Water vapour ↔ liquid water                                 | Coupling between heat, water and vapour conservation equation | ✗                             | ✗                             | ✗ | ✗                          |
|                      | Thermal-induced elastic strains  | Thermo-elasticity   | ✓                             | ✗                             | ✓ | ✗                          |
|                      | Effects of temperature on material strength & magnitude of plastic strains | Yield function and plastic potential depending on temperature | ✗                             | ✗                             | ✗ | ✗                          |

### 3.2 PERFORMANCE CHECK OF CODES FOR REGIONAL SCALE ANALYSIS (UNISA)

At medium-large scale (Fell et al. 2008a, 2008b), a promising approach for the susceptibility analysis of the rainfall-induced shallow landslides source areas relies on the use of the so-called physically based models for their capability in reproducing the physical processes governing the landslides occurrence. Moreover, their general grid-based structure and the wide availability of Geographic Information Systems provide a convenient framework that allows the susceptibility analysis over broad areas.

Although these models have been already presented and discussed in deliverable D1.2, it is worthwhile to summarise some of their main characteristics, in order to allow a better understanding of their performance in the analysis of a relevant case study, which represents the object of the current section.

Physically based models generally couple a hydrologic model, for the analysis of pore water pressure regime, with an infinite slope stability model for the computation of the Factor of Safety. These models rely on several simplifying assumptions that limit their applicability. Particularly, steady or quasi-steady models (e.g. Montgomery and Dietrich 1994; Wu and Sidle 1995) are limited to few unrealistic situations related to both rainfall characteristics and in situ conditions (Iverson 2000). Transient models, used either in saturated or unsaturated conditions of soils, are able to improve the effectiveness of susceptibility analysis, accounting for the transient effects of varying rainfall on slope stability conditions (e.g. Baum et al. 2002, 2008; Crosta and Frattini 2003; Iverson 2000; Savage et al. 2004), but they generally need abundant and accurate spatial information. Moreover, they are sensitive to some of the required input data such as hydraulic properties of soils, initial steady-state groundwater conditions and soil depths, whose correct evaluation is often possible only using empirical

models or inverse deterministic analyses (Godt et al. 2008; Salciarini et al. 2006; Sorbino et al. 2007).

In order to achieve significant results, the application of physically based models requires a deep understanding of the conceptual assumptions, the accurate definition over broad regions of the in situ conditions of soils, of the pore pressure regime characteristics, as well as of the different triggering mechanisms. Moreover, a critical interpretation of results needs a methodology based on the use of quantitative indexes (Crosta and Frattini 2003; Godt et al. 2008; Salciarini et al. 2006; Sorbino et al. 2007).

In the following, a relevant example is presented with reference to an area in Campania Region (southern Italy) of about 60 km<sup>2</sup>, systematically affected during the centuries and in recent times by rainfall-induced shallow landslides of flow-type involving volcanoclastic covers. Particularly, the source areas of the most recent and catastrophic shallow landslides of flow-type event occurred on May 1998 are simulated through the application of three physically based models developed in a GIS framework: SHALSTAB (Montgomery and Dietrich 1994), TRIGRS (Baum et al. 2002) and TRIGRS-unsaturated (Savage et al. 2004).

Finally, the results obtained from the three models are compared by applying a set of quantitative indexes (Sorbino et al. 2007, 2010), and a discussion is provided in order to highlight potential and limitations of these models for the forecasting of the potential source areas.

### 3.2.1 The study area and the available data set

The Campania Region has systematically been affected in the last centuries by shallow landslides of the flow-type occurring in volcanoclastic covers (Cascini et al. 2008a). These covers derive from air-fall deposition of pyroclastic material originating from Late Quaternary-Holocene explosive activity of Somma-Vesuvius and, subordinately, from Campi Flegrei and Roccamonfina volcanic apparatus. The volcanoclastic soils cover three main distinct geoenvironmental contexts (Calcaterra et al. 2004; Cascini et al. 2005b) over an area of about 3,000 km<sup>2</sup> (Fig. 14a). As testified by about 700 events occurred during the last centuries (Cascini et al. 2008b), shallow landslides of the flow-type frequently involve all the three contexts (Fig. 14a), but the most destructive ones mainly occurred in the southern part of the region (Fig. 14b), where volcanoclastic soils cover limestone bedrock (Brancaccio et al. 1999; Calcaterra et al. 2004; Cascini et al. 2008b; Celico and Guadagno 1998; Di Crescenzo and Santo 2005; Guadagno et al. 2005; Olivares and Picarelli 2001).

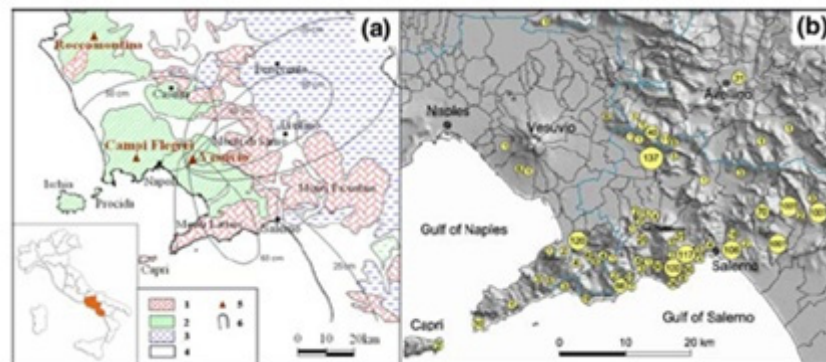


Figure 14: (a) Air-fall pyroclastic deposits in the Campania region (modified after Cascini et al. 2008a): 1 carbonate bedrock; 2 tuff and lava deposits; 3 flysch and terrigenous bedrock; 4 alluvial and continental deposits; 5 volcanic complexes; 6 isopachs of the pyroclastic products from the main eruptions. (b) Casualties in the Campania region caused by flow-type landslides in the period 1570–1998 (modified after Cascini et al. 2005b).

In this area, the most recent and catastrophic event occurred on 5–6 May 1998 and caused 159 casualties and huge damages to four little towns (Bracigliano, Quindici, Sarno and Siano) located at the toe of the so-called Pizzo d'Alvano massif (Fig. 15). According to Cascini (2004), shallow landslides were triggered by a heavy rainfall storm from April 27 to May 5 characterised by a cumulated rainfall value of 300 mm, of which the 80% felt during the last two days. These landslides rapidly propagated downslope and increased their initial volume through the mobilisation and/or erosion of in-place soils and the outermost portion of fractured bedrock, producing a total mobilised volume of about  $2.0 \times 10^6 \text{ m}^3$ .

On the basis of the geological, geomorphological and hydrogeological features, as well as the anthropogenic factors, Cascini et al. (2005a, 2008b) recognised six different triggering mechanisms characterising the source areas of the May 1998 landslides, respectively, named M1, M2, M3, M4, M5 and M6 (Fig. 16). The M1 mechanism essentially occurred inside colluvial hollows associated to zobs (Dietrich et al. 1986; Guida 2003) affected by convergent subsuperficial groundwater circulation and temporary springs coming from the bedrock towards the volcanoclastic covers. The mechanism M2 originated inside triangular-shaped source areas, mainly in the upper portions of open slopes associated to outcropping or buried bedrock scarps. The mechanism M3 produced complex-shaped landslides related to laterally enlarging local instabilities, strictly influenced by anthropogenic elements such as tracks. The mechanism M4 mainly occurred at the head of main channel originating multiple landslides arranged as a grape. These mechanisms are strictly related to heavy superficial water and contribute to the evolution of the head of valleys through the progressive retrogression of the transient channel. The mechanism M5 triggered the soils located along open slopes with a convex longitudinal profile resulting in source areas with shapes elongated in the maximum slope directions. Finally, the mechanism M6 developed at the base of convex–concave hill slopes, in correspondence of natural or man-induced breaks of the slope angle, involving limited volume of the soil covers.

In order to analyse the identified triggering mechanisms by means of geotechnical models, in situ and laboratory investigations were carried out on: the stratigraphical conditions of the source areas; the mechanical properties of volcanoclastic soils in both saturated and unsaturated conditions and the soil suction regime during dry and wet seasons. The obtained results, widely illustrated and commented in several papers (Cascini et al. 2005a, Cascini et al. 2005b, Cascini and Sorbino 2004, Sorbino 2005, Sorbino and Foresta 2002, Bilotta et al. 2005), allowed the setting up of a consistent geotechnical data set of the volcanoclastic covers. Finally, for the description of the landscape topography of the study area prior to the

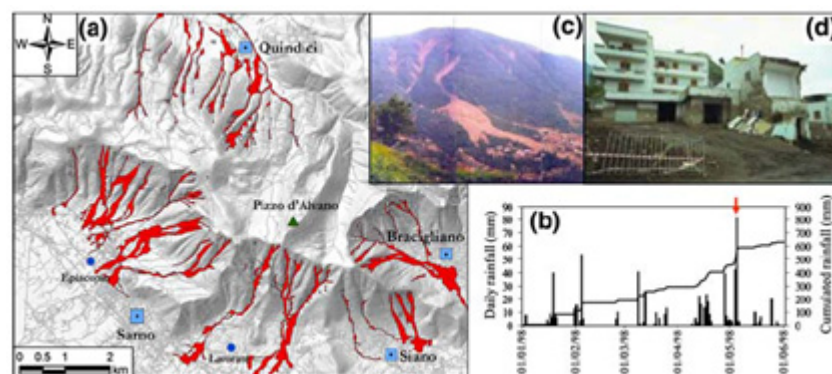


Figure 15: (a) Overview of the Pizzo d'Alvano massif with the main May 1998 shallow landslides of flow-type events; (b) daily rainfall recorded from 1 January to 1 June 1998 (the arrow indicates the landslides occurrence); (c) an example of the occurred phenomena and (d) of the produced damage.

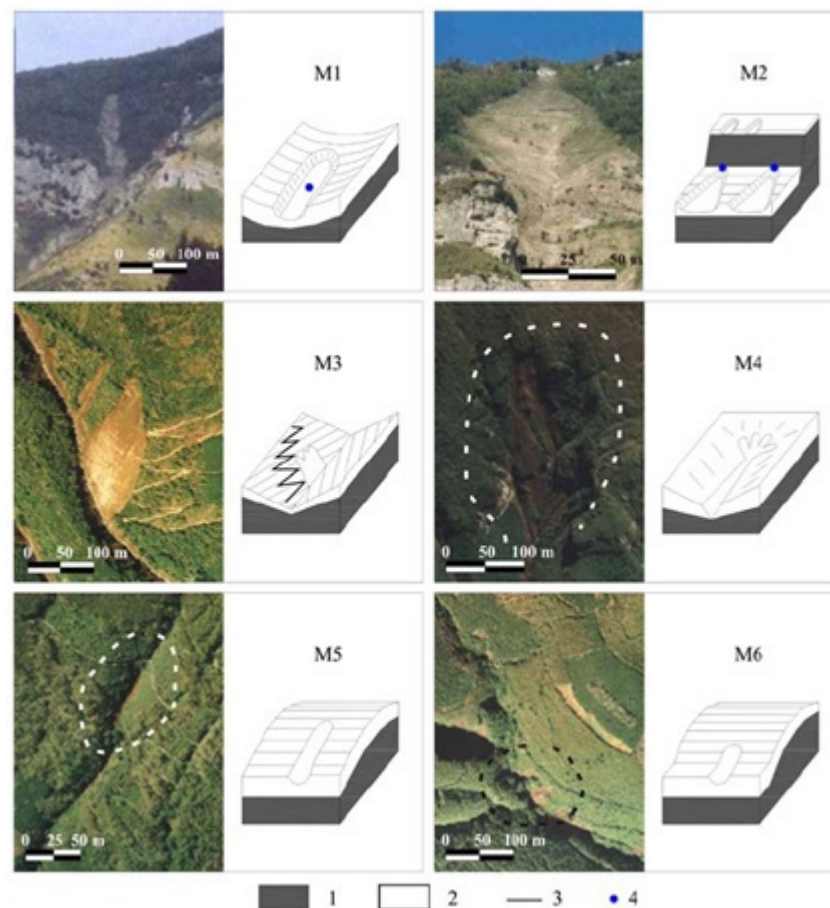


Figure 16: Schematic of the typical triggering mechanisms for the May 1998 shallow landslides of flow-type: 1 bedrock, 2 volcaniclastic deposit, 3 track and 4 spring from bedrock (modified after Cascini et al. 2008a).

landslide events a topographical map at 1:5,000 scale was adopted. From the topographical map, a detailed Digital Terrain Model (3 m × 3 m cells) was derived from interpolation of contour lines and elevation points.

### 3.2.2 The analysis of May 1998 shallow landslides of flow-type

In order to simulate the source areas of May 1998 shallow landslide phenomena, three physically based models SHALSTAB, TRIGRS and TRIGRS-unsaturated were used. To this aim, the study area was divided into four sectors (respectively, named Bracigliano, Quindici, Sarno and Siano) characterised by quite homogeneous in situ conditions and soil properties (Table 5). For the SHALSTAB model, the cover depths were assumed constant inside each sector while, for both TRIGRS models, different cover depths were considered, in agreement with the field data.

Particularly, variable values of soil thickness values were derived from interpolation of the field data collected after the May 1998 events (Cascini et al. 2005b) and geomorphological analyses. As for the mean values of the hydraulic conductivity and diffusivity, their selection was based on the following indirect procedure. Three different infinite slope schemes (Sorbino 2005), representative of the stratigraphic conditions inside the above sectors, were considered (Fig. 17). Referring to these schemes, the transient rainfall-induced pore pressures regime during the period 1 March 1998–5 May 1998 was analysed by using the finite element code SEEP/W (Geo-Slope 2005), which solves the Richards' equation. Referring to Sorbino (2005) for a detailed description of the analyses, the geometric features of the schemes are illustrated in the upper part of figure 17. The hydraulic properties were derived from the

**Table 5: Parameters used for the modelling (constant values of soil unit weight, effective cohesion, and friction angle were assumed respectively equal to 15 kN/m<sup>3</sup>, 5 kPa and 38°).**

| Sector      | Hydraulic conductivity $k$ (m/s) | Soil depth $h_{SHALSTAB}$ (m) | Diffusivity $D_{TRIGRS}$ (m <sup>2</sup> /s) | Parameters of Gardner's curves <i>TRIGRS-unsaturated</i> |                                   |                                    |
|-------------|----------------------------------|-------------------------------|--|--|-----------------------------------|------------------------------------|
|             |                                  |                               |  | $\alpha$ (m <sup>-1</sup> )                              | Residual Water Content $\theta_r$ | Saturated Water Content $\theta_s$ |
| Sarno       | $1.0 \times 10^{-5}$             | 2.65                          | $5.9 \times 10^{-5}$                         | 6.3  | 0.20                              | 0.66                               |
| Siano       | $8.0 \times 10^{-6}$             | 2.80                          | $5.6 \times 10^{-5}$                         | 7  | 0.20                              | 0.60                               |
| Bracigliano | $6.0 \times 10^{-6}$             | 2.00                          | $4.5 \times 10^{-5}$                         | 8  | 0.25                              | 0.53                               |
| Quindici    | $6.0 \times 10^{-6}$             | 2.25                          | $4.5 \times 10^{-5}$                         | 8  | 0.25                              | 0.53                               |

results of the laboratory tests (Sorbino et al. 2010) while rainfall intensities recorded during the analysed period were assumed as boundary conditions at the slope surface. The same schemes were analysed using TRIGRS and TRIGRS-unsaturated with different values of the hydraulic properties varying in the range adopted for the finite element analyses. Finally, the selected values of these properties were those providing the best fit of the pore pressure distributions obtained through the two TRIGRS and SEEP/W codes (Figure 17). In details, for both models, the middle graphs of figure 16 show the adopted initial conditions and the vertical distributions of the pore pressures obtained, respectively, by means of TRIGRS and TRIGRS-unsaturated. Particularly, all the graphs highlight that the selected parameters allow the TRIGRS model to define pore pressure values similar to those computed by SEEP/W exclusively in the lower part of the schemes, characterised by the complete saturation of the soil, while TRIGRS-unsaturated is able to describe the pore pressure regime along the entire profile with good agreement.

As far as the analyses over large areas are concerned, TRIGRS and TRIGRS-unsaturated boundary conditions were represented by hourly rainfall intensities recorded on the 4–5 May 1998 and characterised by a cumulative value of about 240 mm while, for the SHALSTAB model, a critical rainfall intensity was adopted equal to 5 mm/day, corresponding to the mean rainfall intensity during the 10 months before the landslide event.

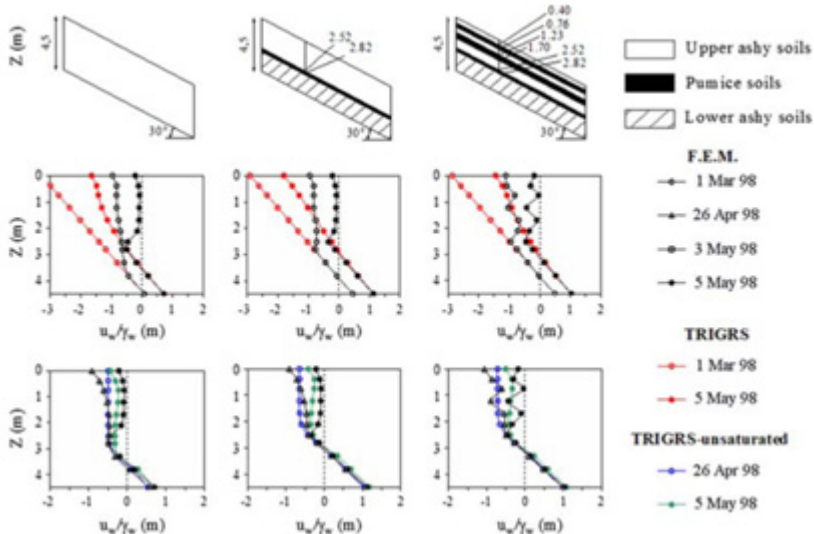


**Figure 17: Pore-water pressure profiles obtained with the SEEP/W, TRIGRS and TRIGRS-unsaturated codes: (from the top to the bottom) the analysed schemes, SEEP/W versus TRIGRS, and SEEP/W versus TRIGRS-unsaturated.**

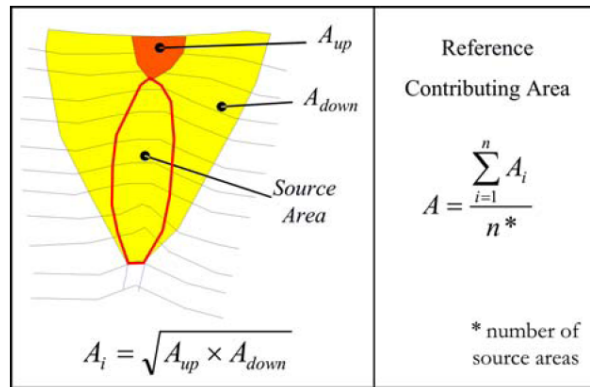


Figure 18: Procedure used to compute the reference contributing area (A) (from Sorbino et al. 2010).

This period was determined according to Iverson (2000) who evidenced that the conceptual assumptions of a steady-state flow model are realistic only if the duration of the rainfall event is much longer than a reference time, defined as the ratio between a representative value of the contributing area and the saturated hydraulic diffusivity. For the Pizzo d’Alvano massif, the hydraulic diffusivity was assumed equal to the mean value of the characteristic saturated diffusivities in Table 5. The representative-contributing area was assumed equal to the arithmetic mean of the contributing areas. These latter were computed as the geometric mean between the contributing areas at both the scar and the toe of each source area (Figure 18).

As regards TRIGRS initial conditions, each sector was characterised by different initial water table depths, providing mean suction values in the range of 0–10 kPa at the bedrock, in agreement with the suction measurements (Cascini and Sorbino 2004). Particularly, the water table configuration obtained by SHALSTAB for the critical steady-state intensity characterising the period antecedent the events was modified to provide mean suction values in the range of available suction measurements. The steady-state suction distributions used to compute mean initial suction values for TRIGRS and TRIGRS-unsaturated were assumed, respectively, linear and exponential, according to the assumptions of both the models. In the adopted procedure, the use of SHALSTAB allowed to take the convergence of subsurface flows during the period antecedent the events into account for the initial conditions of both TRIGRS models.

In order to quantify the results of the two models and evaluate their relative efficacy in the back-analysis of the May 1998 source areas, two indexes, respectively, named “Success Index” (SI) and “Error Index” (EI), were defined (Sorbino et al. 2010). For each source area (Figure 19), the SI is the portion (in percentage) of the observed source area computed as unstable by the models. The EI represents, for each mountain basin, the percentage ratio

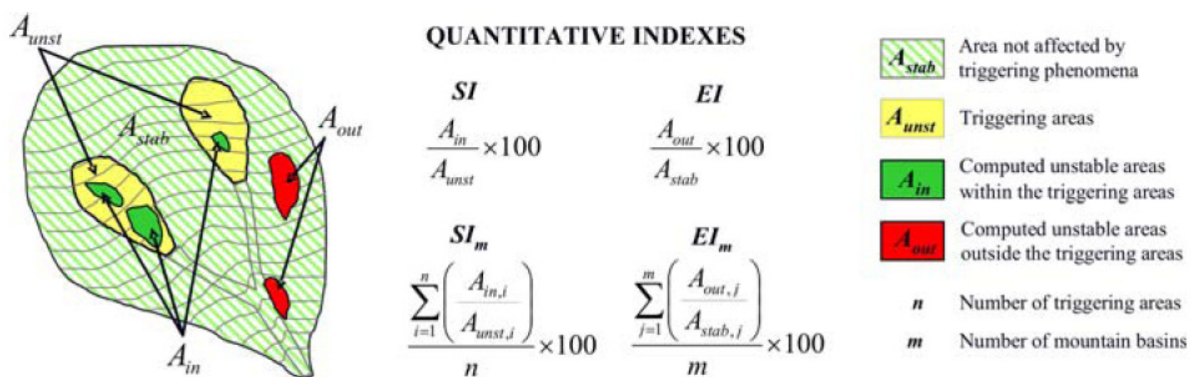


Figure 19: Definition of quantitative Success and Error indexes (from Sorbino et al. 2010).

between the areas computed as unstable located outside the observed source areas ( $A_{out}$ ), and the area of the basin not affected by triggering phenomena ( $A_{stab}$ ). In order to evaluate the efficacy of models for the whole area of figure 15, mean quantities of the earlier-mentioned indexes ( $SI_m$  and  $EI_m$ ) were also defined.  $SI_m$  represents the mean value of  $SI$  referred to the number of the source areas, while  $EI_m$  is the mean value of  $EI$  referred to the number of the mountain basins.

### 3.2.2.1 Results and discussion

The most significant scenarios resulting from SHALSTAB and TRIGRS applications are illustrated in Fig. 20 together with the landslide shapes of the May 1998 event. Fig. 20a depicts the unstable cells computed by SHALSTAB, corresponding to critical rainfall intensity of 5 mm/day while, for the TRIGRS models, Figs. 20b and 20c show the computed unstable areas at the estimated time of occurrence of the 1998 landslides, corresponding to the initial mean suction value of 5 kPa. The figures clearly show the different source areas provided by the three used models. Particularly, also assuming the steady-state rainfall intensity equivalent to the May 1998 rainfall event, the SHALSTAB model furnishes more unrealistic scenarios than TRIGRS.

In order to quantify such differences, Fig. 21 shows the results provided by the models for the whole study area, in terms of the quantitative indexes of Fig. 19. In details, SHALSTAB provides the highest value of  $SI_m$  (77%) that, however, is associated to a very high value of  $EI_m$  (38%) corresponding to a computed unstable area all over the Pizzo d'Alvano massif about 10 times larger than the observed value of the source areas. From the same figure, it can also be noted that, for values of  $EI_m$  lower than 38%, TRIGRS gives more satisfactory results, as it systematically provides higher values of  $SI_m$  than those obtained by SHALSTAB. The same figure shows the values of "Success" and "Error" indexes computed for TRIGRS-unsaturated model, evidencing an increase in the values of "Success" and a decrease in "Error" with respect to the above models, for every assumed initial condition.

However, among the scenarios outlined with the two TRIGRS codes (Figs. 20b and 20c), the best results in terms of Success–Error indexes are certainly represented by those obtained for initial conditions providing mean suction values in the range of 5–10 kPa. It should be noted that these suction values are the same that were used by Cascini et al. (2005a) for the best back-analysis of a shallow landslide occurred inside the sample area. For these initial conditions, the  $EI_m$  values correspond to a computed unstable area all over the Pizzo d'Alvano massif of about twice the extension of the observed source areas. As for the number of source areas, TRIGRS codes provide an estimation of about 20–30% greater than the observed ones.

In order to check the efficacy of both TRIGRS models in simulating the different triggering mechanisms of Fig. 15, the  $EI_m$  values computed for different initial conditions, as well as the

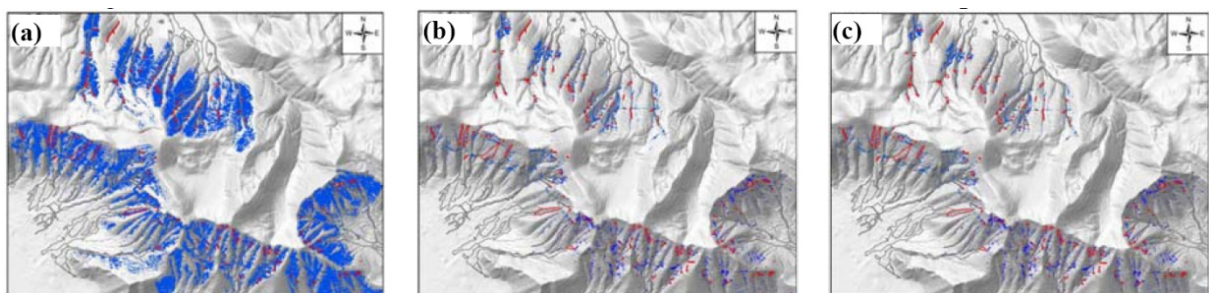


Figure 20: Instability scenarios obtained with (a) SHALSTAB, (b) TRIGRS and (c) TRIGRS-unsaturated: in blue the areas computed as unstable, in red the landslide shapes of the May 1998 event.

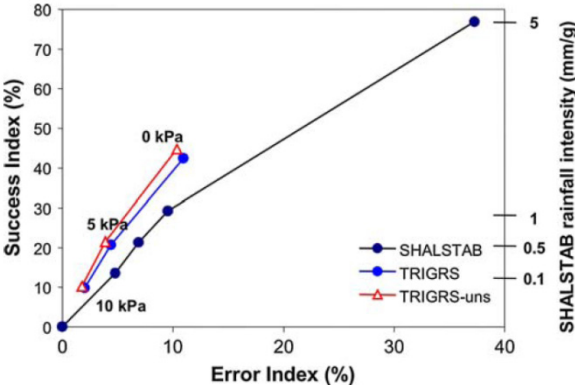


Figure 21: “Success” and “Error” indexes obtained with the SHALSTAB, TRIGRS and TRIGRS-unsaturated (from Sorbino et al. 2010).

$SI_m$  values for each of the considered mechanisms are compared in Fig. 22. It is worth noting that the highest values of  $SI_m$  are systematically provided for the mechanism M4.

With reference to the comparison of the results obtained by the two models, Fig. 22 highlights that, for all the mechanisms except M2, TRIGRS-unsaturated furnishes a slight increase (about 5%) in the value of Success and a subsequent decrease in Error with respect to the values of indexes computed by TRIGRS. For the M2 mechanism, the value of Success index obtained by TRIGRS-unsaturated is about 10% less than the one computed by TRIGRS.

Despite such small differences, it is worth noting that the ratio between the number of source areas related to each mechanism (totally or partially) simulated as unstable by both TRIGRS models, and the number of 1998 shallow landslides’ source areas is quite high. With reference to the M4 mechanism, the earlier-mentioned ratio ranges between 80% and 90%.

Examination of the modelling results provides a basis for some general comments on the use of distributed, physically based models, partially confirming the theoretical assumptions and deepening some aspects deriving from their application.

First, according to conceptual assumptions of all the models, TRIGRS-unsaturated represents the most adequate model for the analysis of shallow landslides source areas occurred within the study area, providing the highest ratio between the “Success” and “Error” indexes. This model is able to take into account both the transient pore-water pressures regime induced by short and intense rainstorms and the unsaturated conditions (Savage et al. 2004; Baum et al. 2008) characterising the volcanoclastic covers (Cascini and Sorbino 2004).

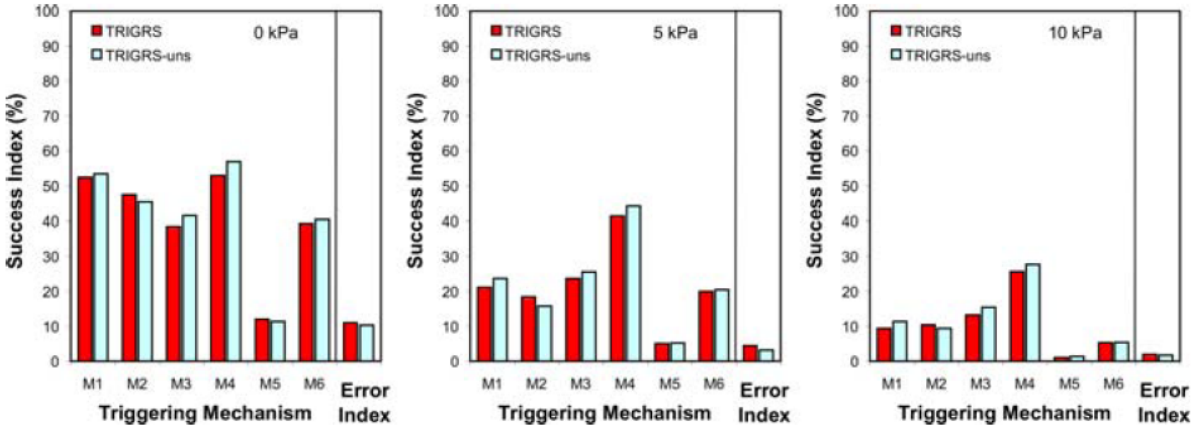


Figure 22: Results obtained with the TRIGRS codes for the different triggering mechanisms and initial mean suction conditions (from Sorbino et al. 2010).

The TRIGRS model furnishes results that are very close to those provided by TRIGRS-unsaturated. However, this finding is strictly related to the use of weighted values of hydraulic properties available for the involved soils. Particularly, such parameters have been selected by means of inverse analyses in order to take the unsaturated conditions of volcaniclastic soils indirectly into account (Sorbino et al. 2007). Although TRIGRS shows potential for the evaluation of transient pore-water pressures and stability conditions of potential landslide source areas during rainfall (Godt et al. 2008, Salciarini et al. 2006), its use is quite costly when the unsaturated conditions play a fundamental role for the porewater pressures regime.

On the other hand, the SHALSTAB theory of steady-state groundwater hydrology is not consistent with the physical process leading to widespread shallow landsliding, and it furnishes an overestimation of the extent and number of source areas. Moreover, results from the application of quasi-steady-coupled models proposed in the literature to part of the study area, yield similar overprediction errors (Chirico et al. 2002, Frattini et al. 2004).

Despite these limitations, the use of SHALSTAB may furnish useful guidance for assessing initial conditions for the transient models. As for the different triggering mechanisms, the M4 mechanism is modeled by all three models as it conforms to the fundamental hypotheses of vertical infiltration and water table accretion adopted by all the models.

As for the remaining mechanisms, lower  $SI_m$  values are mainly associated to local boundary conditions not considered by the models. However, the values of success indexes generally greater than zero indicate a partial modelling of source areas. Particularly, for the M1 mechanism, the failure conditions are influenced by local hydraulic conditions that add their effects to the convergent subsurface flow induced by top morphology. According to the analyses performed by Cascini et al. (2005a), this mechanism is characterised by a retrogressive failure involving the toe of the slope, due to the pore-water pressures increase caused by rainfall infiltration, and the mobilisation of the upper part of slope, due to the local pressure increase induced by the temporary springs from underlying bedrock. The presence of temporary springs is not captured by the TRIGRS models, and the effects of local groundwater gradients should be taken into account to properly simulate springs-induced triggering mechanisms (Cascini et al. 2008a). However, in many circumstances the results partially capture these instabilities and confirm the potential of physically based models to evaluate the failure conditions induced by convergent flows.

Similarly, the partial simulation of M6 mechanism may be addressed to an increase in pore-water pressures related to concentration of subsurface flows, especially due to concavity of slopes.

As for the M3 mechanism, TRIGRS and TRIGRS-unsaturated are theoretically able to simulate the development of overland flows along the preferential patterns caused by trackways and roads. Unfortunately, the cell width (3 m × 3 m) of the used DTM is close to width of typical trackways located in the study area and, moreover, the tortuous trackways paths usually do not match the regular grid discretisation of the landscape. For these reasons, M3 mechanisms are not well simulated by the TRIGRS models. Results for the instabilities generated by this mechanism only identify unstable areas related to high slope angles along road cuts and/or to the direct effects of rainfall infiltration.

In general, the assumptions of the TRIGRS models do not conform to the M2 and M5 mechanisms. Particularly, the effect of springs and impact loading phenomena that originate M2 mechanism are incompatible with theoretical basis of the models and, moreover, the location of source areas close to discontinuities poses some difficulties mainly related to the inconsistency with infinite slope conditions.

## 4 CONCLUSIONS

Geomechanical modelling of landslides involves a handful of challenges. These challenges are related to the multidisciplinary process of landslide modelling to which the geomechanical part belongs. The problem of landslides itself is highly complex for it involves different types of materials and their loading histories, geological configurations and complex environmental conditions. A geomechanical model aims at giving an appropriate idealisation of a certain landslide problem. Appropriate means that the model is able to capture the key physical mechanisms in a given landslide problem and possesses predictive capacities so that it can reproduce qualitatively and quantitatively the observed behaviour in nature and further be used to predict the slope behaviour for other environmental configurations.

This deliverable has addressed in a synthesised form the different key physical mechanisms in landslides and the mathematical frameworks that have been developed in the soil mechanics community to model the time-dependent uncoupled or coupled processes of water flow, pore pressure dissipation and deformation in soil slopes. Shallow landslides, primary triggered during heavy rainfall events, as well as continuously slow moving, large landslides with periodic reactivation phases have been considered.

Guidelines are presented for landslide modelling which provide the user in the first place with some information on the utility of numerical codes. In the second place, these guidelines allow the user to identify the necessary code components for a given landslide problem and to perform the modelling steps, including data pre-processing, the actual numerical calculation, as well as the post-processing of the results. The geomechanical codes for slope-scale and regional-scale analysis used in the SafeLand project are evaluated with respect to the availability of components which are necessary or which allow to obtain additional expertise on a precise landslide problem.

## 5 REFERENCES

- Alonso E.E., Gens A., Delahaye C.H., *Influence of rainfall on the deformation and stability of a slope in overconsolidated clays: a case study*. Hydrogeology Journal, 2003. **11**: 174-192.
- Alonso E.E., Gens A., Josa A., *A constitutive model for partially saturated soils*, Géotechnique, 1990. **40**(3), 405-430.
- Anderland O.B., Ladanyi B., *Frozen Ground Engineering*. Second Edition, The American Society of Civil Engineers and John Wiley & Sons, Ltd. (eds), 2004. 367 pages.
- Argyris J., *Energy theorems and structural analysis*. Aircraft engineering, 1954 and 1955. London: Reprinted by Butterworths Scientific Publications, 1960.
- Baum R.L., Savage W.Z., Godt J.W. *TRIGRS-A Fortran program for transient rainfall infiltration and grid-based regional slope-stability analysis, version 2.0*. US Geological Survey Open-File Report 2008-1159, 2008. Available via: <http://pubs.usgs.gov/of/2008/1159/>.
- Baum R.L., Savage W.Z., Godt J.W., *TRIGRS-A FORTRAN program for transient rainfall infiltration and grid-based regional slope-stability analysis*. US Geological Survey Open-File Report 02-0424, 2002. Available via: <http://pubs.usgs.gov/of/2002/ofr-02-424/>.
- Bell F.G., *Engineering properties of soils and rocks*, Fourth Edition, Blackwell Science Ltd. (eds), 2000. 491 pages.
- Bilotta E., Cascini L., Foresta V., Sorbino G., *Geotechnical characterization of pyroclastic soils involved in huge flowslides*. Geotech Geol Eng, 2005. **23**: 365-402.
- Bishop A.W., *The use of the slip circle in the stability analysis of earth slopes*. Géotechnique, 1955. **5**(1): 7-17.
- Bjerrum, L., *Progressive failure in slopes in overconsolidated plastic clay and clay shales*. Journal of the Soil Mechanics and Foundations Division, ASCE, 1967. **93**(5): 3-49.
- Blatz J.A., Ferreira N.J., Graham J., Effects of near-surface environmental conditions on instability of an unsaturated soil slope. Canadian Geotechnical Journal, 2004. **41**: 1111-1126.
- Bolzon G., Schrefler B.A., Zienkiewicz O.C., *Elasto-plastic constitutive laws generalised to partially saturated states*. Géotechnique, 1996. **46**(2): 279-289.
- Bonnard, C., *Evaluation et prédiction des mouvements des grands phénomènes d'instabilité de pente*. Bulletin angewandter Geologie, 2006. **11**(2): 89-100.
- Brancaccio L., Cinque A., Russo F., Sgambati D., *Osservazioni geomorfologiche sulle frane del 5-6 Maggio 1998 del Pizzo d'Alvano (Monti di Sarno, Campania)*. In: Orombelli (ed) Studi geografici e geologici in onore di Severino Belloni, 1999: 81-123 (in Italian).
- Brooks R. H., Corey A.T., *Hydraulic properties of porous media*. Hydrology Paper N.3, 1964. Colorado State Univ., Fort Collins, Colorado.
- Calcaterra D., de Riso R., Evangelista A., Nicotera M.V., Santo A., Scotto di Santolo A., *Slope instabilities in the pyroclastic deposits of the carbonate Apennine and the Phlegrean district (Campania, Italy)*. In: Picarelli L (ed) Proceedings of International Workshop "Flows 2003—Occurrence and Mechanisms of Flows in Natural Slopes and Earthfill", Sorrento. Patron, Bologna, 2004: 61-75.
- Calvello, M., L. Cascini, and G. Sorbino, *A numerical procedure for predicting rainfall-induced movements of active landslides along pre-existing slip surfaces*. International Journal For Numerical And Analytical Methods In Geomechanics, 2008. **32**(4): 327-351.
- Cancelli A., D'Elia B., Sembenelli P., *Groundwater problems in embankments, dams and natural slopes: General Report*. In Proceedings of IX Symposium of ECSMFE, Dublin, 1987. **3**: 1043-1072.
- Cascini L., and Versace P., *Eventi pluviometrici e movimenti franosi*. Atti del XVI Convegno Nazionale di Geotecnica, 1986. **3**: 171-184 (In Italian).

- Cascini L., Cuomo S., Guida D., *Typical source areas of May 1998 flow-like mass movements in the Campania region, southern Italy*. Engineering Geology, 2008a. **96**:107–125.
- Cascini L., Cuomo S., Sorbino G., *Flow-like mass movements in pyroclastic soils: remarks on the modelling of triggering mechanisms*. Rivista Italiana di Geotecnica, 2005. **4**:11–31.
- Cascini L., Ferlisi S., Vitolo E., *Individual and societal risk owing to landslides in the Campania region (southern Italy)*. Georisk, 2008. **2**(3):125–140.
- Cascini L., Guida D., Sorbino G., *Il Presidio Territoriale: una esperienza sul campo*. Rubbettino Editore, Catanzaro, 2005. (in Italian).
- Cascini L., *Relazione generale: Il regime delle falde idriche*. Atti del Convegno "Il Ruolo dei Fluidi nei Problemi di Ingegneria Geotecnica", Mondovì (CN), 6-7 Settembre 1994, 1996. **2**: I-3 – I-95. (In Italian).
- Cascini L., Sorbino G., *The contribution of soil suction measurements to the analysis of flowslide triggering*. In: Picarelli L (ed) Proceedings of International Workshop "Flows 2003—Occurrence and Mechanisms of Flows in Natural Slopes and Earthfills", Sorrento, Patron, Bologna, 2004: 77–86.
- Cascini L., *The flowslides of May 1998 in the Campania region, Italy: the scientific emergency management*. Rivista Italiana di Geotecnica, 2004. **2**:11–44
- Castelli, M., C. Scavia, C. Bonnard, and L. Laloui, *Mechanics and velocity of large landslides Preface*. Engineering Geology, 2009. **109**(1-2): 1-4.
- Celico P., Guadagno F.M., *L'instabilità delle coltri piroclastiche delle dorsali carbonatiche in Campania: attuali conoscenze*. Quaderni di Geologia Applicata, 1998. **5**(1):129–188 (in Italian)
- Chapuis R.P., Gill D.E., *Hydraulic anisotropy of homogeneous soils and rocks: influence of the densification process*. Bulletin of the International Association of Engineering Geology, 1989. **39**: 75-86.
- Cheng Y.M., Lau C.K., *Slope stability analysis and stabilization – new methods and insights*. Taylor and Francis (eds), 2008. 241 pages.
- Chu J., Leroueil S., Leong W. K., *Unstable behaviour of sand and its implications for slope instability*. Can. Geotech. J., 2003. **40**: 873–885.
- Clough R.W., *The finite element method in plane stress analysis*. Proceedings of the Second ASCE Conference Electronic Computation, Pittsburg, PA, 1960.
- Collin A., *Recherches Expérimentales sur les Glissements Spontanés des Terrains Argileux, accompagnées de Considérations sur Quelques Principes de la Mécanique Terrestre*. Carilian-Goeury and Dalmont, Paris, 1846.
- Collins B.D., Znidarcic D., *Stability Analyses of Rainfall Induced Landslides*. Journal of Geotechnical and Geoenvironmental Engineering, 2004. **130**(4): 362-372.
- Cornforth D.H., *Landslides in Practice - Investigation, Analysis, and Remedial/Preventative Options in Soils*. John Wiley & Sons, 2005.
- Corominas J., Moya J., Ledesma A., Lloret A., Gili J.A., *Prediction of ground displacements and velocities from groundwater level changes at the Vallcebre landslide (Eastern Pyrenees, Spain)*. Landslides, 2005. **2**: 83-96.
- Corominas J., Moya J., Lloret A., Gili J.A., Angeli M.G., Pasuto A., Silvano S., *Measurement of landslide displacements using a wire tensiometer*. Engineering Geology, 2000. **55**: 149-166.
- Coulomb C.A., Mem.Math. et Phys., 1773. **7**: 343.
- Crosta G.B., Frattini R., *Distributed modelling of shallow landslides triggered by intense rainfall*. Nat Hazards Earth Syst Sci, 2003. **3**:81–93
- Cruden, D.M. and D.J. Varnes, *Landslide Types and Processes*, in *Landslides: Investigation and Mitigation*, A.K. Turner and R.L. Schuster, Editors. 1996, National Academy Press: Washington D.C. 673 pages.
- Darve F., Laouafa F., *Instabilities in granular materials and application to landslides*.

- Mechanics of Cohesive-Frictional Materials, 2000. **5**: 627-652.
- Darve F., Laouafa F., *Modelling of slope failure by a material instability mechanism*. Comput. Geotech., 2001. **29**: 301–325.
- Darve F., *Liquefaction phenomenon of granular materials and constitutive instability*. Int. J. Eng. Comp., 1995. **7**: 5-28.
- Delacourt C., Allemand P., Berthier E., Raucoules D., Casson B., Grandjean P., Pambrun C., Varel E., *Remote-sensing techniques for analysing landslide kinematics : a review*. Soc. Géol. Fr., 2007. **178**(2) : 89-100.
- Di Crescenzo G., Santo A., *Debris slides-rapid earth flows in the carbonate massifs of the Campania region (southern Italy): morphological and morphometric data for evaluating triggering susceptibility*. Geomorphology, 2005. **66**:255–276.
- Di Prisco C., Mاتيotti R. and Nova R., *Theoretical investigation of undrained stability of shallow submerged slopes*. Geotechnique. 1995. **45**: 479-496.
- Dietrich W.E., Wilson C.J., Reneau S.L., *Hollows, colluvium, and landslides in soil-mantled landscapes*. In: Abrahams AD (ed) Hillslope processes. Allen and Unwin, Boston, 1986. 361–388.
- Dong J.J., Tzeng J.H., Wu P.K., Lin M.L., *Effects of anisotropic permeability on stabilization and pore water pressure distribution of poorly cemented stratified rock slopes*. International Journal for Numerical and Analytical Methods in Geomechanics, 2006. **30**: 1579-1600.
- Drucker D.C. and Prager W., *Soil Mechanics and Plastic Analysis or Limit Design*. Quart.Appl.Math., 1952. **10**: 157-165.
- Duncan J.M., *State of the art: limit equilibrium and finite-element analysis of slopes*. Journal of Geotechnical Engineering, 1996. **122**(7): 577-596.
- Duncan J.M., Wright S.G., *Soil strength and slope stability*. John Wiley & Sons, Ltd. (eds), 2005. 297 pages.
- Eberhardt, E., A.D. Watson, and S. Loew, *Improving the interpretation of slope monitoring and early warning data through better understanding of complex deep-seated landslide failure mechanisms*. Landslides and Engineered Slopes: From the Past to the Future, Vols 1 and 2, 2008: 39-51.
- Fell R., Corominas J., Bonnard C., Cascini L., Leroi E., Savage W.Z., On behalf of the JTC-1 Joint Technical Committee on Landslides, Engineered Slopes. *Guidelines for landslide susceptibility, hazard and risk zoning for land use planning*. Engineering Geology, 2008. **102**(3–4):85–98.
- Fell R., Corominas J., Bonnard C., Cascini L., Leroi E., Savage W.Z.. On behalf of the JTC-1 Joint Technical Committee on Landslides, Engineered Slopes. *Guidelines' commentary for landslide susceptibility, hazard and risk zoning for land use planning*. Eng Geol, 2008. **102**(3–4): 99–111.
- Fellenius W., *Erdstatische Berechnungen mit Reibung und Kohäsion (Adhäsion) und unter Annahme kreiszylindrischer Gleitflächen*. Ernst & Sohn, Berlin, 1927.
- Fernandez Merodo J.A., Pastor M., Mira P., Tonni L., Herreros M.I., Gonzalez E., Tamagnini R., *Modelling of diffuse failure mechanisms of catastrophic landslides*. Computer Methods in Applied Mechanics and Engineering, 2004. **193**: 2911-2939.
- Fernández Merodo J.A., Tamagnini R., Pastor M., Mira P., *Modelling damage with generalized plasticity*. Rivista Italiana di Geotecnica, 2005. **4**: 32-42.
- Ferrari A., Laloui L., Bonnard C., *Hydro-mechanical modelling of a natural slope affected by a multiple slip surface failure mechanism*. Computer Modelling in Engineering & Sciences, 2009. **52**(3): 217-235.
- François B., Bonnard C. and Laloui L., *Investigation of the Geomechanical Aspects of a Large Landslide by Means of a Finite-element Method : A Case Study*. In Proceedings of the 12th IACMAG Conference, 1-6 Oct. 2008, India. 4577-4585.
- Fredlund, D.G. and H. Rahardjo, *Soil Mechanics for Unsaturated Soils*. 1993, New York:

John Wiley and Sons, INC.

- Gallipoli D., Gens A., Sharma R., Vaunat J., *An elastoplastic model for unsaturated soil incorporating the effects of suction and degree of saturation on mechanical behaviour*. Géotechnique, 2003. **53**: 123-135.
- Gardner W.R., *Some steady state solutions of the un-saturated moisture flow equation with application to evaporation from water table*. Soil Sci., 1958. **85**(4): 228-232.
- Gasmo J.M., Rahardjo H., Leong E.C., *Infiltration effects on stability of a residual soil slope*. Computer and Geotechnics, 2000. **26**: 145-165.
- Geo-Slope, *User's guide*. GeoStudio 2004, Version 6.13. Geo-Slope Int Ltd Calgary, Alberta, Canada, 2005.
- Godt J.W., Baum R.L., Savage W.Z., Salciarini D., Schulz W.H., Harp E.L., *Transient deterministic shallow landslide modelling: Requirements for susceptibility and hazard assessments in a GIS framework*. Engineering Geology, 2008. **102**: 214-226.
- Gonzalez, D.A., A. Ledesma, and J. Corominas, *The viscous component in slow moving landslides: A practical case*. Landslides and Engineered Slopes: From the Past to the Future, Vols 1 and 2, 2008: 237-242.
- Greco R., Guida A., Damiano E., Olivares L., *Soil water content and suction monitoring in model slopes for shallow flowslides early warning applications*. Physics and Chemistry of the Earth, 2010. **35**: 127-136.
- Griffiths D.V., Lane P.A., *Slope stability analysis by finite elements*. Geotechnique, 1999. **49**(3): 387-403.
- Guadagno F.M., Forte R., Revellino P., Fiorillo F., Focareta M., *Some aspects of the initiation of debris avalanches in the Campania region: the role of morphological slope discontinuities and the development of failure*. Geomorphology, 2005. **66**:237–254.
- Guadagno F.M., Revellino P., *Debris avalanches and debris flows of the Campania Region (southern Italy)*. In: Jakob Hungr M, Hungr O (eds) Debris-flow hazard and related phenomena. Springer, Berlin, 2005. 489–518.
- Guida D., *The role of the zero-order basin in flowslide-debris flow occurrence and recurrence in Campania (Italy)*. In: Proceedings of International Conference on ‘Fast Slope Movements – Prediction and Prevention for Risk Mitigation’, Napoli, vol 1. Patron, Bologna, 2003. 255–262.
- Herrera G., Fernández-Merodo J.A., Mulas J., Pastor M., Luzi G., Monserrat O., *Use of ground based SAR data in landslide forecasting models: The Portalet case study* Engng.Geology, 2008. 105: 220-230.
- Huber M. T., *Czasopismo techniczne*, Lemberg, 22, 81 1904.
- Iverson R.M., *Landslide triggering by rain infiltration*. Water Resour Res, 2000. **36**(7):1897–1910.
- Janbu N., *Slope stability computations*. Embankment dam engineering: Casagrande volume, John Wiley & Sons (eds), 1973. 47-86.
- Javadi A.A. and Rezanian M., *Intelligent finite element method: An evolutionary approach to constitutive modelling*. Advanced Engineering Informatics, 2009. **23**(4): 442-451.
- Jing L., Hudson J.A., *Numerical methods in rock mechanics*. International Journal of Rock Mechanics and Mining Sciences, 2002. **39**: 409-427.
- Kawamura, K., *Methodology for landslide prediction*, in *11th International Conference on Soil Mechanics and Foundation Engineering*, R. Publications Committee of the ICSMFE. A.A. Balkema, The Netherlands, Editor. 1985: San Francisco, Calif. 1155–1158.
- Lagioia R. and Nova R., *An experimental and theoretical study of the behaviour of a calcarenite in triaxial compression*. Geotechnique, 1995. **45**(4): 633-648.
- Laloui L., Nuth M., *An introduction to the constitutive modelling of unsaturated soils*. Rev. eur. génie civ., 2005. **9**(5–6): 651–670.
- Li L.C., Tang C.A., Zhu W.C., Liang Z.Z., *Numerical analysis of slope stability based on the*

- gravity increase method*. Computers and Geotechnics, 2009. **36**: 1246-1258.
- Lignon S., Laouafa F., Prunier F., Khoa H.D.V., Darve F., *Hydro-mechanical modelling of landslides with a material instability criterion*. Géotechnique, 2009. **59**(6): 513-524.
- Loret B., Khalili N., *A three phase model for unsaturated soils*. Int. J. Numer. Anal. Meth. Geomech, 2000. **24**(11): 893-927.
- Mabssout M., Pastor M., *A two step Taylor-Galerkin algorithm for shock wave propagation in soils*. Int. J. Num. Anal. Meth. Geomech. 2003. **27**: 685-704.
- Macfarlane, D.F., *Observations and predictions of the behaviour of large, slow-moving landslides in schist, Clyde Dam reservoir, New Zealand*. Engineering Geology, 2009. **109**(1-2): 5-15.
- Malet J.-P., *Les glissements de type écoulement dans les marnes noires des Alpes du Sud. Morphologie, fonctionnement et modélisation hydro-mécanique*. PhD Thesis in Earth Sciences, Université Louis Pasteur, Strasbourg, 2003. 364 pages.
- Malet J.-P., van Asch T.W.J., van Beek L.P.H., Maquaire O., *Forecasting the behaviour of complex landslides with a spatially distributed hydrological model*. Natural Hazards and Earth System Sciences, 2005. **5**(1): 71-85.
- Manzanal D., *Constitutive model based on Generalized Plasticity incorporating state parameter for saturated and unsaturated sand* (Spanish). PhD Thesis School of Civil Engineering, Polytechnic University of Madrid, 2008.
- Manzanal D., Pastor M., Fernandez Merodo J.A., *A Generalized Plasticity model for unsaturated soils under monotonic and cyclic loading*. In proceeding of X International Conference on Computational Plasticity COMPLAS. Oñate and Owen (Eds), CIMNE, Barcelona, 2009.
- Marcato G., Mantovani M., Pasuto A., Silvano S., Tagliavini F., Zabuski L., Zannoni A., *Site investigation and modelling at 'La Maina' landslide (Carnian Alps, Italy)*. Natural Hazards and Earth System Sciences, 2006. **6**: 33-39.
- Mattsson H., Klisinski M., Axelsson K., *Optimisation routine for identification of model parameters in soil plasticity*. Int. J. Numer. Anal. Meth. Geomech., 2001. **25**: 435-472.
- Mayoraz, F. and L. Vulliet, *Neural Networks for Slope Movement Prediction*. International Journal of Geomechanics, 2002. **2**(2): 153-173.
- Mira P., Pastor M., Li T., Liu X., *A new stabilized enhanced strain element with equal order of interpolation for soil consolidation problems*. Comput. Methods Appl. Mech. Engrg., 2003. **192**: 4257-4277.
- Montgomery D.R., Dietrich W.E., *A physically based model for the topographic control on shallow landsliding*. Water Resour Res, 1994. **30**:1153–1171.
- Morgenstern N.R., Price V.E., *The analysis of the stability of general slip surfaces*. Géotechnique, 1965. **15**(1) : 79-93.
- Ng C.W.W., Zhan L.T., Bao C.G., Fredlund D.G., Gong B.W., *Performance of an unsaturated expansive soil slope subjected to artificial rainfall infiltration*. Géotechnique, 2003. **53**(2): 143-157.
- Nicot F. and Wan R. (Eds), *Micromécanique de la rupture dans les milieux granulaires*, Hermes Science Lavoisier, 2008.
- Nova R., *Controllability of the incremental response of soil specimens subjected to arbitrary loading programmes*. J.Mech.Behav.Mater., 1994. **5**: 193-201.
- Nova R., *On the hardening of soils*. Arch.Mech.Stos., 1977. **29**(3): 445-458.
- Olivares L., Picarelli L., *Susceptibility of loose pyroclastic soils to static liquefaction: some preliminary data*. In: Proceedings of International Conference on Landslides—Causes, Impact and Countermeasures, Davos, 2001. 75–84.
- Olivares L., Tommasi P., *The role of suction and its changes on stability of steep slopes in unsaturated granular soils*. In Proceedings of the 10<sup>th</sup> International Symposium on Landslides and Engineered Slopes, Chen Z., Zhang J., Li Z., Wu F and Ho K. (eds.), Taylor & Francis Group, London, 2008. **2**: 203-215.

- Pastor M., Haddad B., Sorbino G., Cuomo S., Drempetic V., *A depth-integrated, coupled SPH model for flow-like landslides and related phenomena*. Int. J. Numer. Analyt. Meth. Geomech., 2008. **33**(2): 143–172.
- Pastor M., Fernandez-Merodo J. A., Gonzalez E., Mira P., Li T., Liu X., *Modelling of landslides: (I) Failure mechanisms*. Degradations and instabilities in geomaterials, CISM course and lectures No. 461, 2004. F. Darve and I. Vardoulakis, eds., Springer, New York: 287–317.
- Petley, D.N., D.J. Petley, and R.J. Allison, *Temporal prediction in landslides - Understanding the Saito effect*. Landslides and Engineered Slopes: From the Past to the Future, Vols 1 and 2, 2008: 865-871.
- Petterson K.E., *The early history of circular sliding surfaces*, Géotechnique, 1955. **5**: 275-296.
- Picarelli L., Urciuoli G., and Russo C., *Effect of groundwater regime on the behaviour of clayey slopes*. Canadian Geotechnical Journal, 2004. **41**(3): 467-484.
- Potts D.M., Zdravkovic L., *Finite element analysis in geotechnical engineering*. Thomas Telford Ltd., London (eds), 1999. 440 pages.
- Potts, D.M., N. Kovacevic, and P.R. Vaughan, *Delayed collapse of cut slopes in stiff clay*. Geotechnique, 1997. **47**(5): 953-982.
- Puzrin A.M., Sterba I., *Inverse long-term stability analysis of a constrained landslide*. Geotechnique, 2006. **56**(7): 483-489.
- Rahardjo H., Ong T.H., Rezaur R.B., Leong E.C., *Factors Controlling Instability of Homogeneous Soil Slopes under Rainfall*. Journal of Geotechnical and Geoenvironmental Engineering, 2007. **133**(12): 1532-1543.
- Regalado, C.M., Munoz Carena, R., Socorro, A.R. and Hernandez Moreno, J.M., *Time domain reflectometry models as a tool to understand the dielectric response of volcanic soils*. Geoderma, 2003. **117**: 313-330.
- Roscoe K.H., Schofield A.N. and Thurairajah A., *Yielding of Clays in States Wetter than Critical*. Géotechnique, 1963. **13**: 211-240.
- Saito M., *Forecasting the time of occurrence of slope failure*, in 6th International Conference on Soil Mechanics and Foundation Engineering. 1965, University of Toronto Press, Toronto, Ont.: Montréal, Québec. 537-542.
- Salciarini D., Godt J.W., Savage W.Z., Conversini P., Baum R.L., Michael J.A., *Modelling regional initiation of rainfall-induced shallow landslides in the eastern Umbria region of central Italy*. Landslides, 2006. **3**:181–194.
- Santagiuliana R., Schrefler B.A., *Enhancing the Bolzon-Schrefler-Zienkiewicz constitutive model for partially saturated soil*. Transport in Porous Media, 2006. **65**: 1-30.
- Savage W.Z., Godt J.W., Baum R.L., *Modelling time-dependent areal slope stability*. In: Lacerda WA, Erlich M, Fontoura SAB, Sayao ASF (eds) Landslides-evaluation and stabilization, Proceedings of 9<sup>th</sup> International symposium on Landslides, vol 1. Balkema, Rotterdam, 2004. 23–36.
- Schmertmann J.H., Hartman J.P., Brown P.R., *Improved strain influence factor diagrams*. Proc. ASCE, Journal of the Geotechnical Engineering Division, 1978. **104** GT8: 1131-1135.
- Shin, H.S. and G.N. Pande, *On self-learning finite element codes based on monitored response of structures*. Computers And Geotechnics, 2000. **27**(3): 161-178.
- Simo J.C., Rifai M.S., *A Class of Mixed Assumed Strain Methods and The Method of Incompatible Modes*. International Journal for Numerical Methods in Engineering, 1990. **29**: 1595-1638.
- Skempton, A.W., *4th Rankine Lecture: Long term stability of clay slopes*. Géotechnique, 1964. **14**(2): 77-101.
- Sladen J. A., D'Hollander R. D., Krahn J. *The liquefaction of sands, a collapse surface approach*. Can. Geotech. J., 1985. **22**: 564–578.

- Sorbino G., Foresta V., *Unsaturated hydraulic characteristics of pyroclastic soils*. In: Proceedings of 3rd International Conference on Unsaturated Soils, Recife, vol 1. Balkema, Rotterdam, 2002. 405–410.
- Sorbino G., *Il regime delle acque sotterranee nelle rocce metamorfiche alterate*. Ph.D. Thesis, Consorzio tra le Università di Roma “La Sapienza” e Napoli “Federico II”, 1994. 245 pages. (In Italian).
- Sorbino G., *Numerical modelling of soil suction measurements in pyroclastic soils*. In: Tarantino A, Romero E, Cui YJ (eds) *Advanced experimental unsaturated soil mechanics*, Proceedings of International symposium, Trento. Taylor and Francis Group, London, 2005. 541–547.
- Sorbino G., Sica C., Cascini L., Cuomo S., *On the forecasting of flowslides triggering areas using physically based models*. In: Proceedings of 1st North American Landslides Conference, vol 1. AEG Special Publication 23, 2007. 305–315.
- Sorbino G., Sica C., Cascini L., *Susceptibility analysis of shallow landslides source areas using physically based models*. *Nat. Hazards*, 2010. **53**:313–332.
- Spencer E., *A method of analysis of the stability of embankments assuming parallel interslice forces*. *Geotechnique*, 1967. **17**: 11-26.
- Spickermann A., *Analyse tiefgreifender Hangdeformationen – Einfluss des Initialspannungszustands und der konstitutiven Formulierung*. No. 18 in Schriftenreihe Geotechnik, Bauhaus-University Weimar, T. Schanz and K.J. Witt (ed.), 2008.
- Stimpson B., Barron K., Kosar K., *Multiple-block plane shear slope failure*. *Canadian Geotechnical Journal*, 1987. **24**(4): 479-489.
- Swan C.C., Seo Y.K., *Limit state analysis of earthen slopes using dual continuum/FEM approach*. *International Journal of Numerical and Analytical Methods in Geomechanics*, 1999. **23**(12): 1359-71.
- Tacher L., Bonnard C., Laloui L., Parriaux A., *Modelling the behaviour of a large landslide with respect to hydrogeological and geomechanical parameter heterogeneity*. *Landslides*, 2005. **2**: 3-24.
- Tamagnini R., *An extended Cam-Clay model for unsaturated soils with hydraulic hysteresis*. *Geotechnique*, 2004. **54**: 223-228.
- Tamagnini R., Pastor M., *A thermodynamically based model for unsaturated soils: a new framework for generalized plasticity*. 2nd International Workshop on Unsaturated Soils, Mancuso (ed), 2004. 1-14.
- Taylor D.W., *The stability of earth slopes*. *J. of Boston Soc. Civil Eng.*, 1937. **24**: p. 337-386.
- Tomer M.D., Clothier B.E., Vogeler I. and Green S., *A dielectric-water content relationship for sandy volcanic soils in New Zealand*. *Soil Sc. Soc. Am. J.*, 1999. **63**: 777-781.
- Topp G.C., Davis J.L., and Annan A.P., *Electromagnetic determination of soil water content: measurement in coaxial transmission lines*. *Water Resour. Res.*, 1980. **16**: 574-582.
- Turner M, Clough R.W., Martin H.C., Topp L.J., *Stiffness and deflection analysis of complex structures*. *J Aeronaut Sci*, 1956. **23**(9): 805-823.
- Van Asch T.W.J., Van Beek L.P.H., Bogaard T.A., *Problems in predicting the mobility of slow-moving landslides*. *Engineering Geology*, 2007. **91**(1): 46-55.
- Van Genuchten M. Th., *A closed-form equation for predicting the hydraulic conductivity of unsaturated soil*. *Soil Sci. Soc. Am. J.*, 1980. **44**: 615-628.
- Vardoulakis I., *Catastrophic landslides due to frictional heating of the failure plane*. *Mechanics of Cohesive-Frictional Materials*, 2000. **5**: 443-467.
- Vardoulakis I., Sulem J., *Bifurcation analysis in geomechanics*. Blackie Academic and Professional, Chapman & Hall, 1995.
- Voight, B., *Materials science law applied to time forecast of slope failure*, in *5th International Symposium on Landslides*, R. C. Bonnard. A.A. Balkema, The Netherlands, Editor. 1988: Lausanne, Switzerland. 1471–1472.

- Von Mises, R., *Gottinger Nachrichten*, math.-phis. Klasse, 582, 1913.
- Vulliet, L., *Modélisation des pentes naturelles en mouvement*, in *Civil Engineering Department*. 1986, Ecole Polytechnique Fédérale de Lausanne: Lausanne. 221 pages.
- Wheeler S. J., Gallipoli D., Karstunen M., *Comments on use of the Barcelona Basic Model for unsaturated soils*. *Int. J. Numer. Anal. Meth. Geomech.*, 2002. **26**: 1561-1571.
- Wilde P., *Two-invariants dependent model of granular media*, *Arch.Mech.Stos.*, 1977. **29**: 799-809.
- Wood D.M., *Geotechnical modelling*. Taylor & Francis Group, ISBN: 0415343046, 2004.
- WP-WLI, *A suggested method for describing the rate of movement of a landslide*. *Bulletin of the International Association of Engineering Geology*, 1995. **52**(1): 75-78.
- Wu W., Sidle R.C. *A distributed slope stability model for steep forested basins*. *Water Resour Res*, 1995. **31**:2097–2110.
- Zienkiewicz O. C., Chan A. H. C., Pastor M., Shrefler B. A., Shiomi T., *Computational geomechanics*, Wiley, New York, 1999.
- Zienkiewicz O. C., Chang C. T., Bettess, P., *Drained, undrained, consolidating dynamic behaviour assumptions in soils*. *Geotechnique*, 1980. **30**: 385–395.
- Zienkiewicz O.C., Humpheson C., Lewis R.W., *Associated and non-associated viscoplasticity and plasticity in soil mechanics*. *Géotechnique*, 1975. **25**: 671-689.
- Zienkiewicz O.C., *The finite element method in Engineering Sciences*. 3<sup>rd</sup> ed. New York: Mc Graw-Hill, 1977.